

# Cellular and Network mechanisms for Learning and Memory Consolidation

## Inauguraldissertation

zur  
Erlangung der Würde eines Doktors der Philosophie  
vorgelegt der  
Philosophisch-Naturwissenschaftlichen Fakultät  
der Universität Basel

von

**Ananya Chowdhury**

von India

Basel, 2017

Original document stored on the publication server of the University of Basel

**edoc.unibas.ch**



This work is licenced under the agreement "Attribution-NonCommercial-NoDerivatives 4.0 International License" (CC BY-NC-ND/4.0). The details can be viewed at [creativecommons.org/licenses/by-nc-nd/4.0](https://creativecommons.org/licenses/by-nc-nd/4.0)

Genehmigt von der Philosophisch-Naturwissenschaftlichen Fakultät  
auf Antrag von

**Prof. Dr. Pico Caroni**  
(Dissertationsleiter)

**Prof. Dr. Silvia Arber**  
(Koreferent)

Basel, 17.10.2017

**Prof. Dr. Martin Spiess**  
(Dekan)

# Table of Contents

<b>Preface</b> .....	4
<b>1. Introduction</b> .....	6
1.1. Memory formation.....	7
1.1.1. Molecular mechanisms	
1.1.2. Cellular and synaptic mechanisms	
1.2 Memory allocation.....	14
1.3. Shaping the network and memory trace.....	15
<b>2. Results</b> .....	18
2.1. Time-units for Learning Involving Maintenance of System-wide cFos expression in Neuronal Assemblies.....	19
2.2. PV plasticity sustained through D1/5 dopamine signaling required for long-term memory consolidation.....	48
2.3. Early- and Late-Born Parvalbumin Basket Cell Subpopulations Exhibiting Distinct Regulation and Roles in Learning.....	87
<b>3. General Discussion</b> .....	124
<b>4. Perspective</b> .....	131
<b>5. Materials and Methods</b> .....	135
<b>6. Abbreviations</b> .....	145
<b>7. References</b> .....	150
<b>Acknowledgements</b> .....	164
<b>Curriculum Vitae</b> .....	165

# Preface

Experience shapes who we become and memories make us who we are. Some memories are so universal and so strong that we might even share it with the world: what were you doing when you heard the news about 9/11? However, most of our memories belong to our everyday life; some fade away fast (what you had for dinner a week ago); some survive time (the sumptuous dessert your mom made especially for your birthday a year back). Some things we strive to keep in mind (an alleyway one should avoid in dark) and some we just remember anyway (the familiar route to your best friend's house).

Adaptability to changing environment gives us the advantage needed to survive. Keeping aside the grand picture of evolution of species, even in our daily life, adaptability is of significant importance. To be safe from predator or danger, to find a source of food faster and easier next time, to perform a necessary skill; at every step, one can improve by adapting. To adapt, however, one needs to perceive the changes in its surrounding (i.e. learn), to remember those information until the next encounter (i.e. memory) and then to apply that knowledge to perform better in future (i.e. retrieval).

The universal necessity for learning and memory across different species has been one of the main driving forces towards understanding its mechanisms and rules for more than a century. The social and economic implications of the various mental disorders leading to learning disabilities (Autism spectrum disorders, Schizophrenia), memory loss in neurological diseases (Alzheimer's, Parkinson's) as well as the psychological effects of post-traumatic stress disorders made the field of learning and memory indispensable. On the other hand, the possibility of studying the mechanisms of memory formation in organisms with relatively simple nervous system and its potential of translation to rodents, non-human primates and human subjects gave a significant advantage to the progress of the field in the last several decades.

With the use of pharmacogenetic tools to reversibly silence or activate specific neuronal populations in different brain areas with temporal and spatial precision

and a wide range of transgenic mouse lines to access these populations, I here ask the following questions:

1) How is learning defined? To create a memory that will be useful later, it is necessary to successfully learn and to define the criteria that determines what to learn and when to learn. Without these boundaries, memories could get all jumbled into intangible information and therefore, inaccessible for coherent retrieval. The first segment of my work will focus on understanding the cellular, molecular and network parameters that dictate the units of learning.

2) What processes are responsible for the formation of long-term memories? Are the plasticity mechanisms over once the short-term memories have been converted into long-term memories, i.e. initial hours after acquisition or could there still be plasticity later in time that determines which memories stay and which are lost? The second segment of my work would deal with a 'second window of consolidation' when the inhibitory Parvalbumin (PV+) interneurons would be shown to be critical in ensuring the formation of long-term memories.

3) How are the inhibitory PV+ interneurons involved in the regulation of learning? Since formation of long-term memory involves structural and molecular changes in the excitatory principal cells, what role does the inhibitory interneurons, specifically PV+ basket cells, play in learning and memory consolidation? The third segment of my work would reveal the existence of distinct sub-populations of PV+ basket cells, specified at the time of birth and required for regulation of different types of learning.

In this thesis, I explore these questions in details to understand how learning leads to memory formation, how memory is strengthened and made long-lasting and how memory-specific cFos+ ensembles and PV+ interneuron subpopulations can be regulating those processes in a temporally-defined manner. This study provides insights into the possible mechanisms that allow associations and informations to become meaningful learning that then can be consolidated into a relevant memory to be successfully retrieved later in life.

# 1. Introduction

## **1.1 Memory formation**

The formation of memory is a protracted temporal phenomenon. While learning has been defined as the process of acquisition and encoding of relevant information from the surrounding (e.g. novel or emotional), the process by which this acquired data becomes a memory that can be successfully retrieved later in time can be described as the phenomenon of consolidation. The credit for the term '*Konsolidierung*' or 'consolidation' (Latin: 'to make firm') was coined by two German scientists Muller and Pilzecker in 1900 (Muller and Pilzecker, 1900). The umbrella term 'consolidation' is used to broadly describe the mechanism by which recently acquired memories (short-term memory) that are vulnerable to disruptions gets converted into stable long-term memories. Several studies have shown that different amnesic agents can disrupt newly acquired memories for a limited time window, after which they are said to have consolidated, i.e. becomes resistant to interference (Davis and Squire 1984, Kandel 2001). However, question remains why consolidate after a certain time? As put forth in the review discussion by Y. Dudai (Dudai 2004), the information could have been stabilized immediately after its acquisition. However, it is highly likely that instantaneously stabilizing each and every encoded information would be wasteful to the computational ability and storage capability of the brain. Not only that, the possibility of assessing the relevance of the acquired information during the hours prior to consolidation increases the effectiveness of the process to maximize the benefit of stabilizing that memory. As will be discussed in details further, the consolidation process goes through several checkpoints during which signalling pathways, molecular changes, cellular (both excitatory and inhibitory) allocation and competition, structural modifications of spines and synapses, synchronized network activities at different frequency ranges, dictate the eligibility, strength and quality of the information to be consolidated into long-term memory.

### **1.1.1 Molecular mechanisms**

Long-lasting forms of synaptic plasticity like long-term potentiation (LTP) and long-term depression (LTD) have been studied extensively as the fundamental basis of learning and memory (Bliss and Collingridge 2013). Upon synaptic input, Ca<sup>2+</sup> entry through N-methyl-D-aspartate-type receptors (NMDARs) was found to

be critical at the onset of LTP via facilitation of  $\alpha$ -amino-3-hydroxy-5-methyl-4-isoxazolepropionic receptor (AMPA) recruitment to the potentiated post-synaptic sites. Several studies with pharmacological inhibition of NMDA and AMPA receptors and genetic deletion of specific NMDAR subunits established the essential role of NMDA and AMPA receptors in the process of long-term potentiation and long-term memory (Abel and Lattal 2001, Schafe, Nader et al. 2001, Fanselow and Poulos 2005, Kessels and Malinow 2009, Kandel, Dudai et al. 2014).

Studies using classical conditioning form of learning in *Aplysia* made several breakthrough into the molecular mechanisms underlying associative learning (Hawkins, Abrams et al. 1983, Walters and Byrne 1983). Experiments in *Aplysia* revealed increase of  $Ca^{2+}$  influx into the presynaptic sensory neuron during the paired firing which led to the enhanced activity of  $Ca^{2+}$ -sensitive adenylyl cyclase, increasing the production of cAMP (cyclic adenosine monophosphate) (Abrams, Karl et al. 1991, Kandel 2001). At the same time, several lines of *Drosophila* with learning deficits were identified by Benzer and his students and revealed to have mutations in different single genes representing different components of cAMP pathway; notable being *dunce* (*Drosophila* Phosphodiesterase 4 homolog) and *rutabaga* (*Drosophila*  $Ca^{2+}$ /CaM-dependent adenylyl cyclase) (Dudai, Jan et al. 1976, Livingstone, Sziber et al. 1984, Lee 2015).

The use of different protein synthesis inhibitors like Anisomycin, Puromycin etc brought forth the seminal findings that has since been used to broadly distinguish between short-term and long-term memory (Davis and Squire 1984, McGaugh 2000, Nader, Schafe et al. 2000, Kandel 2001). Administration of transcription and translation inhibitors immediately after a learning was shown to be detrimental to long-term memory, keeping short-term memory intact (Bourtchouladze, Abel et al. 1998, Igaz, Vianna et al. 2002, Fonseca, Nagerl et al. 2006). Also, an overall increase in translation has been observed after training (Hoeffler, Cowansage et al. 2011). So, which transcription factors might play a role in synthesis of the new proteins essential for consolidation of memories?



One of the key players studied in several systems is cAMP response element binding protein, CREB (Silva, Kogan et al. 1998, Alberini 2009, Kandel 2012). Training or acquisition of an event leads to the activation of cell signalling cascades such as the protein kinase A (PKA) (Dash, Hochner et al. 1990, Martin, Michael et al. 1997), the protein kinase C (PKC), calcium/calmodulin-regulated kinase (CaMKII) (Sheng, Thompson et al. 1991) and the MAPK/extracellular-signal regulated kinases (ERK) cascades (Kelleher, Govindarajan et al. 2004, Xia and Storm 2012), all converging on the phosphorylation and activation of CREB, which may therefore serve to integrate signals from various signal transduction pathways (Kandel 2012). In accordance with this, the phosphorylation of CREB has been shown to increase in the hippocampus, amygdala and parietal cortex shortly following fear conditioning in mice (Stanciu, Radulovic et al. 2001, Dash, Hebert et al. 2004). CREB has been reported to be required for long-term memory formation in several species including *Drosophila*, mice and rats (Bourtchuladze, Frenguelli et al. 1994, Yin, Wallach et al. 1994, Guzowski and McGaugh 1997, Kogan, Frankland et al. 1997, Lamprecht, Hazvi et al. 1997, Kida, Josselyn et al. 2002). Activated pCREB, in turn, is responsible for the transcription of downstream genes like *bdnf* (Tao, Finkbeiner et al. 1998), *c-fos* (Sheng, McFadden et al. 1990), *zif-268* (Davis, Vanhoutte et al. 2000) and others.

Among the downstream factors of CREB, c-Fos is a transcription factor that together with c-Jun, comprises the AP-1 transcriptional complex. *c-fos* is an immediate early gene that has been known to be rapidly upregulated upon different learning tasks (Guzowski 2002, Kubik, Miyashita et al. 2007, Ruediger, Vittori et al. 2011, Ruediger, Spirig et al. 2012). Although initially c-Fos had been widely used as a marker for neuronal activity upon variety of stimulus (Flavell and Greenberg 2008, Joo, Schaukowitch et al. 2016), inhibition of c-Fos expression has been since functionally associated with impairment of long-term memory formation (Lamprecht and Dudai 1996, He, Yamada et al. 2002, Katche, Dorman et al. 2013, Katche and Medina 2017).

Therefore, following acquisition, a cascade of molecular events leads to a sequential activation of essential components of the consolidation program;

upregulation of pERK (MAPK pathway) and pCREB happens almost immediately after (0-60min) while c-Fos protein levels are upregulated at about 45min-60min. However, the consolidation program does not end at these early hours with the classically defined conversion of short-term memory to long-term memory. Recent studies have reported the existence of a delayed consolidation window responsible of strengthening and persistence of long-term memory (Bekinschtein, Cammarota et al. 2007, Rossato, Bevilaqua et al. 2009). Furthermore, studies have since demonstrated a second temporal sequence of recapitulation of the molecular events underlying consolidation about 9-12h onwards after the initial acquisition (Trifilieff, Herry et al. 2006, Bekinschtein, Cammarota et al. 2007, Katche, Bekinschtein et al. 2010, Nakayama, Iwata et al. 2015).

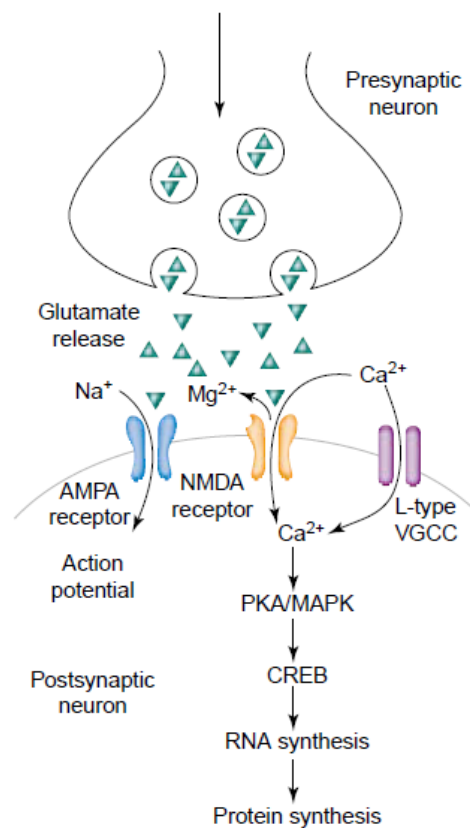


**Fig. 1. Simplistic model depicting the molecular cascades underlying consolidation.** Neuronal activity upon acquisition involves release of glutamate from the presynaptic cell and Ca<sup>2+</sup> influx into the postsynaptic cell through the different channels. Increase in intracellular levels of Ca<sup>2+</sup> leads to the activation of protein kinases, like PKA and ERK/MAPK, which then, translocate to the cell nucleus where they activate transcription factors such as CREB. CREB, in turn, activates transcription of several genes and translation of proteins that are critical for long-term memory formation (Schafe, Nader et al. 2001).

### 1.1.2 Cellular and synaptic mechanisms

Acquisition initiates tightly regulated activation of signalling pathways, expression of genes and proteins, in specific brain areas involved in that particular type of learning. However, the possibility of existence of a physical memory trace has intrigued the neuroscience community for a long time. Where does a memory reside? Seminal concepts were put forth by Richard Semon (1904, 1909, 1921, 1923) as 'the engram theory' and Donald Hebb (1949) as 'synaptic plasticity theory' to explain the memory trace. Semon's insights into the possibility of 'engram' went unnoticed for a while until its revival by Schacter and colleagues (Schacter et al. 1978, 1982). It was the first to suggest the notion of engram as the persistent modifications in specific brain cells that retain the information of the experience responsible for those enduring changes (Law of Engrapy) and capable of reviving or reactivating the experience upon appropriate retrieval conditions (Law of Ecphory). In 1950, Karl Lashley, went on a quest to systematically hunt down the location of engram cells in rodent brain for a maze task. His findings concluded that memory engram was not localized in one part of cortex but was rather distributed (Lashley, 1950). In recent years, harnessing the technologies like genetic targeting of IEGs, transgenic models, pharmacogenetics, optogenetics, single cell recordings, tracings and behavioural paradigms, the quest has continued.

The immediate early genes like c-Fos and Arc are induced within a short time in the involved brain areas upon a certain learning (Kawashima, Okuno et al. 2014). With the advent of chemical and genetic tools, this activity dependent expression of IEGs was exploited to develop the 'TetTag' method (Reijmers, Perkins et al. 2007) and 'TRAP' method (Guenther, Miyamichi et al. 2013). The 'TetTag' method utilizes crossing of two transgenic mouse lines: one in which tTA (tetracycline transactivator) was expressed down-stream of c-fos promoter and other had reporter LacZ protein expressed downstream of tetracycline responsive element (TRE), which is activated by tTA (Reijmers, Perkins et al. 2007). The 'TRAP' (Targeted Recombination in Active Population) method (Guenther, Miyamichi et al. 2013), on the other hand, uses two transgene cassettes to create knock-in mouse lines : in the first cassette, a tamoxifen-dependent Cre

recombinase is expressed under control of an activity-dependent promoter, and in the second cassette, a “STOP signal”, which is flanked by recombination sequences [such as single lox P or double loxP (such as DIO or FLEX)], is placed between the reporter gene of interest and a constitutive promoter. The TetTag method takes advantage of temporal precision of capturing the learning-induced activated cells with Doxycycline on-off regime and the TRAP method uses tamoxifen/hydroxyl-tamoxifen administration within a sharp time window upon learning. Both the methods provide enormous advantage in the study of the properties of the titular engram cells by the means of permanent labelling of these cells upon the brief activation with learning (Kawashima, Okuno et al. 2014, Tonegawa, Liu et al. 2015, Tonegawa, Pignatelli et al. 2015).

With access to the neuronal ensembles activated during a learning, several studies have shown that recall of that memory preferentially reactivates the tagged cells in region-specific manner (Reijmers, Perkins et al. 2007, Deng, Mayford et al. 2013, Tayler, Tanaka et al. 2013).

Furthermore, combining the TRE-dependent (for TetTag method) or CRE-dependent (for TRAP method) approaches for tagging neuronal ensembles with chemogenetics or optogenetics provided the chance to manipulate the tagged cells in different brain areas involved, successfully demonstrating their sufficiency and necessity for retrieval of the memory (Liu, Ramirez et al. 2012, Cowansage, Shuman et al. 2014, Denny, Kheirbek et al. 2014, Tanaka, Pevzner et al. 2014, Gore, Schwartz et al. 2015).

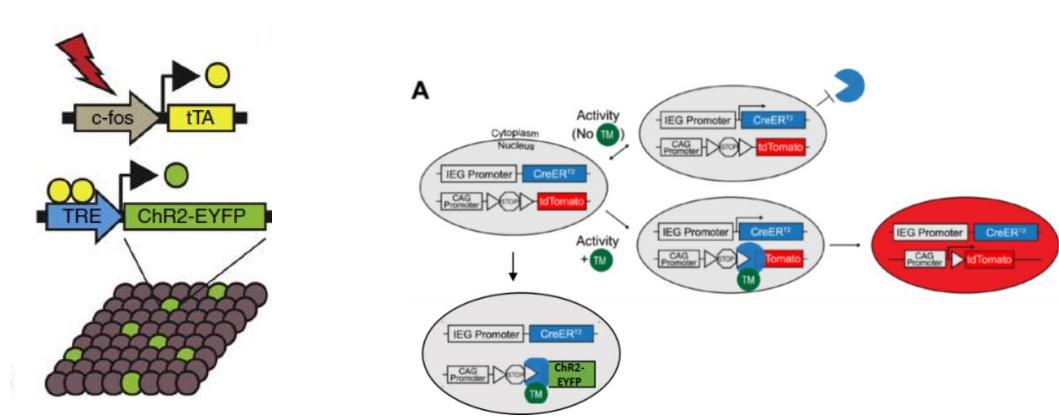


**Fig. 2. Basic components of ‘TetTag’ and ‘TRAP’ method for tagging and manipulating the engram.** In ‘TetTag’ method, virus expressing TRE-ChR2 and optic

fibers are targeted to a specific brain area in a c-Fos-tTA transgenic mice. In the absence of DOX, the neurons that are active during the formation of a memory are labelled with ChR2 and thereby, the engram can be manipulated with light and studied (Tonegawa, Pignatelli et al. 2015).

In 'TRAP' method, the activity-promoter dependent expression of CreERT2, in presence of tamoxifen, allows the expression of either td-tomato or ChR2 to label the neurons active during learning and manipulate their response subsequently (Modified partially from (Guenther, Miyamichi et al. 2013)).

The neurons communicate with each other through synaptic connectivity and dendritic spines are the postsynaptic structures for most excitatory neurons. So, if neurons are responding to a learning event with the regulation of myriad molecular pathways, the dendritic spines and synapses onto them like would have corresponding alterations to adjust that response. As proposed by Donald Hebb, neurons that encode a memory undergo enduring strengthening of some of their synapses by virtue of their simultaneous activation from the presynaptic neurons: hence neurons that "fire together wire together" (Hebb, 1949, Tonegawa, Liu et al. 2015). Indeed, several studies have demonstrated that learning and relevant experience leads to long-lasting structural modifications in the synaptic units with increase of spine dynamics, stabilization and pruning of synapses as well as increase of selective synaptic strength (Hofer, Mrcic-Flogel et al. 2009, Xu, Yu et al. 2009, Yang, Pan et al. 2009, Lai, Franke et al. 2012, Caroni, Chowdhury et al. 2014), revealing another physical representation of memory trace (Rogerson, Cai et al. 2014, Holtmaat and Caroni 2016). In a recent study, using AS-PaRac1 (activated synapse targeting photoactivatable Rac1; a novel optical probe), the newly potentiated spines could be specifically tagged and selectively compromised by light-dependent activation of Rac1, leading to disruption of the acquired motor task (Hayashi-Takagi, Yagishita et al. 2015), providing a causal link between learning-specific newly formed and potentiated spines and subsequent performance. Connecting the two theories of cellular and synaptic engram even further, studies showed evidence of increased synaptic strength and dendritic spine density in the engram cells (tagged after contextual fear learning) when compared to neighbouring non-engram cells in dentate gyrus of hippocampus (Ryan, Roy et al. 2015), upregulation of post-synaptic calcium-permeable AMPA receptors in the engram cells of ACC after trace fear conditioning (Descalzi, Li et al. 2012) while engram cells of CA1 were revealed to

have significant reduction of spines 24h post fear conditioning in comparison to non-engram cells (Sanders, Cowansage et al. 2012).

## **1.2 Memory allocation**

With the emergence of the concept of neuronal ensemble 'engram' specifically dedicated to formation of a memory and ensuring its long-term retrieval, an equally perplexing question came forth. How is the size of such ensemble determined? Majority of the neurons in a particular brain area are equipped with the molecular and synaptic machinery to participate in learning; however, only a small fraction of them actually become part of the memory trace for one particular memory (Repa, Muller et al. 2001, Rumpel, LeDoux et al. 2005, Johansen, Tarpley et al. 2010). As discussed in a current review (Rogerson, Cai et al. 2014), there has to be a fine balance in the size of the memory trace: too big and there won't be enough capacity to store further memories; too small and the representation will be unstable and easily disrupted. Excitability of the neurons was found to be an important determinant for neuronal allocation. The neurons with higher excitability immediately before a learning event were demonstrated to have higher propensity to be incorporated into the memory trace (Choi, Stettler et al. 2011, Yiu, Mercaldo et al. 2014). The existence of highly excitable strongly interconnected neuronal ensemble embedded within the network might serve as such nodes (Yassin, Benedetti et al. 2010). In those lines, CREB was found to a key player in allocating the eligible neurons to memory traces; neurons with higher CREB expression at the time of learning were shown to have higher probability to become integral part of that memory trace (Han, Kushner et al. 2007, Han, Kushner et al. 2009, Kim, Kwon et al. 2014, Sano, Shobe et al. 2014) and exhibit higher excitability and synaptic efficacy (Zhou, Won et al. 2009).

Therefore, the size-constrained neuronal assemblies have to be organized to form memory trace with maximal efficiency. Indeed, it was demonstrated that though fewer neurons responded to stimulation of the trained whisker in an associative fear learning paradigm studied in primary somatosensory or barrel cortex, their evoked responses were stronger than those in control non-associative condition (Gdalyahu, Tring et al. 2012). The emergence of sparser but more robust ensemble upon learning puts forth the possibility of network

subcomponents which might be essential to dictate neuronal allocation by adjusting the excitability of neurons through tightly-controlled excitatory-inhibitory balance onto them.

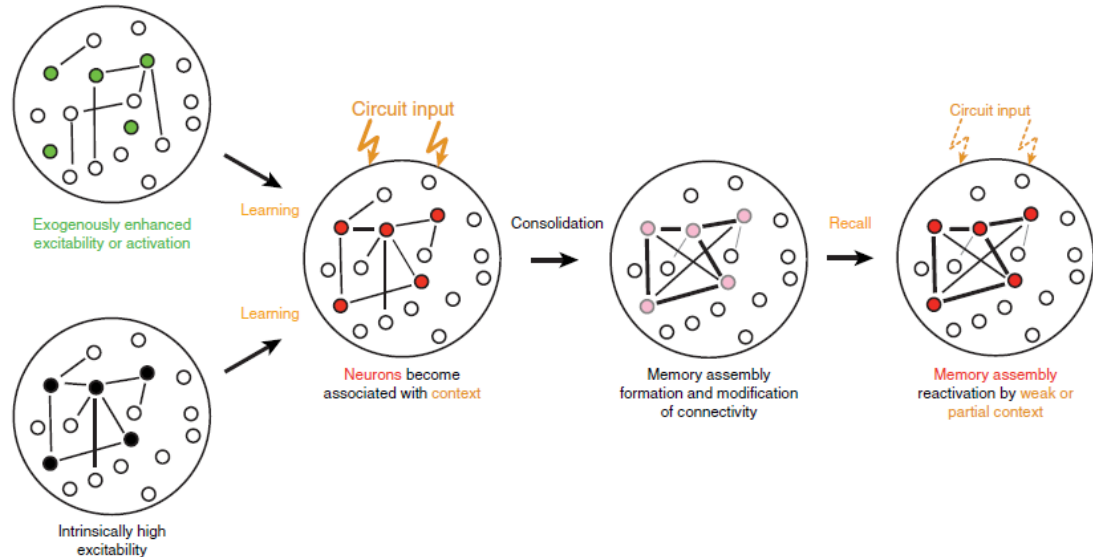


**Fig. 3. Putative mechanism of engram formation and allocation during learning.** Increased excitability in a random subset of neurons, whether exogenously enhanced or due to intrinsic properties, becomes a crucial factor in deciding their recruitment to the memory engram during associational learning. Upon consolidation, the neuronal assembly that was activated and recruited during learning gets modified, possibly exhibiting stronger synaptic connections within them such that a weak or partial cue can reactivate the assembly and retrieve the memory (Holtmaat and Caroni 2016).

### 1.3 Shaping the network and memory trace

The brain is composed of a large repertoire of neurons, each type with its distinct morphological, biochemical, physiological and functional feature. Very broadly, they can be divided into excitatory (projection) and inhibitory (interneurons) cells (Klausberger and Somogyi 2008). The excitatory cells respond with increased activity which needs to be temporally constricted by inhibition onto them to generate the multitudes of network oscillations necessary for neuronal communication within and across areas (Klausberger and Somogyi 2008, Isaacson and Scanziani 2011, Kepecs and Fishell 2014). Temporally defined inhibition and disinhibition of principal cells through increase and decrease of the activity of inhibitory interneurons respectively represents the perfectly balanced window for acquisition and processing of memory (Letzkus, Wolff et al. 2015).

Among the different classes of GABAergic interneurons, parvalbumin basket cells (PV+) comprises the fast-spiking interneurons that provide strong feedforward and feedback perisomatic inhibition to principal neurons. The feedforward inhibition temporally restricts the response of principal cells, as the same glutamatergic input excites both the principal cell and the PV+ basket cell which then perisomatically inhibits that principal cell. The lateral feedback inhibition, instead, spatially restricts the incorporation of principal cells into an active ensemble, as the principal cells activate the PV+ interneurons that in turn inhibits the neighbouring cells (Ruediger, Vittori et al. 2011, Hu, Gan et al. 2014). Due to these features, PV+ interneurons could potentially shape the memory trace by restricting the size of the active ensemble. Indeed, recent studies have indicated that PV+ interneurons in amygdala are involved in limiting the recruitment of principal cells to the memory trace in a competitive manner (Morrison, Rashid et al. 2016, Rashid, Yan et al. 2016).

The recruitment of PV+ interneurons has been shown to support various synchronized and fast network activities such as sharp-wave ripples, spindles, theta rhythm and gamma-range oscillations in both hippocampus and cortical areas, which in turn are found to be critical for memory processing (Cardin, Carlen et al. 2009, Girardeau, Benchenane et al. 2009, Stark, Roux et al. 2014, Amilhon, Huh et al. 2015, Stark, Roux et al. 2015, Ognjanovski, Schaeffer et al. 2017, Roux, Hu et al. 2017).

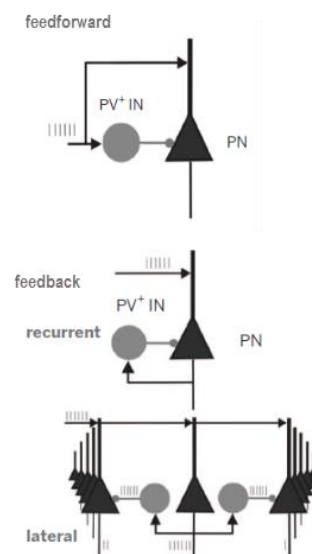
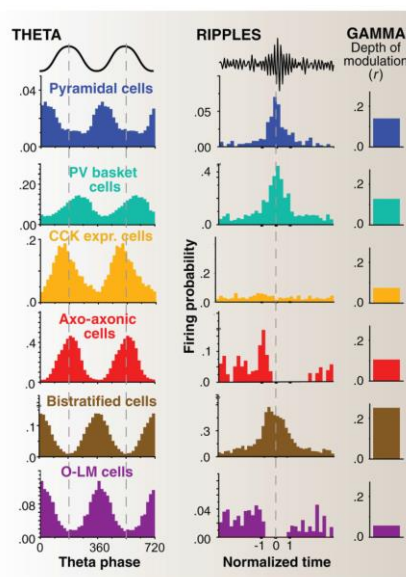




**Fig. 4. Properties of interneurons and PV+ basket cells.** Interneurons are known to fire with distinct temporal patterns during the theta and ripple oscillations, and their spike timing has been shown to be coupled to the field gamma oscillations to differing degrees, depending on where they innervate the principal cells, as depicted in the firing probability histograms (Klausberger and Somogyi 2008).

In feedforward inhibition, afferent glutamatergic axons activate principal cell and PV+ interneuron in parallel, the PV+ interneurons in turn, inhibiting the principal cell. In feedback (recurrent and lateral) inhibition, afferent glutamatergic axons activate principal cells, which then activate interneurons in series. In case of recurrent inhibition, the PV+ interneuron inhibit the same principal cell that activates it while in lateral inhibition, the PV+ interneuron inhibits the surrounding cells (Hu, Gan et al. 2014).

PV+ interneurons are found to be critical during learning (Donato, Rompani et al. 2013, Wolff, Grundemann et al. 2014) and necessary for consolidation of memory (Ruediger, Vittori et al. 2011, Ognjanovski, Schaeffer et al. 2017). Interestingly, PV+ basket cells themselves exhibit plasticity and undergo synaptic remodelling upon learning. It was observed that earlier experience inclines the PV+ basket cell distribution towards either elevated PV and GAD67 (enzyme important for GABA production) expressing population or reduced PV and GAD67 expressing population, which are accompanied by increase or decrease of E/I balance of inputs onto the PV+ cells. The PV+ network state upon prior experience influences the subsequent learning (Donato, Rompani et al. 2013).

## 2. Results

2.1

**Time Units for Learning Involving  
Maintenance of System-wide cFos  
Expression in Neuronal Assemblies**

Ananya Chowdhury and Pico Caroni

Submitted: Nature Neuroscience (2017)

### **2.1.1 Summary**

In learning, repeated experiences might be integrated individually as they occur, or they might be combined within dedicated time windows, possibly promoting quality control. Here we show that in Pavlovian, incremental and incidental learning, related information acquired within time windows of 5h (time units for learning) is combined to determine whether and what mice learn. Trials required for learning had to occur within 5h, when learning-related shared partial cues could produce association and interference with learning. Upon acquisition, cFos expression was elevated during 5h throughout specific system-wide neuronal assemblies. Time unit function depended on network activity and cFos expression. Local cFos activity was required for distant assembly recruitment through network activity and distant BDNF. Activation of learning related cFos assemblies was sufficient and necessary for time unit function. Therefore, learning processes consist of dedicated 5h time units, involving maintenance of specific system-wide neuronal assemblies through network activity and cFos expression.

### **2.1.2 Introduction**

An isolated experience can produce long-lasting memories, but learning often involves multiple interactions with related information<sup>1-3</sup>. The outcome of these interactions could be integrated incrementally, independent of when individual interactions occur. Alternatively, integration might occur within dedicated periods of time, breaking down learning processes into discrete time units. The latter possibility might provide brain mechanisms for content and quality control in learning, and to avoid interference through spurious observations, but whether learning processes involve dedicated time windows for associative learning has remained unclear.

Learning and memory processes can be influenced by the temporal schedule of individual trials. Thus, learning protocols in which individual trials are a few minutes apart (spaced learning) are more effective than massed protocols (trials less than 1min apart)<sup>2,4</sup>. Furthermore, local pharmacological manipulation of dopamine D1 receptor signaling within about 5h from acquisition modulates the strength of long-term memories<sup>5</sup>, and neuronal assemblies accounting for

memories can be combined within a time window of about 5h from acquisition<sup>6,7</sup>. These findings suggest the existence of molecular, cellular and network mechanisms that might support the combination of related memories in learning during a time window of about 5h, but whether and how these proposed mechanisms might play together to determine what is learned is currently poorly understood.

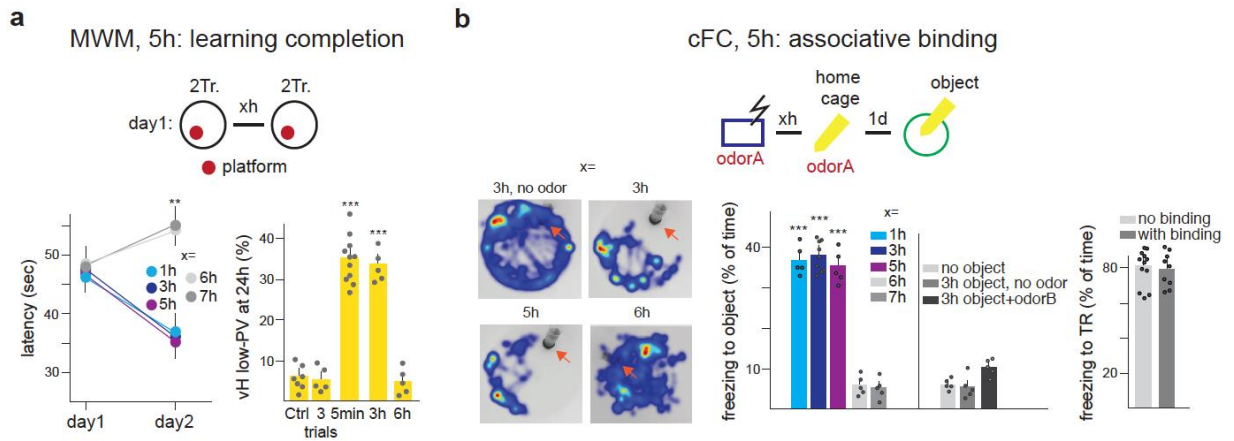
Here we investigated whether learning might involve dedicated time windows for integration of individual related experiences, and what might be the underlying molecular/cellular, circuits and systems mechanisms. We show that in spatial, motor, fear, and incidental learning, related information acquired within time windows of 5h is combined to determine whether and what is learned. For learning to occur, sufficient trials had to be executed within 5h, and learning-related shared partial cues produced association of otherwise unrelated information and interference with learning when occurring within 5h. Single related but goal-contradicting trials within 5h were sufficient to disrupt learning, and such interference could not be overcome within the same time unit. Addressing cellular and network mechanisms underlying time unit duration and function, we show that these involve maintenance of specific system-wide neuronal assemblies<sup>8,9</sup> through network activity<sup>10</sup>, cFos expression<sup>11,12</sup> and BDNF signaling<sup>12-14</sup>.

### **2.1.3 Results**

#### **A 5h time window for learning and associative binding.**

To investigate possible temporal constraints in learning, we first defined numbers of individual trials that, under our experimental conditions, led to behaviourally detectable progress in Morris water maze<sup>15</sup> (MWM; incremental spatial learning) or rotarod training protocols<sup>16</sup> (RR; incremental motor skill learning). Under our experimental conditions, regimes of 4 daily trials led to detectable progress, whereas regimes of 2 daily trials did not (Suppl. Fig. 1). We then determined whether there might be critical time windows within which those 4 trials needed to be completed in order to promote learning. We assessed MWM learning behaviorally as incremental improvement in daily performance<sup>15</sup>, and cellular-molecularly as learning-related increase in the fraction of parvalbumin (PV)

neurons exhibiting low expression levels of PV (PV plasticity) in ventral hippocampus (vH)<sup>17,18</sup>. We tested MWM protocols consisting of 2+2 (2 not sufficient, 4 sufficient) trials, separated by increasingly long time intervals (Fig. 1a). Any time interval up to 5h produced learning and hippocampal PV plasticity that were undistinguishable from that detected upon a conventional 5min inter-trial interval protocol (Fig. 1a). By contrast, intervals of 6h or more not only produced no behavioral learning, but also no learning-related PV plasticity in vH (Fig. 1a). In closely comparable 2+2 trials protocols, RR learning was equally effective when the total of 4 trials was delivered within a time window of up to 5h, whereas time windows of 6h or more led to no learning and no PV plasticity in primary motor cortex<sup>18</sup> (M1; Suppl. Fig. 2). These findings suggested that training essential for behavioral learning needs to be integrated within time units of 5h. The 5h time window might reflect a time when learning-related information is most effectively integrated, which would be reminiscent of recent findings concerning the merging of memory engrams<sup>6,7</sup>. To investigate this notion, we placed a neutral object (Falcon tube), together with the odor associated with Pavlovian conditioning (partial cue) during a period of 30min into the home cage of mice that had undergone contextual fear conditioning (cFC; Fig. 1b). Supporting the notion that partial cues are associated effectively to learning within time windows of 5h, mice exposed on the next day to a novel (i.e. neutral) context with the object, but without the odor, avoided the object and froze only if object + partial cue presentation had occurred within 5h after cFC (Fig. 1b). This associative binding to fear memory occurred 5h but not 7h after acquisition regardless of whether the initial cFC was carried out at 4am, 10am, 4pm or 10pm (Suppl. Fig. 3), suggesting that the duration of the time window for associative binding was not affected by the circadian rhythm. In control experiments, the associative binding protocol, which led to freezing values of 35-40% of the time in a new context with the object, did not influence the magnitude of freezing responses to the conditioning context, which were about 80% of the time regardless of whether mice had learned the additional association between object and fear.



Chowdhury and Caroni Fig. 1

### Figure 1. A 5h time window for learning and associative binding.

**(a) Time window to complete MWM learning.** Left: latencies as a function of time interval between first and second group of 2 trials on day1 (one-way ANOVA,  $F(4,23)=45.81$ ,  $P<0.0001$ ,  $n=5$  in each group, except  $n=8$  for 3h); right: PV plasticity (low-PV contents in vH at 24h; Ctrl: swim control without platform; one-way ANOVA,  $F(4,28)=105.6$ ,  $P<0.0001$ ,  $n=7,5,11,5,5$ ). Tr.: trial, x: numbers of hours as indicated in different protocols; day2: 4 trials.

**(b) Associative binding of neutral object to fear memory during 5h time unit.** x: number of hours following acquisition of cFC. Schematic: boxes of different colors indicate different contexts; object: Falcon tube. Left, center: Representative heat maps (left) and quantitative analysis (center; one-way ANOVA,  $F(7,36)=104.9$ ,  $P<0.0001$ ,  $n=5$  for each group, except  $n=9$  for 3h) of novel context exploration in the presence of object (Falcon tube; orange arrows). Right: Fear memory binding (3h after acquisition) does not influence fear response to conditioning context (tested at 26h; unpaired t-test,  $t(19)=0.8568$ ,  $P=0.4022$ ,  $n=12,9$ ).

### Interference through shared partial cues within 5h time units.

We then explored experimental conditions under which learning of distinct but behaviorally related content within time units of 5h might produce interference and disruption of learning. We first investigated delivery of two cFC protocols (same type of learning) in different contexts (conflicting conditioned stimulus associations). cFC in a first context (TR1), and then again in a different context (TR2) 3h later, led to a dramatic reduction of freezing (35% instead of 80% of the time) to TR1 or TR2 on the next day (Fig. 2a). By contrast, no interference with freezing was detected when the two conditioning contexts separated by 3h were identical, or when cFC in TR1 and TR2 were separated by 6h (Fig. 2a). These

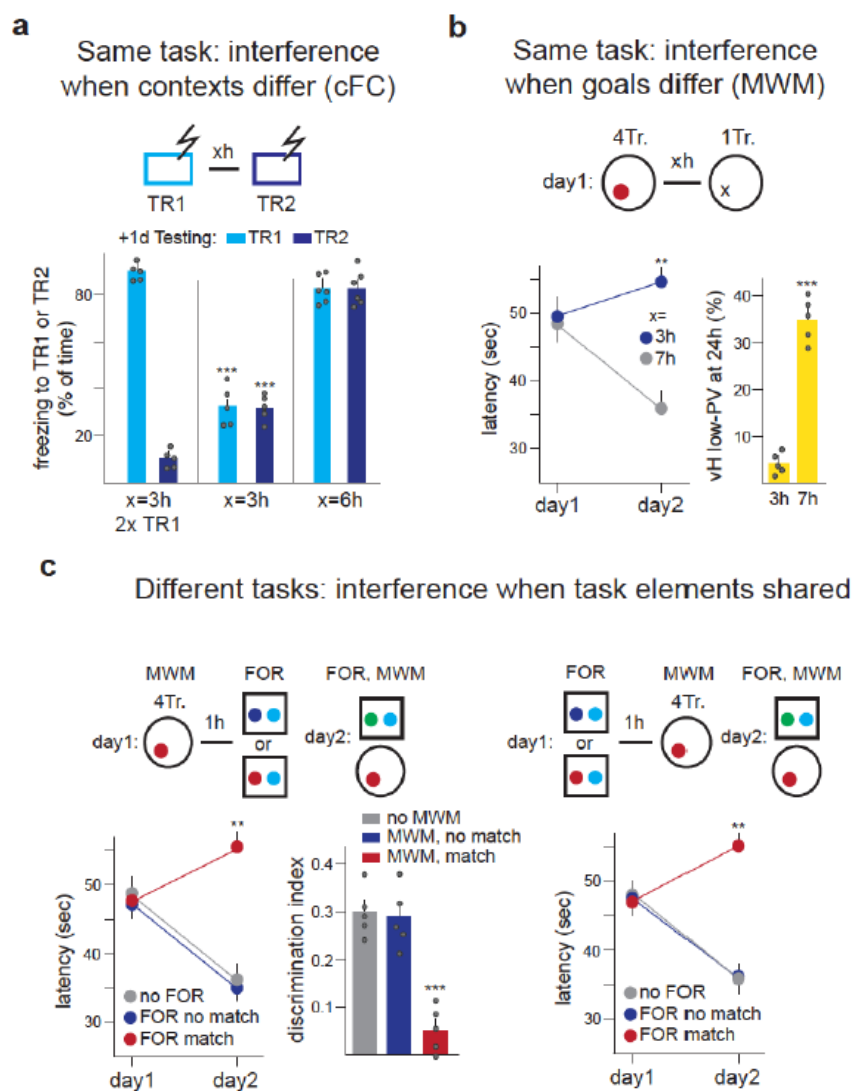
results suggested that when the two cFC protocols in different contexts were carried out within 3h (or 5h, not shown) from another, none of the two contexts was associated with a robust fear memory, possibly because detection of the US in TR2 conflicted with association of the US with TR1.

We then investigated the possible impact of a single trial without escape platform (same task; closely comparable behavior but no escape goal) for MWM learning. Remarkably, when 4 trials required for learning were completed within 25 minutes (conventional 5min inter-trial interval), a single trial without platform delivered at 3h, but not at 7h was sufficient to suppress any learning-related improvement in performance and learning-related PV plasticity in the MWM as detected on the next day (Fig. 2b). Therefore, and like the two cFC protocols in different contexts, these results suggested that when the association between water maze setting and goal (the escape platform) was contradicted within a 5h time window, mice did not associate the maze setting with the escape platform, and did not learn to navigate to the platform.

Finally, we investigated whether interference might also occur among entirely distinct learning tasks, in cases where we provide a task-relevant element that is shared between the two tasks. First, we found that when an object recognition memory task (incidental learning; familiar object recognition; FOR<sup>18</sup>) and MWM training were carried out in the absence of shared elements within the same 5h time unit, the two tasks did not interfere with each other (Fig. 2c). Notably, however, when one of the objects during acquisition of FOR closely resembled the escape platform (for these particular experiments FOR object and MWM escape platform were the same), learning of FOR and MWM were both disrupted as detected by performance on the next day (Fig. 2c). The outcome of these experiments was not influenced by whether MWM was carried out before or after FOR (Fig. 2c). Taken together, these results provided evidence that, within the 5h time unit, contrasting task-related goals among trials belonging to the same or closely related tasks, or individual shared task related goals between different tasks are sufficient to profoundly disrupt learning. In a further set of behavioral experiments to define features of time units for learning, we investigated the possibility that initiation of a new time unit might be necessary to overcome



interference in learning. Indeed, in MWM learning, 4 additional trials with platform carried out within the same time unit for learning failed to overcome the impact of a single trial without escape platform (Fig. 2d). By contrast, when the additional 4 trials were carried out after the end of the time unit (7h), they produced robust learning undistinguishable to carrying out a single unperturbed MWM learning unit (Fig. 2d). Finally, when a second set of 4 trials was carried out within the same time unit, it was not associated with improved performance, whereas the improved performance was undistinguishable from that detected on a subsequent training day when the second set of 4 trials were carried out 7h after the first one (Fig. 2e). Therefore, overcoming associational interference or producing improved performance as a consequence of MWM learning requires initiation of a new time unit.



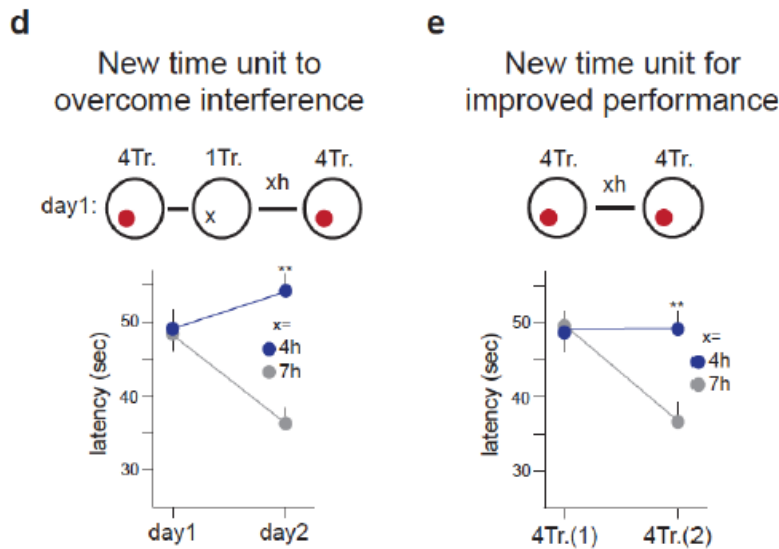


**Figure 2. Interference through shared partial cues within 5h time units.**

**(a) Interference when cFC in TR1 is followed within 5h time unit by cFC in different context TR2.** Freezing at recall 1d after acquisition assessed in TR1 or TR2 (one-way ANOVA,  $F(5,26)=96.36$ ,  $P<0.0001$ ;  $n=5,5,5,5,6,6$ ).

**(b) Interference in MWM learning by single trial without platform carried out during 5h time window.** Left: latencies (3h versus 7h on day2; unpaired t-test,  $t(8)=4.692$ ,  $P=0.0016$ ,  $n=5$  each); right: PV plasticity (unpaired t-test,  $t(8)=9.272$ ,  $P<0.0001$ ,  $n=5$  for each group).

**(c) Interference between different tasks (MWM learning and object recognition memory (FOR))** carried out during same 5h time unit only if they share one task-related element (red: platform same as one object; one-way ANOVA,  $F(2,12)=14.28$ ,  $P=0.0007$ , FOR; one-way ANOVA,  $F(2,12)=41.94$ ,  $P<0.0001$ , MWM, first; one-way ANOVA,  $F(2,12)=53.9$ ,  $P<0.0001$ ;  $n=5$  for each group).

**(d) Overcoming interference by single trial without platform in MWM learning** through further 4 trials with platform not achieved within same learning unit (unpaired t-test,  $t(8)=6.171$ ,  $P=0.0003$ ,  $n=5$  each group).

**(e) Behaviorally detectable improved performance in MWM learning** detected upon initiation of new learning unit (unpaired t-test,  $t(8)=4.588$ ,  $P=0.0018$ ,  $n=5$  each group).

### **Time unit for learning dependent on 5h network activity and cFos function.**

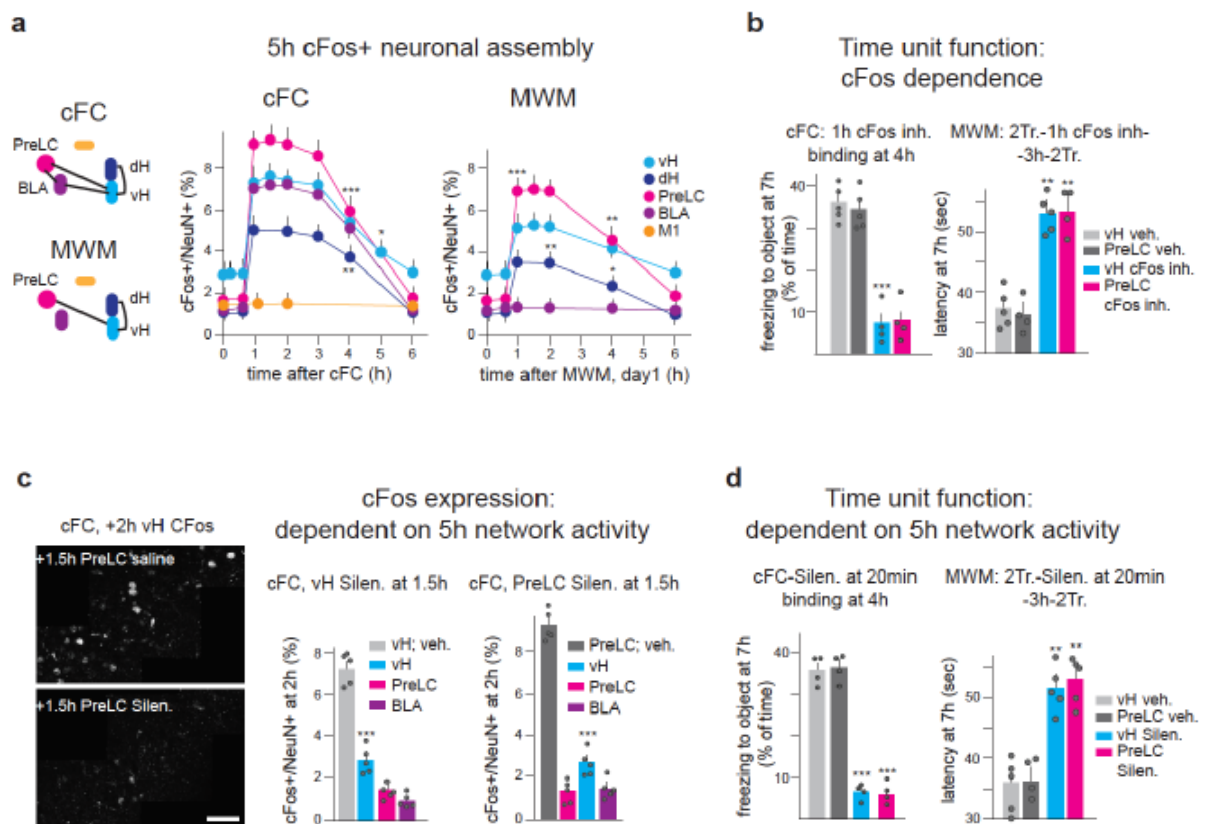
To investigate cellular and systems mechanisms that might underlie 5h time units for learning, we focused on the induction of cFos expression in brain regions

known to be involved in cFC<sup>19</sup> or MWM learning<sup>20</sup>. The immediate early gene and transcription factor cFos is a reporter of learning-related plasticity in neurons<sup>12,21</sup>, and activity in assemblies of learning-related cFos+ neurons is involved in memory recall<sup>8,9,22</sup>. For cFC<sup>19</sup>, we focused on ventral and dorsal hippocampus (vH, dH), basolateral amygdala (BLA) and prelimbic cortex (PreLC) (primary motor cortex (M1) as negative control; i.e. not implicated in this form of learning); for MWM<sup>20</sup> we focused on vH, dH and PreLC (BLA and M1 as negative controls) (Fig. 3a). Contents of cFos+/NeuN+ neurons in vH CA3 were markedly elevated 1h after cFC (Fig. 3a; Suppl. Fig. 4). Peak contents of cFos+ neurons were sustained from 1h to 3h, cFos values were still half-maximally elevated at 4h, and had returned to baseline cage control values at 6h (Fig. 3a; Suppl. Fig. 4). Comparable time courses of cFos induction and maintenance were detected in dH, BLA and PreLC, whereas no cFos induction was detected in M1 (Fig. 3a). Upon MWM learning, cFos induction up to 4-5h after training was detected in vH, dH, PreLC but not BLA (Fig. 3a). To determine whether cFos function might be causally involved in learning unit function, we inhibited cFos activity locally in vH or PreLC 1h after acquisition with a small-molecule compound that prevents transcriptional activity of cFos-containing AP1 complex<sup>23</sup>. Indeed, local treatment (Suppl. Fig. 5) with the cFos inhibitor was sufficient to suppress learning unit function (cFC, freezing to object; MWM, 2+2 trials; Fig. 3b).

In control experiments, freezing to context (as opposed to freezing to object) at 7h was not affected by vH cFos inhibition at 1h (Suppl. Fig. 6), consistent with the notion that cFos activity was specifically required for associative learning during the time unit for learning.

These findings raised the question of what might be the mechanisms underlying cFos+ neuronal assembly maintenance throughout brain regions used for learning a task. To determine whether network activity<sup>3,10</sup> might have a role in maintaining cFos expression and learning unit function throughout the 5h time window, we carried out silencing experiments in single brain regions implicated in the studied behavior. These experiments involved activation of local parvalbumin+ (PV+) inhibitory interneurons in PV-Cre mice through ligand-induced triggering of pharmacogenetic activator delivered locally (Suppl. Fig. 5)

through a Cre-dependent AAV<sup>5,24-26</sup>. Under these experimental conditions, silencing lasts about 30min<sup>25</sup>. Silencing vH any time from just after (5min) to 4h after acquisition of cFC led to rapid (within 15min) and complete loss of cFos in vH as well as throughout the memory network, including dH, BLA and PreLC (Fig. 3c; Suppl. Fig. 7). Likewise, silencing PreLC led to loss of cFos in PreLC, vH and BLA (Fig. 3c). Furthermore, silencing vH or PreLC 1h after acquisition also led to network-wide loss of cFos induced upon MWM learning (Suppl. Fig. 7). In control experiments, silencing M1 did not affect vH or PreLC cFos induced upon cFC, and silencing BLA did not affect cFos induced upon MWM learning (Suppl. Fig. 7). In parallel to system-wide loss of cFos, silencing vH or PreLC at +20min suppressed associative binding to fear memory at +4h (measured as freezing to object at 7h), and learning-unit function at 4h in the 2+2 trials MWM training protocol (Fig. 3d). Therefore, activity in distributed networks involved in learning is required during a 5h time window to prevent loss of cFos and of learning unit function.



Chowdhury and Caroni Fig. 3

**Figure 3. Time unit for learning dependent on 5h network activity and cFos function.**

**(a) Time course of cFos induction in systems involved in cFC or MWM learning.** Schematics on right: systems analyzed involved in cFC or MWM (connected by lines). cFC, vH:  $F(6, 39) = 30.33$  ( $n=11,7,5,10,4,4,5$ )  $p<0.0001$  for time points 0, 1, 2, 3, 4, 5, 6 hs; MWM, vH:  $F(4, 24) = 67.09$  ( $n=6, 9, 5, 5, 4$ )  $p<0.0001$  for time points 0, 1, 2, 4, 6 hs.

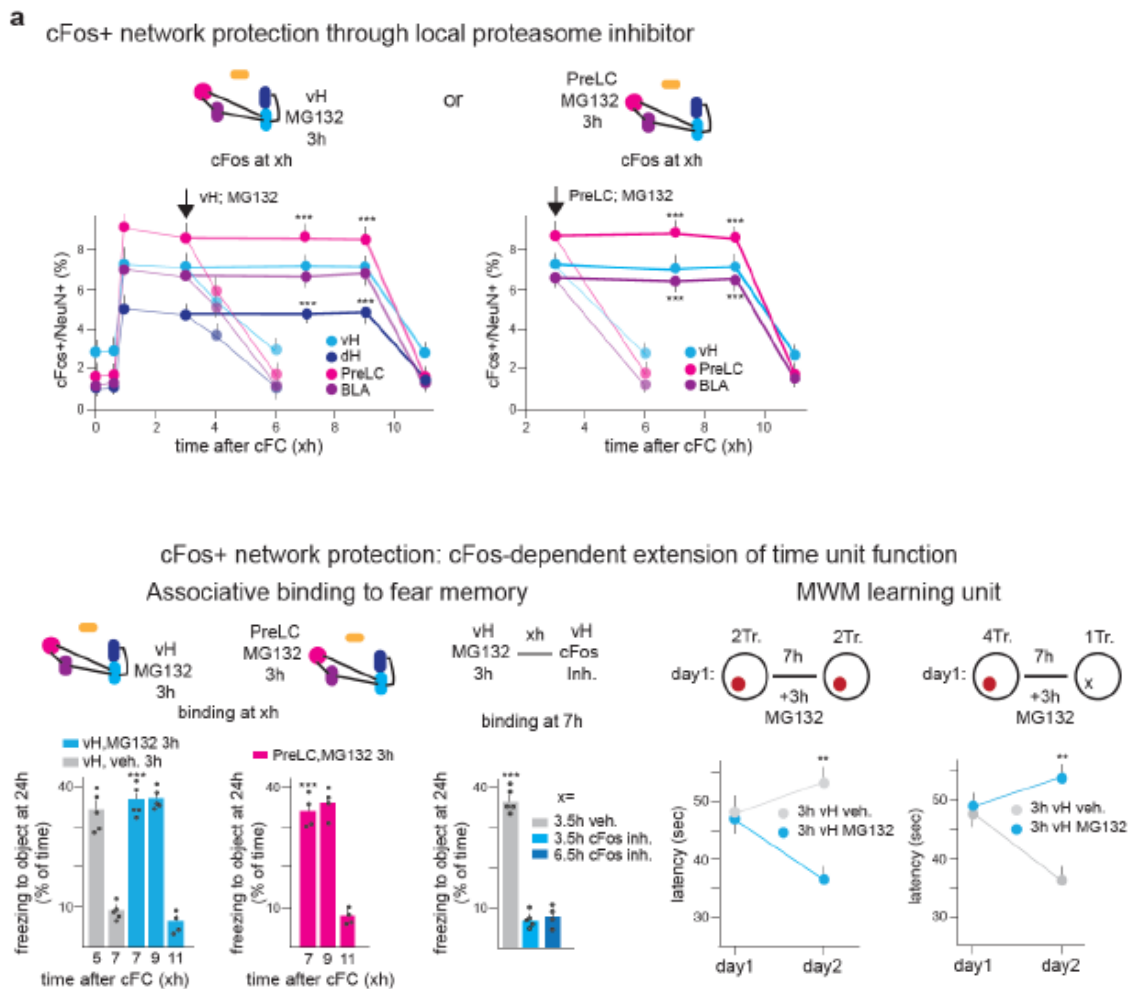
**(b) Inhibiting cFos activity 1h after acquisition locally in vH or PreLC prevents further time unit function in cFC and MWM learning.** cFos inh.: local delivery of cFos inhibitor; veh.: vehicle (cFC: one-way ANOVA,  $F(3,14)=29.05$ ,  $P<0.0001$ ,  $n=5,5,4,4$ ; MWM: one-way ANOVA,  $F(3,14)=17.62$ ,  $P<0.0001$ ,  $n=5,4,5,4$ ).

**(c, d) 5h network activity at systems used in learning required for system-wide cFos expression** (right: representative examples of vH cFos immunoreactivity with and without PreLC silencing; bar=50  $\mu\text{m}$ ; vH silencing: one-way ANOVA,  $F(3,16)=69.44$ ,  $P<0.0001$ ,  $n=5$  each; PreLC silencing: one-way ANOVA,  $F(3,16)=80.17$ ,  $P<0.0001$ ,  $n=5$  each) (c) and time unit function (cFC: one-way ANOVA,  $F(3,12)=104.8$ ,  $P<0.0001$ ,  $n=4$  each; MWM: one-way ANOVA,  $F(3,15)=11.02$ ,  $P=0.0004$ ,  $n=5,4,5,5$ ) (d). Silen.: local and reversible silencing of brain system through pharmacogenetic PV neuron activation.

**cFos-dependent extension of time unit for learning upon local inhibition of protein degradation.**

To further relate cFos expression in distributed neuronal assemblies to learning unit function, we sought to extend the duration of learning-induced cFos expression. Local blockade of protein synthesis<sup>27</sup> by delivery of Anisomycin 30min after acquisition led to loss of vH cFos induction at 60min (and any time thereafter), and to suppression of memory binding at +4h (Suppl. Fig. 8). However, local delivery of Anisomycin to vH at +1h failed to affect vH cFos levels at +2h and time unit function (Suppl. Fig. 8), suggesting that ongoing translation might not be critically important to maintain cFos expression<sup>28</sup> (but see Ref 29 for super-induction of cFos upon inhibition of translation as a possible alternative explanation for these findings). Indeed, local delivery of proteasome inhibitor MG132<sup>28,30</sup> to vH at +3h produced a long-lasting extension of elevated cFos+ neuron contents in vH, with values at +7h and at +9h that were comparable to those at +3h, and return to baseline values at +11h (Fig. 4a). Notably, local delivery of MG132 to vH also effectively extended learning related cFos expression in dH, BLA and PreLC (Fig. 4a). Likewise, MG132 delivery to PreLC extended cFos expression in PreLC and vH (Fig. 4a). In parallel to extension of cFos expression by local delivery of the proteasome inhibitor, the time window for

learning unit function as detected by binding to fear memory or by sufficient trials for MWM learning was now extended to up to +9h (Fig. 4b). Prevention of protein degradation with MG132 followed by local delivery of cFos inhibitor abolished binding to fear memory, indicating that the extended time window for memory binding depended on cFos expression and activity (Fig. 4b). Local interference with protein degradation also extended the time window during which a single interfering trial was sufficient to suppress MWM learning (Fig. 4b). Taken together, these results provided evidence that time units for learning can be extended in a cFos-dependent manner through local interference with protein degradation.



Chowdhury and Caroni Fig. 4

**Figure 4. cFos-dependent extension of time unit for learning upon local inhibition of protein degradation.**

**(a) Preventing protein degradation locally with proteasome inhibitor is sufficient to extend time window of cFos expression throughout the cFos network.** Local delivery of MG132 at 3h to vH (arrow, left; one-way ANOVA,  $F(4,35)=48.26$ ,  $P<0.0001$ ,  $n=11,9,5,9,6$ ) or PreLC (arrow, right; one-way ANOVA,  $F(4,24)=148.8$ ,  $P<0.0001$ , comparison between vehicle and MG132 at each time point,  $n=9,5,5,5,5$ ).

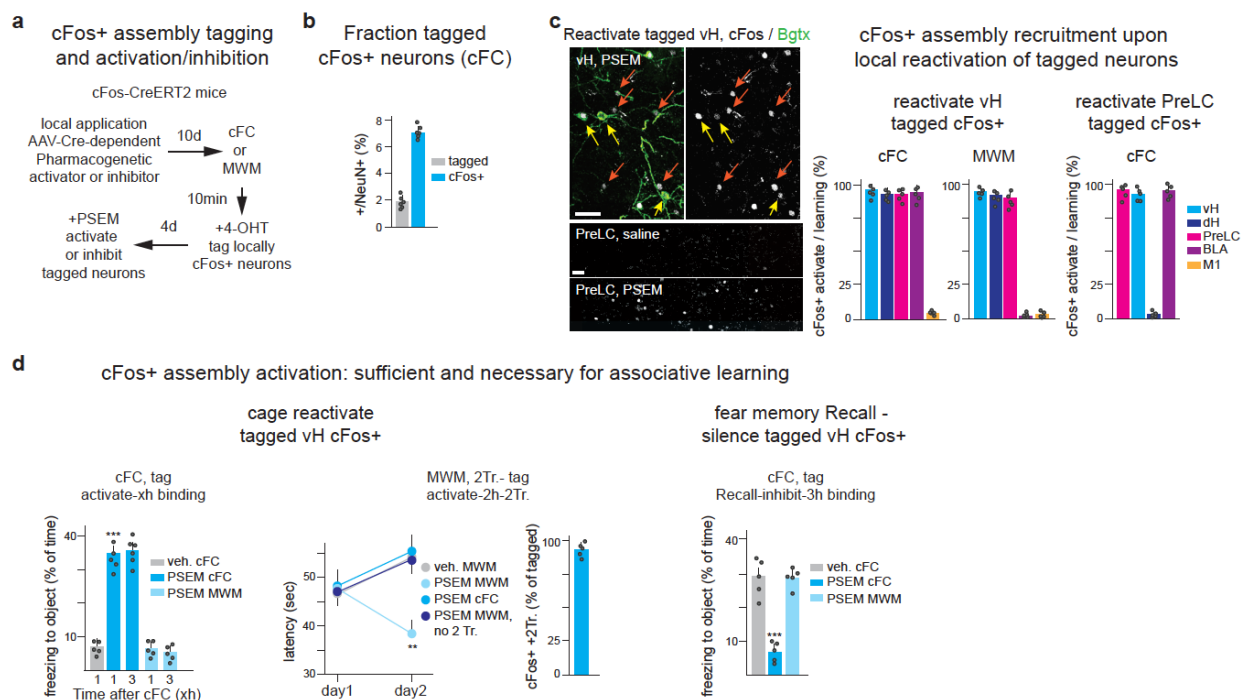
**(b) cFos-dependent extension of time unit function.** Left: extension of fear memory binding time unit by local delivery of proteasome inhibitor (one-way ANOVA,  $F(7,28)=52.16$ ,  $P<0.0001$ ,  $n=5,5,5,5,4,4,4,4$ ); compare to vH 3h vehicle and to 7h binding); center: cFos dependence of time unit extension (one-way ANOVA,  $F(2,11)=76.85$ ,  $P<0.0001$ ,  $n=5,5,4$ ); right: extension of time unit for trial completion (left) and for single trial interference in MWM learning (unpaired t-test;  $t(8)=4.96$ ,  $p=0.0011$  (left), and  $t(8)=5.942$ ,  $P=0.0006$  (right);  $n=5$  for each group).

### **Activity in local cFos+ neuronal assemblies sufficient and necessary for time unit function.**

To investigate the role of neuronal activity for time unit function specifically in learning-related cFos+ assemblies rather than generally in implicated brain regions, we carried out cFos assembly activation and inhibition experiments<sup>8,9,22</sup>. We tagged cFos+ neurons by delivery of hydroxy-Tamoxifen shortly after acquisition to activate Cre recombinase in mice expressing Tamoxifen-dependent CreERT2 in the cFos locus<sup>31</sup>. We combined these manipulations with previous local delivery (Suppl. Fig. 5) of AAV carrying Cre-dependent pharmacogenetic activator or inhibitor channels<sup>24</sup>, to activate or inhibit the learning-related cFos+ neurons (Fig. 5a). In these experiments, 16-22% of the total fraction of cFos+ neurons induced upon learning were labeled and hence accessed by the tagging procedure in vH or PreLC (Fig. 5b). Pharmacogenetic reactivation of tagged vH cFos+ fear memory neurons induced robust expression of cFos (to an extent up to 80-95% of the fraction of cFos+ neurons induced upon learning) in vH, dH, PreLC and BLA, but not M1 (Fig. 5c).

Likewise, reactivation of tagged PreLC cFos+ fear memory neurons induced robust expression of cFos (again up to 80-95% of the fraction of cFos+ neurons induced upon learning) in PreLC, vH and BLA (Fig. 5c). Whether, and to what extent, the cFos+ neurons induced upon reactivation of tagged neurons are identical to those originally expressing cFos upon acquisition remains to be determined (but see Fig. 5d). However, supporting specificity in cFos induction, pharmacogenetic reactivation of tagged vH MWM cFos+ neurons induced robust

expression of cFos in vH, dH, PreLC, but not BLA (Fig. 5c). Reactivation of vH cFos+ fear memory neurons in the home cage 4 days after cFC, followed 1h or 3h later by presentation of (object + odor) produced effective binding of fear memory to object (Fig. 5d). In control experiments, reactivation of vH MWM cFos+ memory neurons did not produce binding of fear memory to object, indicating that binding specifically involved activation of cFos+ fear memory neurons (Fig. 5d). In a second test, we tagged cFos+ neurons after 2 trials of MWM (Fig. 5d). Reactivation of those cFos+ MWM neurons in vH was sufficient to replace the first 2 trials in a new MWM time unit (Fig. 5d). Most (>90%) of the reactivated tagged cFos+ neurons were cFos+ upon 2 additional MWM trials (Fig. 5d). In control experiments, reactivation of cFC cFos+ neurons or omission of the subsequent 2 trials failed to produce MWM learning (Fig. 5d). Finally, in related experiments addressing necessity of cFos+ neurons for associative memory binding, recall of fear memory upon placing mice in training context reopened a time window for (object + odor) associative binding, which was suppressed by pharmacogenetic silencing of tagged vH cFos+ fear memory neurons (Fig. 5d). Taken together, these results provided evidence that activity in learning related cFos+ neuronal assemblies is sufficient and necessary for time unit function.



Chowdhury and Caroni Fig. 5



**Figure 5. Activity in local cFos+ neuronal assemblies sufficient and necessary for time unit function.**

**(a) Schematic of cFos+ neuron tagging and reactivation protocols.** 4-OHT: Tamoxifen derivative used in these experiments.

**(b) Fractions of tagged and total cFos+ neurons** upon cFC acquisition in vH. N=6 mice each.

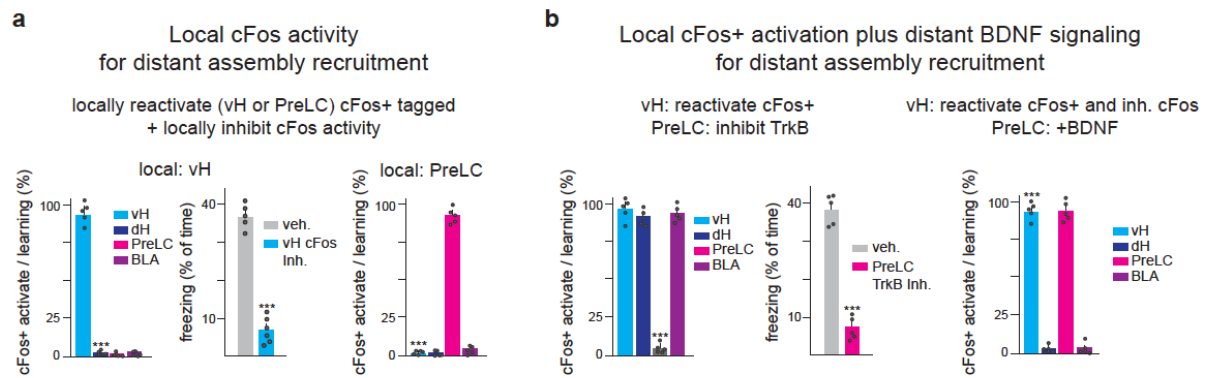
**(c) System-wide cFos+ neuronal assembly recruitment upon local reactivation of tagged cFos+ neurons.** Left: representative images of vH tagged neuron re-activation experiment; yellow arrows: tagged (Bgtx+) and cFos+ neurons; orange arrows: cFos+ neurons induced by activation of tagged neurons; bars: 40  $\mu$ m. N=5 mice for each group.

**(d) Role of cFos+ assembly re-activation and inhibition for time unit function.** Left: Reactivation of cFC (but not MWM) tagged vH cFos+ neurons is sufficient for associative fear memory binding (one-way ANOVA,  $F(4,22)=83.76$ ,  $P<0.0001$ ,  $n=5,6,6,5,5$ ); MWM learning: re-activating, four days later (now defined as day1), vH cFos+ neurons tagged after 2 trials is sufficient to replace the first 2 trials in MWM learning (one way ANOVA,  $F(3,16)=10.21$ ,  $P=0.0005$ ,  $n=5$  for each group); right: fraction of vH 2-trials MWM tagged neurons that are cFos+ after 2 more trials ( $n=5$  mice). Right: fear memory recall 4 days after acquisition reopens a time unit for memory binding, which is suppressed by inhibition of tagged cFos+ fear memory neurons (one-way ANOVA,  $F(2,12)=38.81$ ,  $P<0.0001$ ,  $n=5$  for each group).

**Distant assembly recruitment involving local cFos activity and distant BDNF signaling.**

To investigate the function of cFos protein in memory network recruitment and memory binding, we carried out cFos+ neuron tagging and reactivation experiments combined with local pharmacology experiments. Reactivation of tagged vH cFos+ fear memory neurons followed by local delivery of cFos inhibitor (block cFos transcriptional activity) to the same vH did not prevent robust induction (80-90% of the total fraction of cFos+ neurons induced upon cFC) of learning-related cFos+ neurons in vH (Fig. 6a). Notably, however, in the same experiments, local inhibition of cFos activity in vH prevented induction of cFos+ neurons in distant memory network systems such as PreLC, dH or BLA (Fig. 6a). In parallel, local inhibition of cFos in vH prevented re-induction of associative memory binding (Fig. 6a). Likewise, reactivation of tagged PreLC cFos+ fear memory neurons followed by local delivery of cFos inhibitor to PreLC did not prevent induction of learning-related cFos+ neurons in PreLC, but suppressed

distributed network cFos induction, e.g. in vH (Fig. 6a). Therefore, together with local memory network reactivation, local cFos activity is necessary to induce distant memory network induction and time unit function. To investigate the mechanisms through which cFos activity in local memory neurons might be necessary to induce distant memory network cFos expression upon local tagged neuron reactivation, we focused on the neurotrophin BDNF<sup>11,12</sup>. This growth factor has powerful roles in promoting learning-related plasticity<sup>12,32,33</sup>, and its presynaptic release depends on robust depolarization and calcium entry<sup>12-14,34</sup>. Furthermore, BDNF is required for long-lasting translation and synaptic plasticity during a 4-5h time window after acquisition<sup>33</sup>. Indeed, local delivery of a specific small-molecule inhibitor of the BDNF receptor TrkB<sup>35</sup> to PreLC prevented cFos expression specifically in PreLC upon reactivation of tagged vH cFos+ fear memory neurons (Fig. 6b). In parallel, and further supporting the notion that recruitment of the entire distributed memory network is required for binding, local delivery of the TrkB inhibitor suppressed memory binding in the vH tagged neuron reactivation experiment (Fig. 6b). Furthermore, consistent with the notion that local BDNF signaling is critically important for time unit function, delivery of TrkB inhibitor to PreLC 1h after cFC suppressed freezing to object at 7h in the associational fear memory binding experiment (Suppl. Fig. 9). To investigate whether BDNF might also be sufficient, together with network activity, for distant cFos+ neuron induction, we carried out BDNF delivery experiments. Indeed, local delivery of BDNF into PreLC rescued induction of cFos+ neurons specifically in PreLC upon reactivation of tagged vH cFos+ fear memory neurons when local vH cFos activity was inhibited (Fig. 6b). In control experiments, although BDNF by itself did induce some cFos+ neurons, it was not sufficient to induce an amount of cFos+ neurons comparable to fear memory-associated cFos+ neuron expression in PreLC in the absence of pharmacogenetic ligand to activate tagged vH cFos+ fear memory neurons (Suppl. Fig. 9). Together, these results are consistent with the notion that the activity of cFos in activated local memory neurons is critically important to mediate distant memory network recruitment through activity-dependent BDNF signaling in distant target regions.



Chowdhury and Caroni Fig. 6

**Figure 6. Distant assembly recruitment involving local cFos activity and distant BDNF signaling.**

**(a) Local re-activation of tagged cFos+ neurons, combined with local inhibition of cFos activity prevents network-wide recruitment of cFos+ neurons without affecting local recruitment** (local vH: one-way ANOVA,  $F(3,16)=207.7$ ,  $P<0.0001$ ,  $n=5$  each; local PreLC: one-way ANOVA,  $F(3,16)=289.3$ ,  $P<0.0001$ ,  $n=5$  each). Center: absence of network-wide cFos recruitment prevents time unit function (unpaired t-test,  $t(9)=10.17$ ,  $P<0.0001$ ,  $n=5,6$ ).

**(b) Role of BDNF signaling for distant cFos+ neuron recruitment.** Left: local re-activation of tagged cFos+ neurons in vH, combined with local delivery of TrkB inhibitor to PreLC specifically prevents induction of cFos expression in PreLC (one-way ANOVA,  $F(3,16)=139.7$ ,  $P<0.0001$ ,  $n=5$  each) and time unit function (unpaired t-test,  $t(8)=8.525$ ,  $P<0.0001$ ,  $n=5$  each). Right: local delivery of BDNF to PreLC is sufficient to disinhibit cFos induction upon local re-activation of tagged vH cFos+ neurons, combined with local inhibition of cFos activity in vH (one-way ANOVA,  $F(3,16)=199.2$ ,  $P<0.0001$ ,  $n=5$  each).

## 2.1.4 Discussion

We have shown that learning processes consist of dedicated 5h time units, during which sufficient numbers of trials need to be carried out in order to produce learning, and individual shared learning-relevant elements are sufficient to combine otherwise unrelated behavioral experience, and to interfere with learning (Supplementary Fig. 10). Learning unit function depended critically on sustained competence by specific system-wide assemblies of cFos expressing neurons, ensured through neuronal network activity, cFos protein expression and BDNF signaling in used brain structures.

## **Activity in system-wide cFos+ learning-related network for time unit function**

Activity throughout brain structures used in the particular learning was critically important to maintain cFos expression and time unit function. Whether and in what way the ongoing distributed network activity was a specific consequence of learning remains to be determined. In principle, however, network activity might initiate spontaneously at any part of the network, e.g. as ripples or spindles<sup>3,10,36</sup>, and might then recruit and maintain system-wide networks in a cFos-dependent manner, e.g. through enhanced neuronal excitability and BDNF signaling. Notably, reactivating subsets of local cFos+ neurons was sufficient to recruit learning-specific system-wide assemblies for time unit function, providing a potential mechanism through which partial memory recall might open up a new time unit for further learning. Our results are in good agreement with the notion that cell assemblies involved in learning and memory consist of interconnected neurons in multiple brain systems<sup>8,9,22</sup>.

Our findings are further consistent with the notion that the 5h time unit coincides with a time window during which memories can be linked through a shared neural ensemble<sup>6,7</sup>. Accordingly, our findings suggest that facilitated memory ensemble merging during about 5h upon acquisition<sup>6,7</sup> might be a key mechanism in learning, underlying integration of validated, related information to ensure learning, and preventing learning of spuriously or inconsistently linked experiences.

Our results provide evidence as to the mechanisms critically important to sustain time unit function during and beyond 5h. We suggest that time unit function involves protracted processes of system-wide formation, active off-line maintenance and evidence-driven modification of cFos+ neuronal assemblies ensured through network wide activity and coordinated throughout specific circuitry by cFos and BDNF activity (Supplementary Fig. 10). The endogenous mechanisms that limit time unit function to about 5h remain to be determined. However, the sharp termination at 5-6h seems to argue against the possibility that learning unit function just reflects enhanced excitability of learning-related neurons since that plasticity was shown in past work to be maximal 24h after

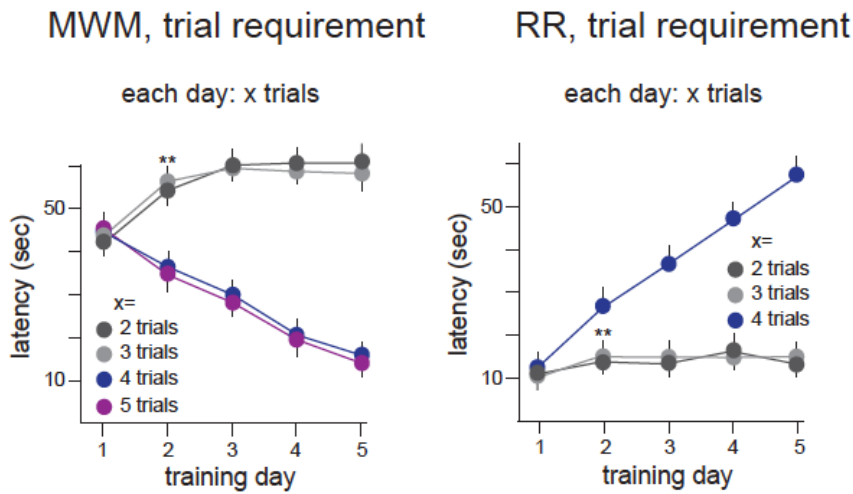
acquisition<sup>37,38</sup>. Our results further suggest that a major role of cFos expression induced upon learning is to implement time unit function through neuronal assembly maintenance. On the other hand, our findings do not exclude the possibility that plasticity induced during the 5h time window, and involving cFos expression and function, might have additional roles in learning and memory, e.g. as a prerequisite for long-term memory consolidation<sup>5,32</sup>.

### **Roles of dedicated 5h time units for learning**

Our study uncovers remarkable implications of the dedicated 5h time units on learning. This included a dramatic sensitivity to learning-related but contradicting information during a 5h time window after initial learning. In unfavorable cases, the high sensitivity to inconsistent associations might interfere with efficient learning. On the other hand, in addition to providing opportunities for validation in learning, a key advantage of the sensitivity to interference might involve preventing linkage of unrelated information in memory, a process that might majorly interfere with adaptive behavior and cognition. Future studies should define the molecular/cellular and circuit mechanisms that suppress learning in the presence of inconsistent information, and their possible impairment in conditions affecting mental health.

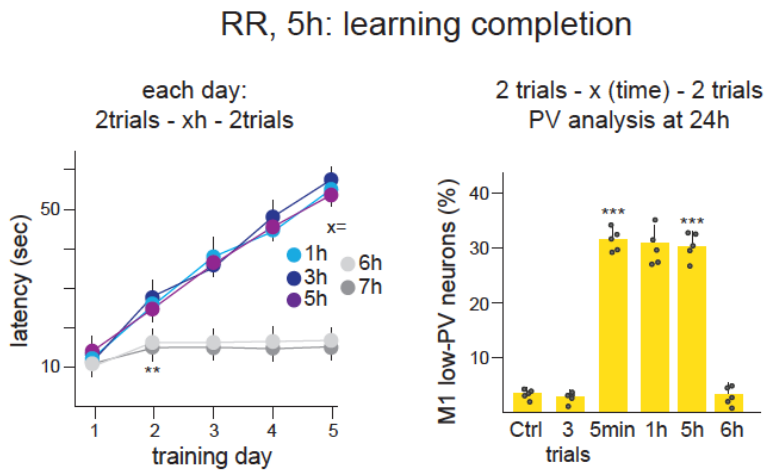
That a single interfering episode was sufficient to disrupt learning, and that additional successful trials within the same time unit failed to rescue learning suggests that learning within the time unit does not resemble a process of quantitative evidence evaluation<sup>39</sup>. Instead, these observations suggest that, within the time unit, learning involves goal definition (i.e. learning content) through associative merging, mechanisms that link sufficient interactions with the task to thresholds for learning, and mechanisms that suppress learning upon contradicting evidence. We also provide evidence that exhibiting learning-related improved performance requires the initiation of a new time unit. Accordingly, the time units for learning uncovered in this study might represent basic elements of a broader scheme to effectively and independently manage the identity of the learning content that enters memory networks in the brain.

## 2.1.5 Supplementary Figures



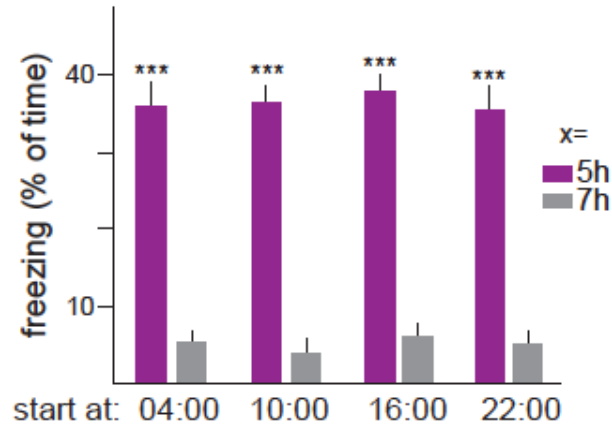
Chowdhury and Caroni Suppl. Fig.1

**Suppl. Fig 1. Daily trial number requirements in water maze and rotarod learning under our experimental conditions.** Left: Morris water maze learning; right: Rotarod learning. Learning curves as a function of daily trial numbers.  $P=0.002$ ,  $P=0.006$  \*\*,  $n=5$  mice each.



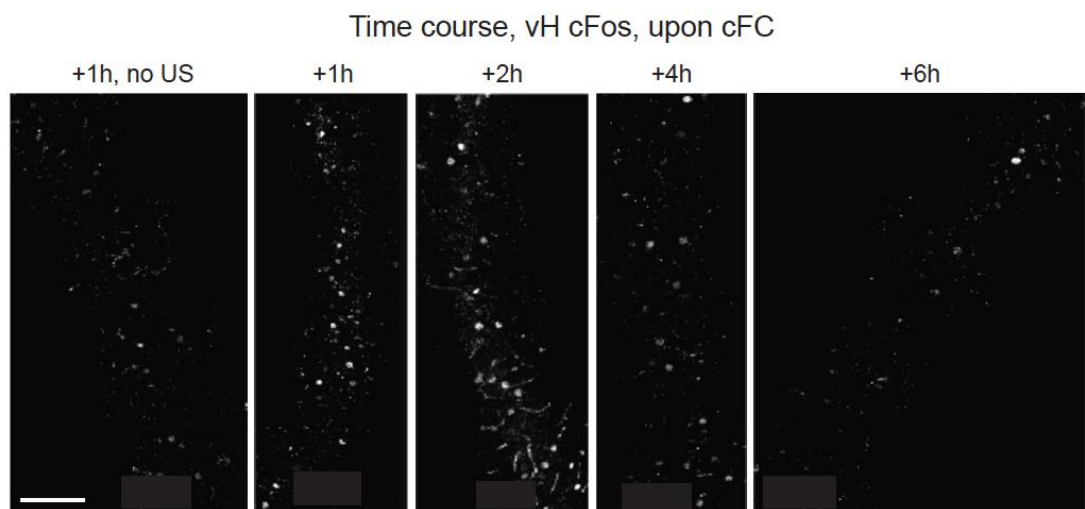
Chowdhury and Caroni Suppl. Fig.2

**Suppl. Fig 2. Time unit for learning in rotarod training.** x: numbers of hours between first and second group of 2 trials; right: PV plasticity (low-PV contents in M1 at 24h).  $P=0.008$  \*\* (left),  $P<0.0001$  (right),  $n=5$  mice each.



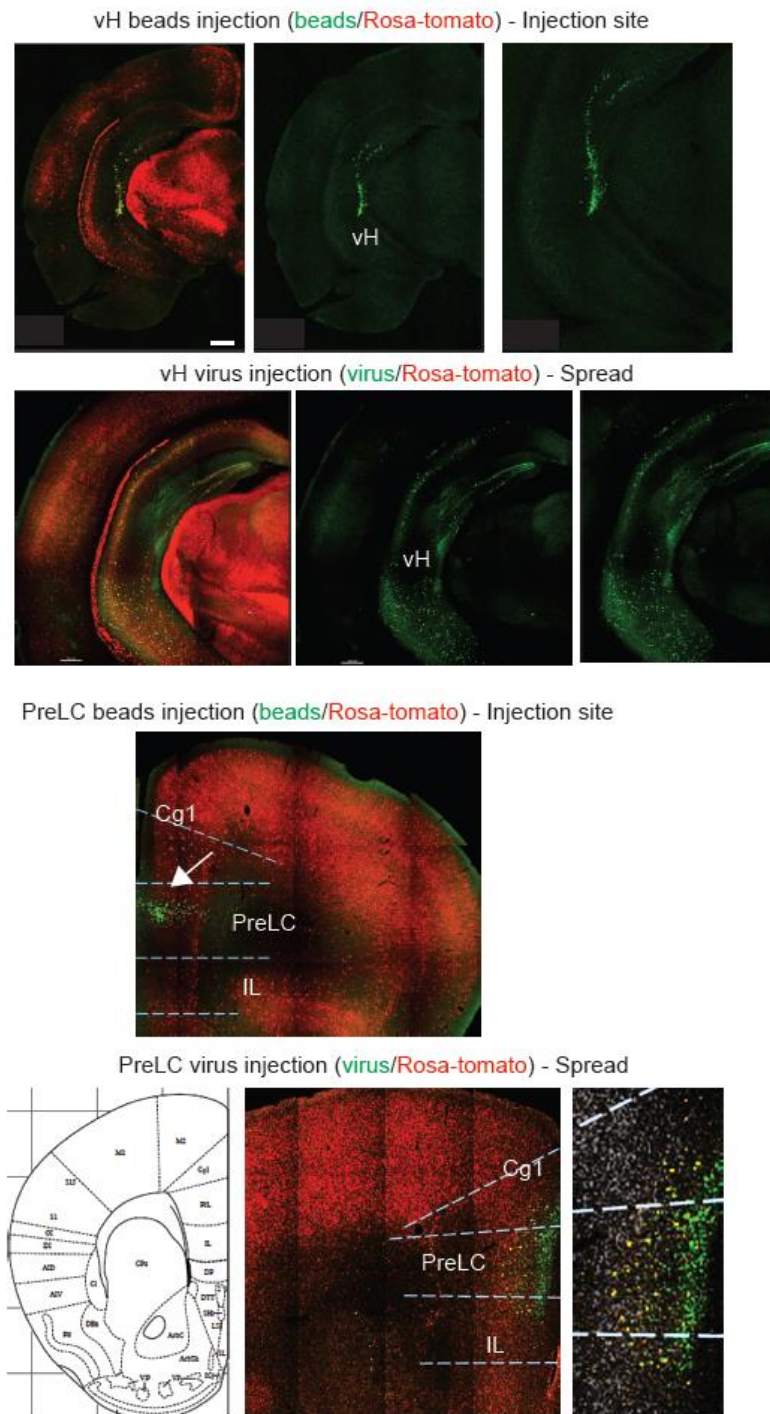
### Chowdhury and Caroni Suppl. Fig.3

**Suppl. Fig 3. The duration of the time unit for learning is not affected by the time of the day at which learning is initiated.** Associational binding to fear memory; experimental conditions as in Fig. 1b;  $P < 0.0001$ ,  $n = 5$  mice each.



Chowdhury and Caroni Suppl. Fig.4

**Suppl. Fig 4. Time course of cFos expression in vH upon cFC.** Representative examples of data as shown in Fig. 3a; vH CA3. Bar: 100  $\mu$ m.

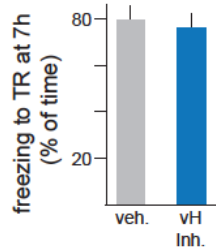


Chowdhury and Caroni Suppl. Fig.5

**Suppl. Fig 5. Local delivery of AAV to vH and to PreLC.** Representative examples of local treatment experiments as applied throughout the study. Beads: fluorescent beads to visualize injection site (arrow in PreLC); Virus: Bungarotoxin signal; Rosa-tomato: global histology marker. Right panels: higher magnification of images shown in left and center panels. Bar: 500  $\mu$ m.



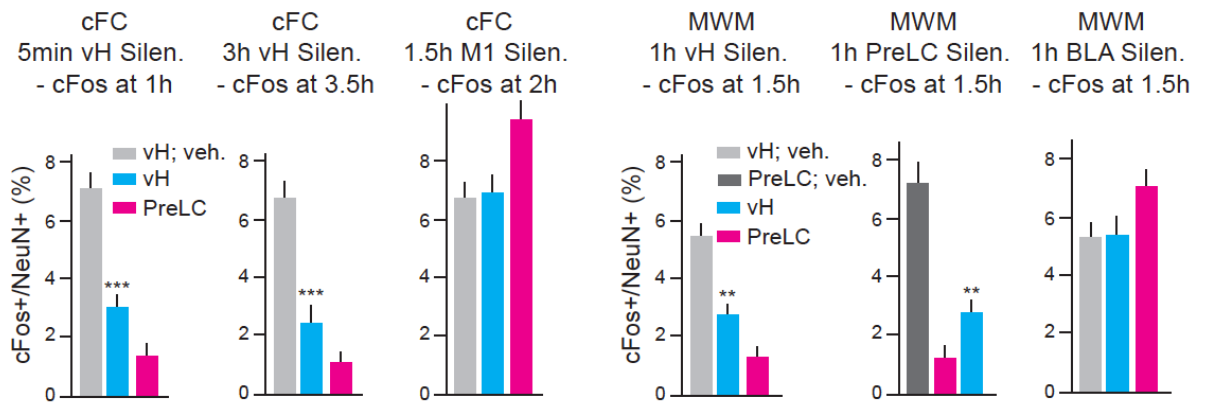
cFC(TR)-1h vH Inh.  
freezing to TR at 7h



Chowdhury and Caroni Suppl. Fig.6

**Suppl. Fig 6.** Preventing binding to fear memory through vH inhibition at 1h does not interfere with fear memory to context as tested at 7h. N=5 mice each.

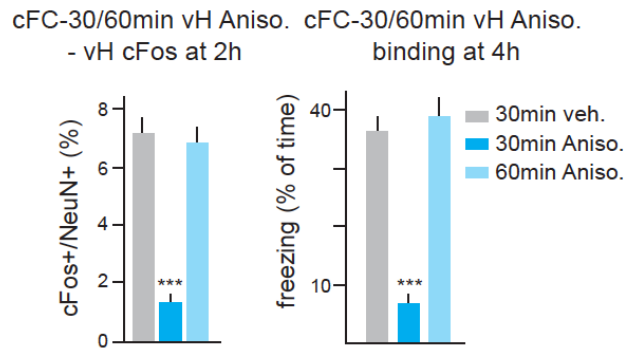
Network activity for sustained cFos expression



Chowdhury and Caroni Suppl. Fig.7

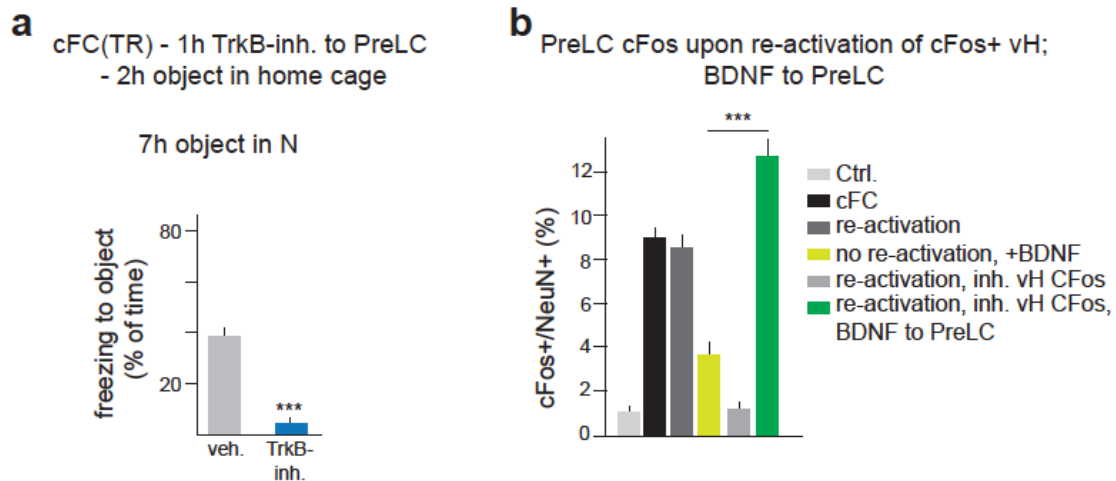
**Suppl. Fig 7. Network activity for sustained cFos expression.** Left panels: Silencing vH at 5min or 3h upon cFC produces network-wide loss of cFos protein; in control experiments, silencing M1 at 1.5h does not affect cFos expression upon cFC. Right panels: Silencing vH or PreLC, but not BLA, at 1h upon MWM learning produces network-wide loss of cFos protein at 1.5h. P=0.0006, 0.0005, 0.003, 0.001; n=5 mice each.

## cFos expression: translation



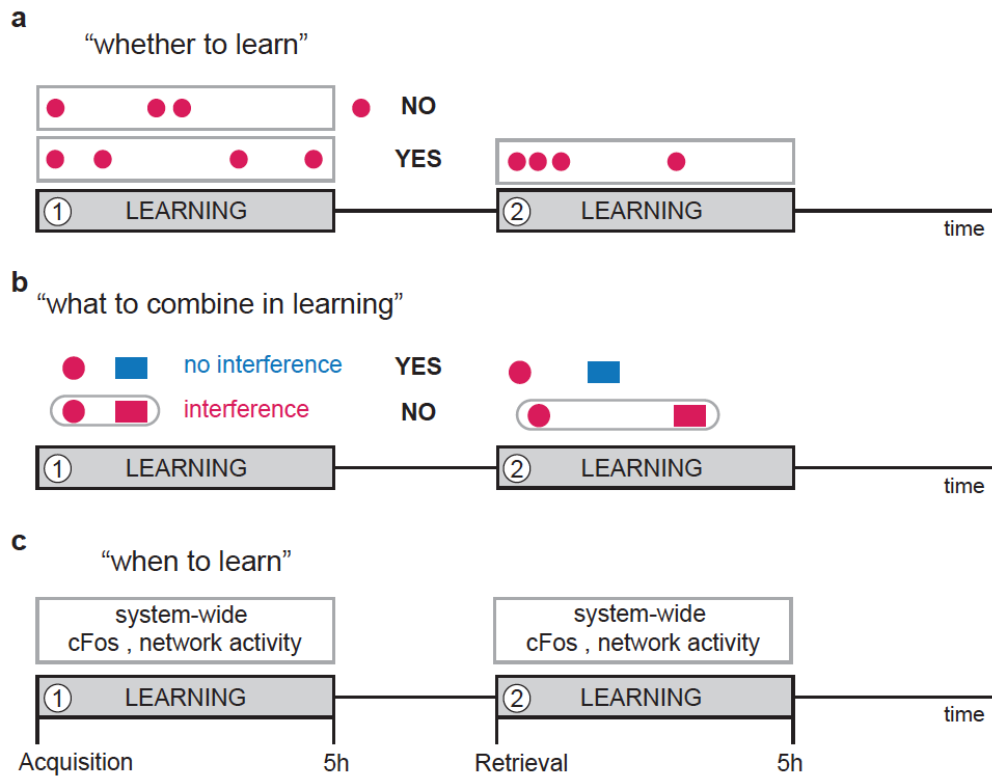
## Chowdhury and Caroni Suppl. Fig.8

**Suppl. Fig 8.** Anisomycin interferes with cFos expression and time unit function when delivered 30min but not 60min after acquisition.  $P < 0.0001$ ;  $n=5$  for each group.



## Chowdhury and Caroni Suppl. Fig.9

**Suppl. Fig 9. Role of local BDNF signaling for time unit function and distant cFos induction.** (a) Local TrkB signaling during time unit for learning is critically important for time unit function.  $P=0.0002$ ,  $n=5$  each. (b) cFos+ neuron contents in PreLC 1.5h after reactivation of tagged vH cFos+ neurons; vH cFos inhibitor and PreLC BDNF were delivered within 30min from tagged vH cFos+ neuron reactivation. Note how local delivery of BDNF to PreLC in the absence of tagged vH cFos+ neurons reactivation only induced a modest increase in cFos+ neuron contents in PreLC.  $P < 0.0001$ ;  $n=5$  for each group.



Chowdhury and Caroni Suppl. Fig. 10

**Suppl. Fig 10. Time units for learning involving maintenance of system-wide cFos expression in neuronal assemblies.** (a) Within 5h time units for learning (1, 2) sufficient trials need to be executed (red circles) to determine whether learning occurs (no/yes). (b) Within the time units, learning-related shared features are associated to determine what to learn; associations (red circle/red square), if leading to contradictions, can produce interference, disrupting learning within the time unit. (c) Induction (acquisition) and maintenance of network activity and cFos expression in distributed brain systems involved in the particular type of learning determine when to learn. Subsequent time units can be initiated upon memory retrieval, which is followed by expression of cFos in learning-related neuronal assemblies.

## 2.1.6 Acknowledgments

We thank S. Arber (FMI) for valuable comments on the manuscript and for reagents, Kerstin Leptien (FMI) for assistance with some of the analysis, and Smitha Karunakaran (FMI) for the first interference experiments in cFC. A.C. was supported by the Swiss National Science Foundation. The Friedrich Miescher Institut is part of the Novartis Research Foundation.

### 2.1.7. Author contributions

A.C. devised carried out and analyzed all experiments; P.C. helped devise the experiments and wrote the manuscript. All authors discussed the results and commented the manuscript.

### 2.1.8 References

- 1 Botvinick, M.M. Hierarchical reinforcement learning and decision making. *Curr.Opin. Neurobiol.* **22**, 956-62 (2012).
- 2 Smolen, P., Zhang, Y. & Byrne, J. H. The right time to learn: mechanisms and optimization of spaced learning. *Nat. Rev. Neurosci.* **17**, 77-88 (2016).
- 3 Robertson, E.M., Pascual-Leone, A., & Miall, R.C. Current concepts in procedural consolidation. *Nat. Rev. Neurosci.* **5**, 576-582 (2004).
- 4 Menzel, R., Manz, G., Menzel, R. & Greggers, U. Massed and spaced learning in honeybees: the role of CS, US, the intertrial interval, and the test interval. *Learn.Mem.* **8**, 198-208 (2001).
- 5 Karunakaran, S., et al. PV plasticity sustained through D1/5 dopamine signaling required for long-term memory consolidation. *Nature Neurosci.* **19**, 454-464 (2016).
- 6 Cai, D. J. et al. A shared neural ensemble links distinct contextual memories encoded close in time. *Nature* **534**, 115-118 (2016).
- 7 Rashid, A. J. et al. Competition between engrams influences fear memory formation and recall. *Science* **353**, 383-387 (2016).
- 8 Josselyn, S. A., Köhler, S. & Frankland, P. W. Finding the engram. *Nat. Rev.Neurosci* **16**, 521-34 (2015).
- 9 Holtmaat, A., & Caroni, P. Functional and structural underpinnings of neuronal assembly formation in learning. *Nature Neurosci.* **19**, 1553-1562 (2016).
- 10 Carr, M.F., Jadhav, S.P., & Frank, L.M. Hippocampal replay in the awake state: a potential substrate for memory consolidation and retrieval. *Nature Neurosci.* **14**, 147-153 (2011).

- 11 Sheng, M. & Greenberg, M.E. The regulation and function of c-fos and other immediate early genes in the nervous system. *Neuron* **4**, 477-485 (1990).
- 12 Flavell, S. W. & Greenberg, M. E. Signaling mechanisms linking neuronal activity to gene expression and plasticity of the nervous system. *Ann. Rev. Neurosci.***31**, 563-90 (2008).
- 13 Kuzniewska, B., Rejmak, E., Malik, A.R., Jaworski, J., Kaczmarek, L. & Kalita, K. Brain-derived neurotrophic factor induces matrix metalloproteinase 9 expression in neurons via the serum response factor/c-Fos pathway. *Proc. Natl. Acad. Sci. U.S.A.***33**, 2149-2162 (2013).
- 14 Joo, J.-Y., Schaukowitch, K., Farbiak, L., Kilaru, G. & Kim, T.-K. Stimulus specific combinatorial functionality of neuronal c-fos enhancers. *Nature Neurosci.* **19**, 75-83 (2016).
- 15 Morris, R. Development of a water-maze procedure for studying spatial learning in the rat. *J. Neurosci. Methods.* **11**, 47-60 (1984).
- 16 Buitrago, M.M., Schultz, J.B., Dichgans, J., & Luft, A.R. Short and long-term motor skill learning in an accelerated rotarod training program. *Neurobiol. Learn. Mem.* **81**, 211-216 (2004).
- 17 Ruediger, S., Spirig, D., Donato, F. & Caroni, P. Goal-oriented searching mediated by ventral hippocampus early in trial-and-error learning. *Nature Neurosci.* **15**, 1563-1571 (2012).
- 18 Donato, F., Rompani, S. B. & Caroni, P. Parvalbumin-expressing basket-cell network plasticity induced by experience regulates adult learning. *Nature* **504**, 272-276 (2013).
- 19 Maren, S., Phan, K.L., & Liberzon, I. The contextual brain: implications for fear conditioning, extinction and psychopathology. *Nat. Rev. Neurosci.* **14**, 417-428 (2013).
- 20 Chersi, F., & Burgess, N. The cognitive architecture of spatial navigation: hippocampal and striatal contributions. *Neuron* **88**, 64-77 (2015).

- 21 Minatohara, K., Akiyoshi, M. & Okuno, H. Role of immediate-early genes in synaptic plasticity and neuronal ensembles underlying the memory trace. *Front. Mol. Neurosci.* **8**, 78 (2015).
- 22 Liu, X., et al. Optogenetic stimulation of a hippocampal engram activates fear memory recall. *Nature* **484**, 381-385 (2012).
- 23 Aikawa, Y. et al. Treatment of arthritis with a selective inhibitor of cFos/activator protein-1. *Nature Biotechnol.* **26**, 817-823 (2008).
- 24 Sternson, S. M. & Roth, B. L. Chemogenetic tools to interrogate brain functions. *Ann. Rev. Neurosci* **37**, 387-407 (2014).
- 25 Kato, H.K., Gillet, S.N., Peters, A.J., Isaacson, J.S. & Komiyama, T. Parvalbumin-expressing interneurons linearly control olfactory bulb output. *Neuron* **80**, 1218-1231 (2014).
- 26 Li, N., Chen, T.-W., Guo, Z.V., Gerfen, C.R., & Svoboda, K. A motor cortex circuit for motor planning and movement. *Nature* **519**, 51-56 (2015).
- 27 Rossato, J. I. et al. On the role of hippocampal protein synthesis in the consolidation and reconsolidation of object recognition memory. *Learn. Mem.* **14**, 36-46 (2007).
- 28 Basbous, J., Jariel-Encontre, I., Gomard, T., Bossis, G. & Piechaczyk, M. Ubiquitin-independent- versus ubiquitin-dependent proteasomal degradation of the c-Fos and Fra-1 transcription factors: is there a unique answer? *Biochimie* **90**, 296-305 (2008).
- 29 Edwards, D.R. & Mahadevan, L.C. Protein synthesis inhibitors differentially superinduce c-fos and c-jun by three distinct mechanisms: lack of evidence for labile repressors. *EMBO J.* **11**, 2415-1424 (1992).
- 30 Lee, D.H., & Goldberg, A.L. Proteasome inhibitors: valuable new tools for cell biologists. *Trends Cell Biol.* **8**, 397-403 (1998).
- 31 Guenther, C. J., Miyamichi, K., Yang, H. H., Heller, H. C. & Luo, L. Permanent genetic access to transiently active neurons via TRAP: targeted recombination in active populations. *Neuron* **78**, 773-784 (2013).

- 32 Bekinschtein, P. et al. Persistence of long-term memory storage requires a late protein synthesis- and BDNF- dependent phase in the hippocampus. *Neuron* **53**, 261-277 (2007).
- 33 Leal, G., Comprido, D., & Duarte, C.B. BDNF-induced local protein synthesis and synaptic plasticity. *Neuropharmacology* **76**, 639-656 (2014).
- 34 Walsh, J. J. et al. Stress and CRF gate neural activation of BDNF in the mesolimbic reward pathway. *Nature Neurosci.* **17**, 27-29 (2014).
- 35 Cazorla, M. et al. Identification of a low-molecular weight TrkB antagonist with anxiolytic and antidepressant activity in mice. *J. Clin. Invest* **121**, 1846-1857 (2011).
- 36 Carr, M.F., Karlsson, M.P., & Frank, L.M. Transient slow gamma synchrony underlies hippocampal memory replay. *Neuron* **75**, 700-713 (2012).
- 37 Moyer, J.R., Thompson, L.T., & Disterhoft, J.F. Trace eyeblink conditioning increases CA1 excitability in a transient and learning-specific manner. *J. Neurosci.* **16**, 5536-5546 (1996).
- 38 Disterhoft, J.F. & Oh, M.M. Learning, aging and intrinsic neuronal plasticity. *Trends Neurosci.* **29**, 587-599 (2006).
- 39 Shadlen, M.N., & Kiani, R. Decision making as a window on cognition. *Neuron* **80**, 791-806 (2013).

## 2.2

# **PV plasticity sustained through D1/5 dopamine signaling required for long-term memory consolidation**

Smitha Karunakaran<sup>\*</sup>, Ananya Chowdhury<sup>\*</sup>, Flavio Donato, Charles Quairiaux, Christoph M Michel and Pico Caroni

Published: Nature Neuroscience

Nat. Neurosci. 19, 454–464 (2016)

<sup>\*</sup> Equal contribution



### **2.2.1 Summary**

Long-term consolidation of memories depends on processes occurring many hours after acquisition. Whether this involves plasticity that is specifically required for long-term consolidation remains unclear. We found that learning-induced plasticity of local parvalbumin (PV) basket cells was specifically required for long-term, but not short/intermediate-term, memory consolidation in mice. PV plasticity, which involves changes in PV and GAD67 expression and connectivity onto PV neurons, was regulated by cAMP signaling in PV neurons. Following induction, PV plasticity depended on local D1/5 dopamine receptor signaling at 0–5 h to regulate its magnitude, and at 12–14 h for its continuance, ensuring memory consolidation. D1/5 dopamine receptor activation selectively induced DARPP-32 and ERK phosphorylation in PV neurons. At 12–14 h, PV plasticity was required for enhanced sharp-wave ripple densities and c-Fos expression in pyramidal neurons. Our results reveal general network mechanisms of long-term memory consolidation that requires plasticity of PV basket cells induced after acquisition and sustained subsequently through D1/5 receptor signaling.

### **2.2.2 Introduction**

Memories ensure that what is learned and might be important will be available for later retrieval following appropriate cues<sup>1,2</sup>. Synaptic plasticity can be triggered in seconds, long-term potentiation of synaptic transmission in minutes and the emergence of new synapses in 1–2 h, but long-term consolidation of memories is also regulated by late protein synthesis, BDNF and local dopamine (DA) D1/5 receptor signaling about 12 h after acquisition<sup>3,4</sup>. The mechanisms that couple learning at the time of acquisition to long-term consolidation of memories 12 h later are poorly understood. Their elucidation should provide fundamental insights into how learning and memory produce adaptive behavior.

Memories are subdivided into short- (up to 30 min), intermediate- (hours) and long-term (days to years) memories<sup>1</sup>. Short-term memories do not depend on de novo gene expression and protein synthesis, whereas long-term memories depend on de novo transcription and, presumably, on the establishment of new functional synapses<sup>1,5</sup>. Mechanistic studies of learning and memory have focused on sequences of synaptic and cellular plasticity processes, suggesting that

cascades of memory consolidation processes starting at the time of acquisition might gradually lead from short- to intermediate- and long-term consolidation of memories<sup>1,3-8</sup>. However, whether early consolidation processes are required for long-term consolidation and which early processes might be important for late long-term consolidation have remained unclear. In parallel with plasticity processes initiated at the time of acquisition at individual synapses and neurons, ensembles of synapses and neurons specifically involved in learning can be recruited again through local and system-wide network events that are thought to involve replay of learned sequences<sup>9-12</sup>. Replay processes have been shown to occur during quiet wakefulness and during non-REM sleep, and they are thought to have important roles in memory consolidation<sup>13-19</sup>. Such off-line network replay processes might provide attractive candidate mechanisms for influencing synaptic plasticity processes up to many hours after acquisition.

PV-positive basket cells are abundant GABAergic inhibitory interneurons that provide powerful feedforward and feedback inhibition to somas and proximal dendrites of principal neurons, and have important roles in shaping network oscillations, including ripples, spindles and long-range neuronal synchronization<sup>20-26</sup>. PV neurons are critical for enhancing cortical functions and regulate plasticity<sup>27-29</sup>. It recently became apparent that local PV basket cells exhibit marked plasticity following behavioral learning in the adult<sup>30</sup>. Incremental learning (defined here as learning involving gradual acquisition of task-related information to improve behavioral performance), for example, in Morris water maze (MWM) or rotarod training, leads to large increases in the fraction of PV basket cells expressing low levels of PV and GAD67 and receiving high densities of inhibitory synaptic puncta (designated here as low-PV plasticity). By contrast, definite learning (defined here as learning leading to adherence to validated rules), for example, following contextual fear conditioning (cFC) or at completion of MWM or rotarod learning, leads to large increases in the fraction of PV basket cells expressing high levels of PV and GAD67 and receiving high densities of excitatory synaptic puncta (designated here as high-PV plasticity)<sup>30</sup>. These opposite forms of PV neuron plasticity are implemented by two distinct subpopulations of PV basket cells that are defined by their distinct time lines of neurogenesis<sup>31</sup>. Thus, early-born PV basket cells specifically exhibit plasticity

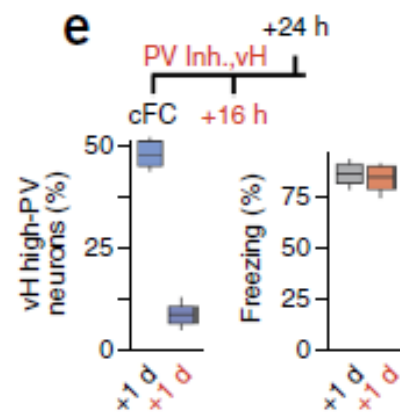
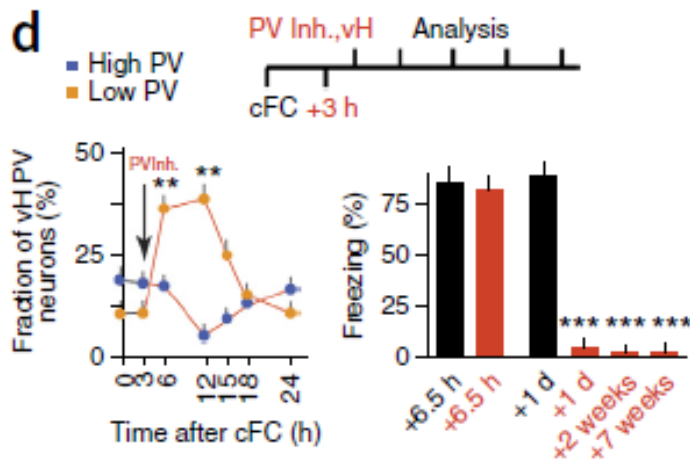
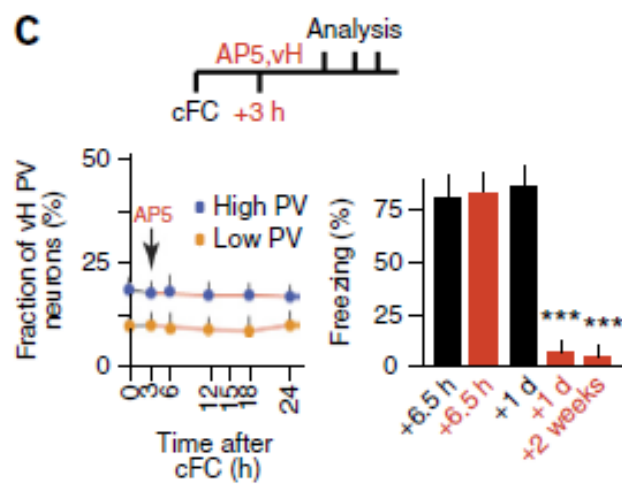
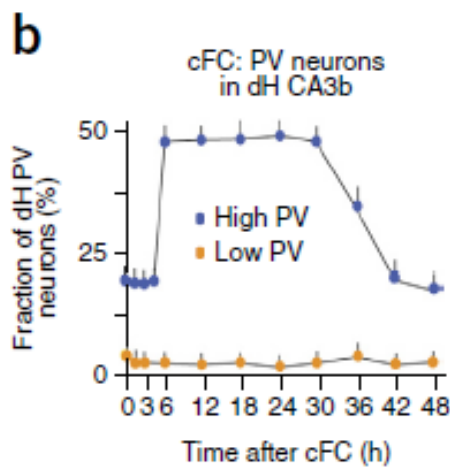
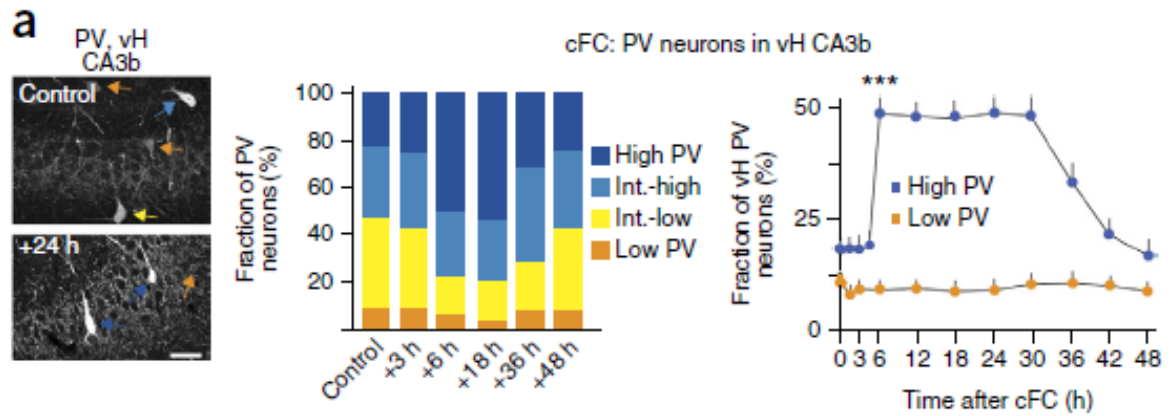
following definite learning, whereas late-born PV basket cells specifically exhibit plasticity following incremental learning<sup>31</sup>. Furthermore, plasticity in early-born PV neurons is specifically regulated through changes in excitation, whereas plasticity in late-born PV neurons is specifically regulated through changes in inhibition<sup>31</sup>. In spite of the extent and behavioral specificity of this plasticity, its role in learning and memory remains unclear. Given the importance of PV basket cells in modulating network activities, their learning-related plasticity might provide an attractive mechanism for influencing local network events during memory consolidation processes.

We investigated circuit mechanisms of long-term memory consolidation, focusing on the time line of relevant plasticity processes after acquisition, and the possible role of PV basket cells and their plasticity in memory consolidation. We found that dynamic regulation of PV basket cell plasticity specifically was required for long-term memory consolidation during two protracted phases at +0–5 h and at +12–14 h after acquisition (we designate time points after acquisition as ‘+’ and before acquisitions as ‘-’). Regulation involved local D1/5 DA receptor signaling to ensure long-term memory consolidation through PV plasticity sustained throughout a +12–14-h time window.

### **2.2.3 Results**

#### **Time course of high-PV plasticity following cFC**

To investigate which aspects of learning and memory might be influenced by learning-induced plasticity in local PV neurons, we first monitored the time course of high-PV plasticity induced in mouse hippocampal CA3 following cFC. We designated the time at which a learning protocol was completed (in cFC: the last of five foot shocks (US) in training context) as the time of acquisition, or time +0 h. In ventral and dorsal hippocampus (vH and dH, respectively), PV neuron labeling distributions were not detectably altered up to +4.5 h and reached peak high-PV values at +6 h (Fig. 1a,b). These were maintained until +30 h, decreased to half-maximal values around +36 h and reached baseline values at +48 h after acquisition (Fig. 1a,b).



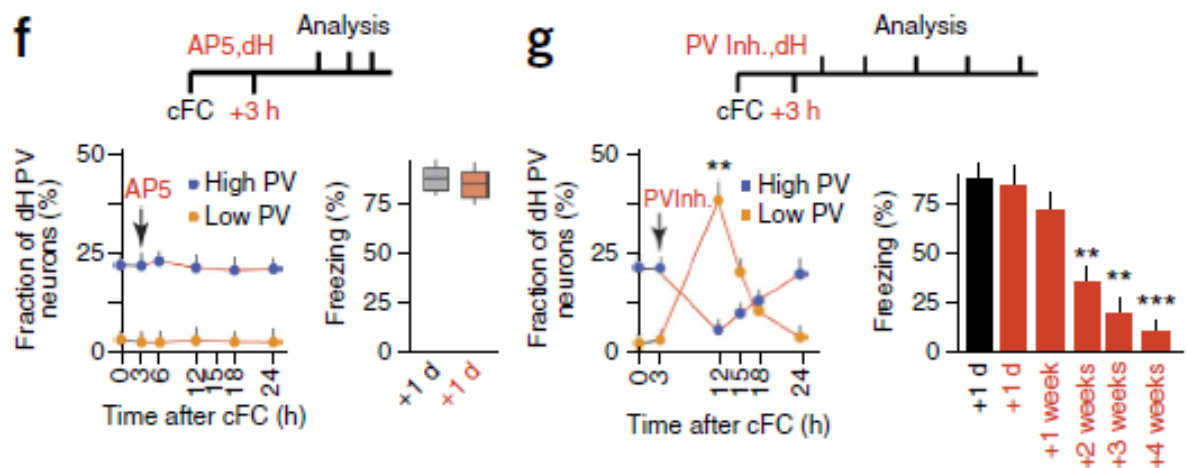


**Figure 1. Sustained high-PV plasticity required for long-term memory in definite learning.**

**(a) Time course of vH high-PV plasticity following cFC.** Left, representative examples of PV immunocytochemistry under control conditions and 24 h after cFC. Color code of arrows: high-PV (dark blue), intermediate-high (pale blue), intermediate-low (yellow), low-PV (orange). Scale bar represents 50  $\mu$ m. Center and right, quantitative analysis of PV neurons in vH CA3b.

**(b) Time course of dH high-PV plasticity following cFC.**

**(c–e) Interference with vH high-PV plasticity following cFC by local delivery** of AP5 (c) or pharmacogenetic ligand (d) to vH at +3 h suppressed long-term (but not intermediate-term) fear memory, whereas interference at +16 h did not (e).

**(f,g) Interference with dH high-PV plasticity following cFC by local delivery** of AP5 (f) or pharmacogenetic ligand (g) to dH at +3 h had no effect on fear memory at +24 h, but had an increasing effect on fear memory retrieved between 1 and 4 weeks (g; stars refer to control cFC values).

Average values from 6 (except (a, e, c, f, g) 3 h (5), 18 h, 30 h, 42 h (4)) mice and 60 PV neurons each; ANOVA followed by Dunnett's post hoc; F/R2: 58.21/0.936 (b), 130/0.9559 (c, right), 126/0.9521 (g); P = 0.00033, 0.00046 (b), 0.0054, 0.0021, 0.00027 (c), 0.0031, 0.0044, 0.0065 (g). \*\*P < 0.01, \*\*\*P < 0.001. Data are presented as mean  $\pm$  s.e.m. Whisker plots: median, upper and lower quartile, and upper and lower extreme.

### Sustained high-PV plasticity is required for long-term memory in definite learning

To determine the time window during which elevated high-PV values might influence behavioral expression of cFC, we locally interfered with the high-PV shift after acquisition. In a first set of experiments, we locally delivered the NMDA

receptor inhibitor AP5 to specifically interfere with high-PV plasticity in late-born PV basket cells<sup>31</sup>. Delivery of AP5 at +3 h to vH selectively prevented learning-induced high-PV plasticity in vH and abolished freezing to context from the next day on while not affecting freezing at +6.5h (Fig. 1c). In a second approach, we pharmacogenetically imposed a low-PV shift at +3 h specifically in vH PV neurons<sup>30,32</sup> (Fig. 1d). Although intermediate memory at +6.5 h was not affected, the procedure led to a suppression of freezing to context at +24 h, which lasted at least 7 weeks (Fig. 1d). When treatments were started at +16 h after acquisition, we still found no excess vH high-PV at +24 h, but freezing to context exposure was not detectably affected (Fig. 1e; data not shown for AP5). Unlike vH, abolishing high-PV plasticity with AP5 or through pharmacogenetic PV inhibition at +3 h in dH did not affect freezing to context on the next day (Fig. 1f,g; but see below). Consistent with previous reports of time-dependent requirement for dH in contextual fear memory<sup>33</sup>, we detected a gradual loss of freezing response when mice were tested in conditioned context between 1 and 4 weeks after cFC in these long-term consolidation interference experiments (Fig. 1g). Taken together, these results indicate that counteracting long-lasting high-PV plasticity in vH CA3 before +16 h specifically prevents behavioral long-term fear memory consolidation while leaving intermediate memory unaffected. Counteracting long-lasting high-PV plasticity in dH also interfered with long-term fear memory consolidation, but the behavioral consequences of this intervention only became detectable weeks after acquisition. For this reason, we focused on long-term fear memory consolidation processes in vH.

### **Sustained low-PV plasticity required for long-term memory in incremental learning**

We next determined whether learning-induced low-PV plasticity is also required for long-term consolidation of corresponding memories. MWM learning is a trial-and-error hippocampus-dependent learning protocol involving hippocampal low-PV plasticity as mice learn the task, and high-PV plasticity when the spatial navigation task has been learned<sup>30</sup>. As in cFC, low-PV plasticity induced after 1 d of MWM training became detectable at +6 h (Fig. 2a). In MWM learning, low-PV plasticity depends on local VIP receptor signaling<sup>30</sup>. Local delivery of VIP antagonist to vH at +3 h specifically suppressed the low-PV shift (Fig. 2b). In

parallel, mice lost all behavioral benefits of previous training (Fig. 2b). Similarly, pharmacogenetic imposition of a high-PV shift in vH at +3 h suppressed the low-PV shift and previous learning, as detected by maze performance on day 3 (Fig. 2c). Imposing a high-PV shift at +16 h suppressed the low-PV shift at the time of retrieval (+24 h), but did not detectably affect navigation performance (Fig. 2d).

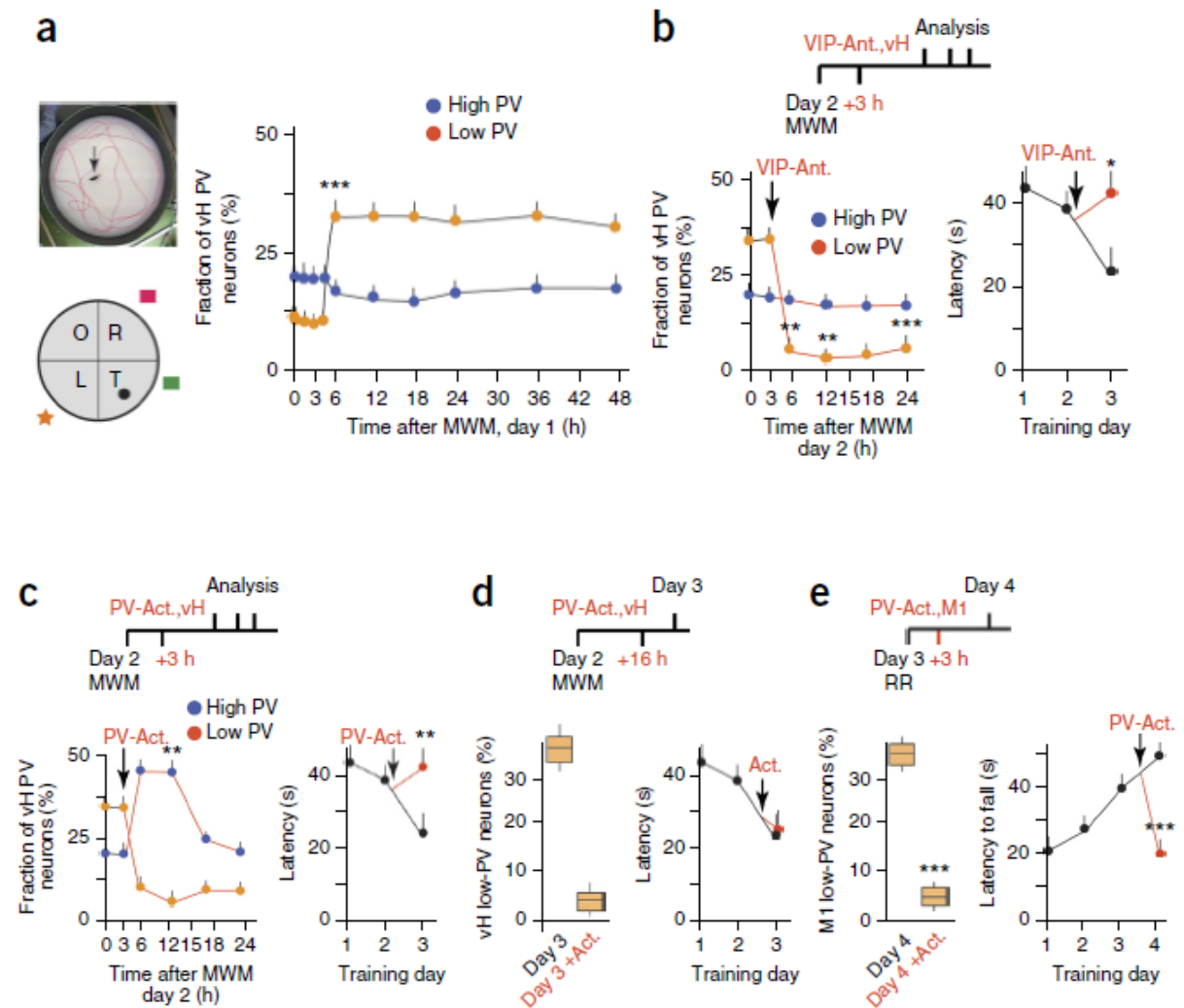


**Figure 2. Sustained low-PV plasticity required for long-term memory consolidation in incremental learning.**

**(a) Time course of vH low-PV plasticity following MWM training.** Top left, representative photograph of water maze and mouse (arrow) search trace (red). Bottom left, schematic of water maze experiment with hidden platform (black circle), quadrants (T, target; O, opposite; L, left; R, right) and spatial cues (rectangles and star). Right, quantitative analysis of PV neurons in vH CA3b.

**(b–d) Interference with vH low-PV plasticity following MWM training by local delivery** of VIP antagonist (b) or pharmacogenetic ligand (c) to vH at +3 h suppressed maze navigation memory, whereas interference at +16 h did not (d).

**(e) Long-term memory consolidation in rotarod (RR) learning.** Suppression of low-PV plasticity and motor learning by pharmacogenetic ligand at +3 h is shown.

Data are average values from 6 (except a–c) 3 h (5), 18 h, 30 h, 42 h (4)) mice and 60 PV neurons each; Student's t test;  $P = 0.00094$  (a), 0.0034, 0.0044, 0.00083 (b, left), 0.021 (b, right), 0.0032, 0.0038 (c), 0.00089, 0.00048 (e). \* $P < 0.05$ , \*\* $P < 0.01$ , \*\*\* $P < 0.001$ . Data are presented as mean  $\pm$  s.e.m. Whisker plots: median, upper and lower quartile, and upper and lower extreme.

To determine whether learning-induced PV basket cell plasticity might also be required for long-term memory consolidation in learning tasks that don't depend on the hippocampus, we interfered with low-PV plasticity in primary motor cortex (M1) after 3 d of accelerating rotarod training<sup>30</sup>. Imposing a high-PV shift in M1 at +3 h early (3 d) in rotarod training suppressed learning-related low-PV plasticity and all benefits of previous training following testing on the next day (Fig. 2e). Taken together, these results suggest that sustained learning-related local PV basket cell plasticity is specifically required for long-term consolidation of the corresponding memories, regardless of whether learning induces high or low-PV plasticity.

### **PV plasticity sustained through D1/5 DA signaling**

We next focused on the mechanisms that might ensure sustained learning-induced PV neuron plasticity up to the time window critical for long-term memory consolidation. Similar to high or low-PV plasticity induced following learning, pharmacogenetically induced PV plasticity became detectable at +6 h (but not by +4.5 h) following induction (Fig. 3a,b). However, unlike plasticity induced after learning, elevated contents of high or low-PV neurons began to decline after 10–11 h following induction and returned to baseline values at +15 h (Fig. 3a,b). These observations suggest that the long-lasting PV plasticity necessary for long-term memory consolidation might require additional signals delivered locally. Given the role of late DA signaling in fear memory consolidation<sup>34–39</sup>, we hypothesized that this might involve local DA signaling acting through D1/5 receptors. Indeed, local delivery of a specific D1 receptor agonist<sup>40</sup> to vH at +12 h



rescued and extended both the high and the low-PV shifts up to at least +24 h (Fig. 3a,b). In control experiments, D1 receptor agonist failed to induce a high-PV (or low-PV) shift in naive mice in the absence of previous triggering through PSEM ligand (Fig. 3a).

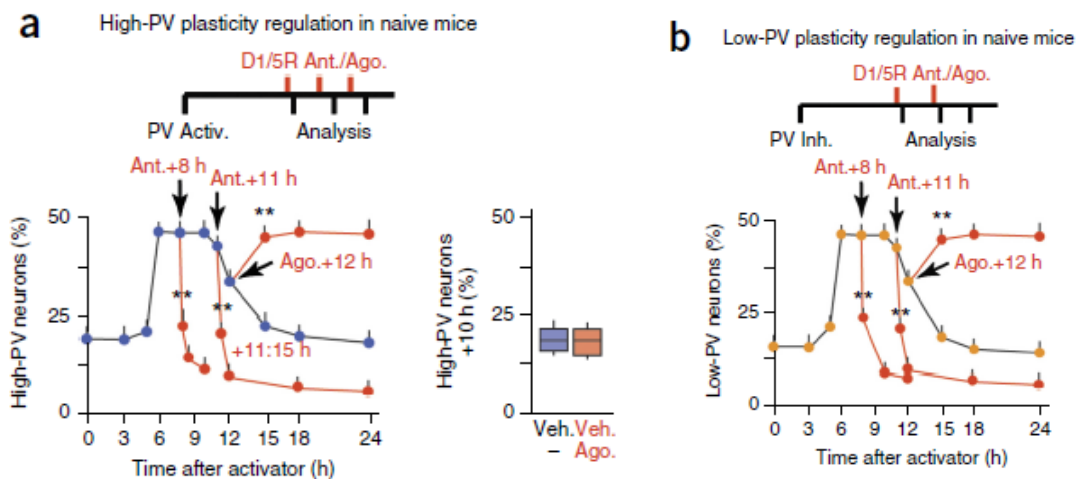
Given that enhancing D1 receptor signaling extended the duration of PV plasticity, we wondered whether interfering with local D1 receptor signaling might accelerate loss of PV shifts in pharmacogenetically treated naive mice. Indeed, local delivery of a D1/5 receptor antagonist at +8 h or +11 h led to a rapid loss (return to baseline levels in 15 min) of excess high or low PV neurons in these experiments (Fig. 3a,b). To determine whether enhancing D1 receptor signaling might strengthen plasticity in primed PV neurons, we locally delivered D1 receptor agonist at +3 h after pharmacogenetic stimulation. The early treatment with D1 agonist did not accelerate the appearance of detectable PV shifts (absent at +4.5 h), but rather greatly delayed the spontaneous decline of high-PV neuron contents in pharmacogenetically treated mice (Fig. 3c). Furthermore, D1 agonist at +3 h slowed down high-PV neuron losses induced by D1/5 receptor antagonist at +8 h (Fig. 3c). Taken together, these results suggest that local stimulation of D1 receptor signaling strengthens plasticity (high or low PV) in PV neurons, whereas local interference with D1/5 receptor signaling disrupts PV plasticity in pharmacogenetically treated PV neurons of naive mice.

To determine whether modulation of D1/5 receptor activation influences DA-related signaling in PV neurons, we analysed contents of phosphorylated DARPP-32 (pDARPP-32; Thr34 phosphorylation involving D1 signaling) and ERK (pERK) in PV (Neun+ PV+) and non-PV (NeuN+ PV-) neurons<sup>41</sup>. Local delivery of D1 agonist to vH of naive mice induced marked increases in the fraction of pDARPP-32+ and pERK+ PV neurons, whereas corresponding changes in non-PV neurons were much more modest (pDARPP-32) or absent (pERK) (Fig. 3d). These results indicate that local activation of D1/5 receptor in vH initiates signaling selectively in PV neurons.

### **PV level regulation through cAMP in PV neurons**

To investigate mechanisms that might interface with D1/5 receptor signaling to regulate PV levels in PV basket cells, we carried out pharmacological

experiments aimed at altering cAMP levels in vH of naive mice. Local delivery of the phosphodiesterase (PDE-4) inhibitor Rolipram to vH was sufficient to produce a shift to higher PV levels in a large fraction of local PV neurons at +6 h (Fig. 3e). Conversely, local delivery of the adenylate cyclase (AC) inhibitor SQ22536 produced a shift to lower PV values in a large fraction of local PV neurons in naive mice at +6 h (Fig. 3e). To determine whether cAMP levels in PV neurons influence their PV levels, we expressed an AC-activating DREADDs<sup>42</sup> construct specifically in PV neurons using a Cre-dependent AAV in PV-Cre mice. Activation with ligand led to an increase in PV levels in virus-expressing neurons (Fig. 3f). Comparable end contents of high-PV neurons were induced in early- and late-born PV neuron subpopulations by the AC activation construct, suggesting that early-born PV neurons might exhibit higher endogenous levels of AC activation, for example, as a result of higher levels of endogenous cAMP (Fig. 3f). Local delivery of D1/5 receptor antagonist at +11 h did not interfere with high-PV contents in these PV neuron-specific DREADDs experiments, consistent with the notion that, although D1/5 signaling modulates the plasticity response of PV neurons, cAMP might directly regulate PV levels in PV neurons, for example, through PKA activity (Fig. 3g).



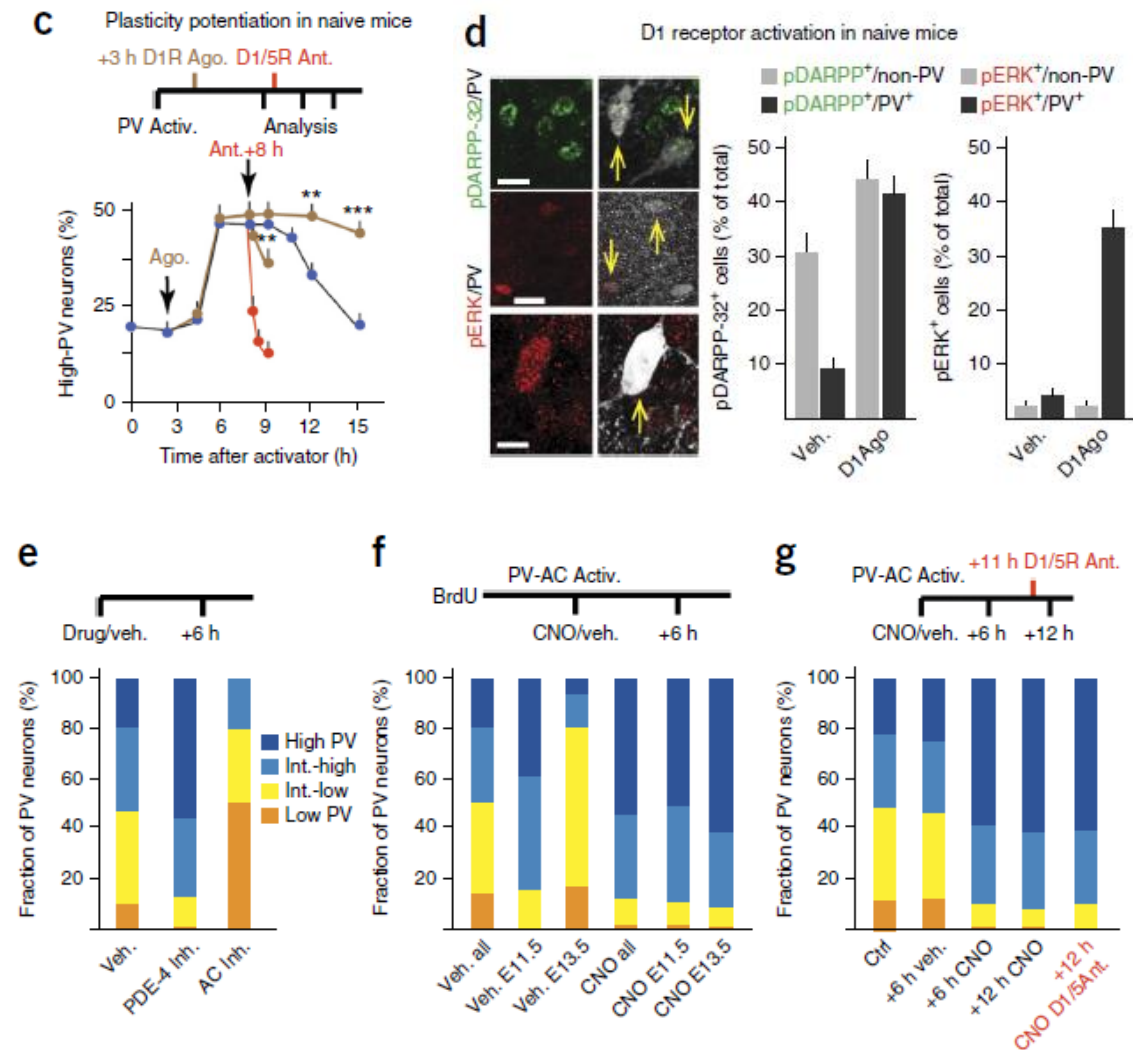


**Figure 3. PV neuron plasticity sustained through D1/5 dopamine receptor signaling and regulated by cAMP in PV neurons.**

**(a,b) Pharmacogenetic induction of high-PV (a) or low-PV (b) plasticity in vH of naive mice:** time course, specific extension by D1 receptor agonist and rapid loss following D1/5 receptor antagonist delivery. In the absence of previous pharmacogenetic activation, D1 receptor agonist did not affect PV content distributions (right, a).

**(c)** Delivery of D1 agonist at +3 h extended the duration of PV plasticity in naive mice and slowed down its decline following D1/5 antagonist delivery.

**(d) D1 receptor signaling in PV neurons.** Left, representative examples of pDARPP-32/PV and of pERK/PV double immunocytochemistry in vH CA3b; arrows: double-labeled cells. Right, quantitative analysis of pDARPP-32+ and pERK+ PV (NeuN+ PV+) and non-PV (NeuN+ PV-) neurons in vH CA3b 15 min after delivery of vehicle or D1 agonist. Scale bars represent 15  $\mu$ m.

**(e–g) Regulation of PV plasticity by cAMP in PV neurons.** Local delivery (vH, CA3) of PDE-4 inhibitor induced high-PV plasticity, whereas delivery of AC inhibitor induced low-

PV plasticity at +6 h (e). High-PV plasticity induced by DREADDs-mediated AC activation in vH PV neurons led to comparable high-PV neuron contents in virus-expressing early- (labeled with BrdU at E11.5) and late-born (labeled at with BrdU at E13.5) PV neurons at +6 h (f); plasticity at +12 h was resistant to delivery of D1/5 receptor antagonist at +11 h (g).

Average values from 6 (except 3 h, 4.5 h (5), 24 h (4)) (a–c) and 5 (except vehicle pERK (3) and vehicle pDARPP-32 (4)) (d) mice and 60 PV vH CA3b neurons each; Student's t test;  $P = 0.0024, 0.0032, 0.0061$  (a),  $0.0019, 0.0037, 0.0044$  (b),  $0.0054, 0.0037, 0.00040$  (c). \* $P < 0.05$ , \*\* $P < 0.01$ , \*\*\* $P < 0.001$ . Data are presented as mean  $\pm$  s.e.m. Whisker plots: median, upper and lower quartile, and upper and lower extreme.

### **Long-term memory consolidation dependent on D1/5 signaling at +12–14 h**

To identify processes that might influence long-term memory consolidation through regulation of local PV plasticity, we determined the time window during which local delivery of D1/5 receptor antagonist might interfere with long-term memory consolidation in cFC. Consistent with previous reports that local DA signaling is important in fear learning<sup>37,43,44</sup>, D1/5 receptor antagonist delivery to vH 10 min before acquisition (–10 min) prevented long-term (but not intermediate-term) fear memory consolidation in cFC (Fig. 4a and Supplementary Fig. 1). After acquisition, D1/5 receptor antagonist weakened, but did not suppress, long-term fear memory when delivered at up to +5 h, did not interfere with fear memory when delivered between +6 h and +10 h after acquisition, and suppressed long-term fear memory when delivered between +12 h and +14 h (Fig. 4a). Interfering with D1/5 receptor signaling after +15 h did not affect fear memory (Fig. 4a).

To determine whether endogenous local D1 receptor signaling is necessary to ensure a long-lasting PV shift and long-term memory consolidation following learning, we delivered D1/5 receptor antagonist to vH at +12 h after acquisition of cFC<sup>34</sup>. Previous studies have shown that, under local in vivo delivery conditions comparable to those used here, the antagonist is effective as soon as 5 min and up to 60–90 min following delivery<sup>45</sup>. Indeed, high-PV neuron contents in vH dropped to nearly baseline levels by 15 min after antagonist delivery (Fig. 4b). At subsequent time points, high-PV neuron contents dropped further and then recovered to baseline levels (Fig. 4b). In parallel, fear memory was undetectable up to at least 7 weeks (Fig. 4b). Suppression of freezing by D1/5 antagonist was not correlated with enhanced locomotor activity, and reconditioning on day +1

produced robust freezing on day +2, ruling out lasting damage to fear learning by the D1/5 antagonist treatment to vH (Supplementary Fig. 2). In control experiments aimed at testing specificity of the requirement for D1/5 receptor signaling<sup>40</sup>, local delivery of D2 dopamine receptor agonist or antagonist to vH at +12 h did not influence PV levels or freezing (Fig. 4c) following cFC at +24 h. In further control experiments, delivery of noradrenergic receptor antagonist at +12h also failed to affect PV levels or freezing following cFC (Supplementary Fig. 2). Consistent with the observation that D1/5 receptor antagonist during a time window at +6–10 h did not affect fear memory at +24 h, delivery of D1/5 antagonist at +8 h had no detectable effect on PV level distributions in vH (Fig. 4d). Notably, cFC led to robust increases in the fraction of pDARPP-32+ and pERK+ PV neurons at +5 h and at +12 h (Fig. 4e). Local delivery of D1/5 receptor antagonist at +12 h led to a nearly complete loss of pDARPP-32+ and pERK+ PV neurons, consistent with the notion that, following cFC, activation of D1/5 receptor signals in PV neurons act to sustain PV plasticity. Taken together, these results suggest that local D1/5 receptor signaling during a critical time window +12–14 h after acquisition is necessary to maintain learning-induced high-PV plasticity and to ensure long-term consolidation of fear memory.

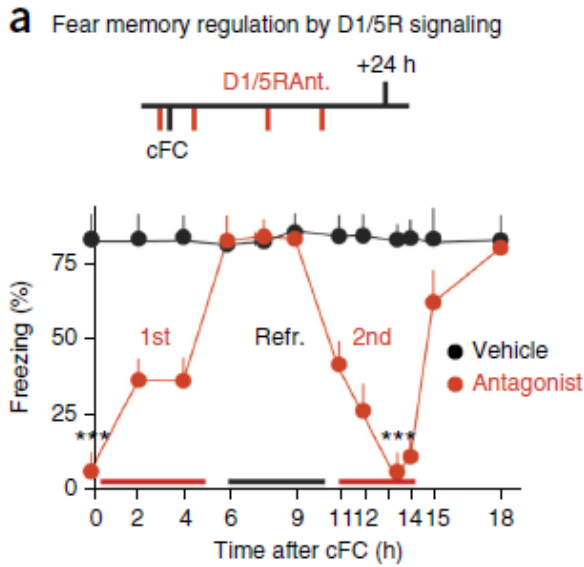
To determine whether a local D1/5 receptor signaling requirement at +12–14 h reflects consolidation processes specific for each memory separately, we carried out fear learning experiments at different times of day and night and analyzed consolidation of separate memories during the same acquisition day. Fear memory consolidation depended on local D1/5 receptor signaling at +12 h regardless of whether acquisition occurred at the beginning, in the middle or at the end of the day-night cycle (Supplementary Fig. 3). Furthermore, when mice were fear conditioned to two different contexts, TR1 and TR2, with a 6-h interval between conditioning protocols, consolidation of fear memory to TR1 or TR2 each specifically depended on local D1/5 receptor signaling at +12 h after acquisition of the particular fear memory association (Supplementary Fig. 3). Consistent with the notion that long-term consolidation of fear memory to TR2 depended on a high-PV shift at its long-term consolidation time window, conditioning to TR2 induced excess high-PV contents in vH, and delivery of D1/5 antagonist at +12 h led to only a partial loss of high-PV neurons (Supplementary

Fig. 3). Thus, a requirement for local D1/5 receptor signaling at +12–14 h after acquisition is a specific feature of each memory consolidation process regardless of day-night cycle.

To determine whether local D1/5 receptor signaling is also required during a late time window for long-term consolidation of memories involving low-PV plasticity, we investigated mice that underwent MWM training. During the first 4 d of maze training, navigation learning depends on vH<sup>45</sup>, where low-PV plasticity induced after the first 3 d of training is followed by high-PV plasticity after day 4 of training. Delivery of D1/5 receptor antagonist to vH at +12 h after training on day 2 suppressed the low-PV shift and all benefits of training when mice were tested on day 3 (Fig. 4f). The same treatment to vH after day 4 of training suppressed the high-PV shift in vH on the next day, indicating that, in the same maze learning procedure, D1/5 receptor signaling at +12 h is required to support PV plasticity regardless of whether this involves low-PV or high-PV plasticity (Fig. 4f).

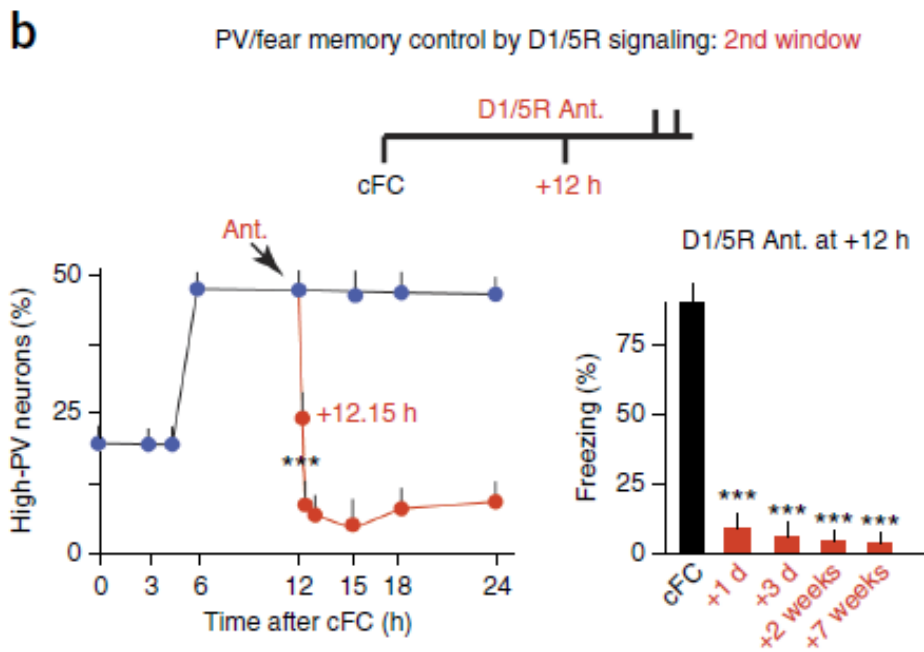
Consistent with the notion that learning of a spatial map depends on dH<sup>46</sup>, local delivery of D1/5 antagonist to dH at +12 h after 8 d of training suppressed a high-PV shift in dH and led to a loss of spatial memory (Fig. 4g). Finally, consistent with the notion that PV plasticity in rotarod learning depends on local D1/5 receptor signaling<sup>47</sup> during a long-term consolidation time window in M1, local bilateral delivery of D1/5 antagonist to M1 at +12 h after 3 d of training suppressed low-PV plasticity and motor skill memory on day 4 (Fig. 4h).

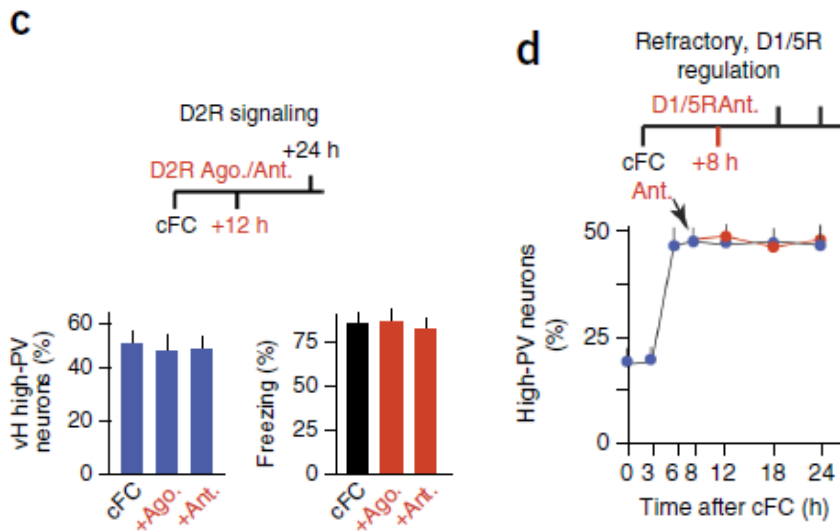
Taken together, these results suggest that endogenous local D1/5 receptor signaling at a late time window +12–14 h after acquisition is important for maintaining learning-induced PV plasticity and for ensuring long-term consolidation of the corresponding memories.



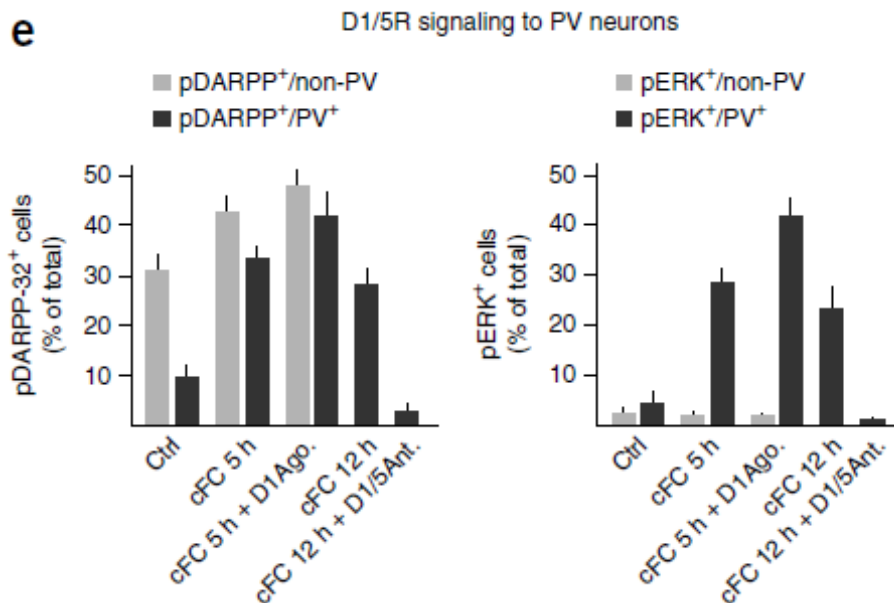
**Figure 4. Critical late time window of long-term memory consolidation depending on D1/5 receptor signaling.**

**(a) Time windows** at which local delivery of D1/5 receptor antagonist to vH interferes with long-term consolidation of fear memory (Refr: refractory time window).

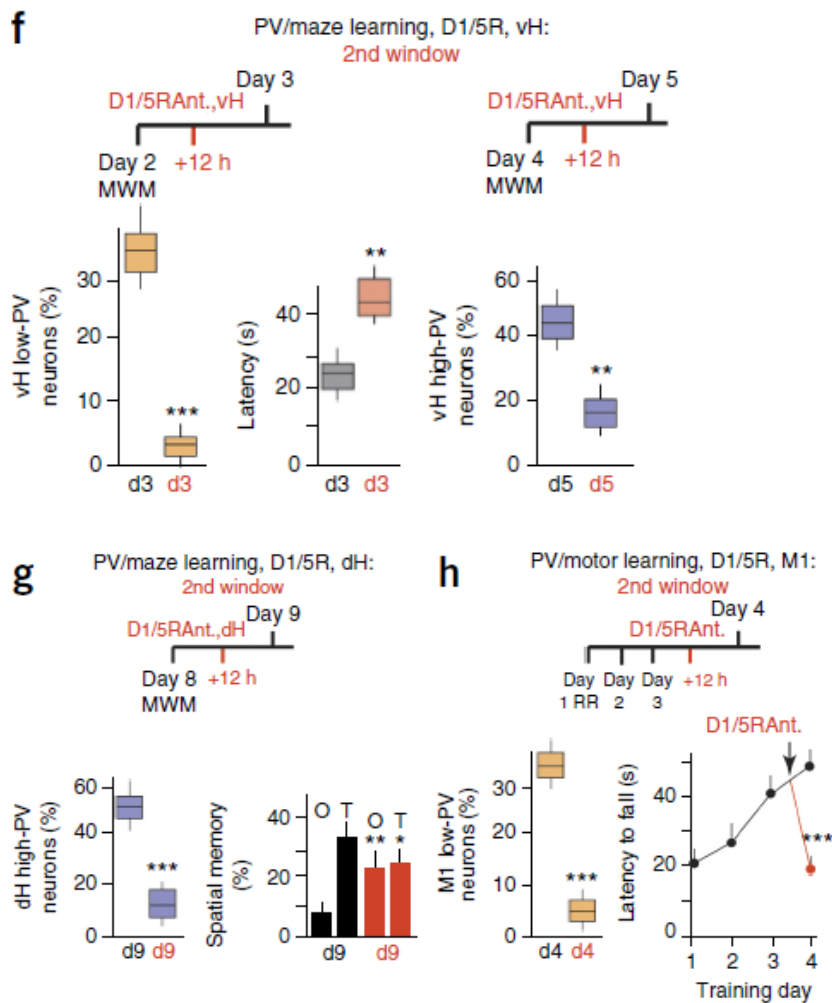




**(b–d) Long-term fear memory consolidation specifically depends on vH D1/5 receptor signaling at +12 h.** Rapid loss of high-PV neuron contents (left) and suppression of fear memory consolidation (right) following delivery of D1/5 receptor antagonist to vH (b). Local delivery of D2 receptor agonist or antagonist to vH at +12 h did not influence consolidation of fear memory (c). Delivery of D1/5 antagonist during refractory time window (+8 h) did not affect PV plasticity (d).







**(e) D1/5 receptor signaling to PV neurons in cFC.** Quantitative analysis of pDARPP-32+ and pERK+ PV and non-PV neurons in vH CA3b, 5 h and 12 h after cFC; drug treatments: analysis 15 min after delivery of D1 agonist, and 30 min after delivery of D1/5 antagonist.

**(f–h) Requirement for D1/5 receptor signalling at +12 h in water maze learning.** After day 2, D1/5 receptor antagonist to vH at +12 h suppressed low-PV plasticity and reset performance (f, left). After day 4, D1/5 antagonist to vH suppressed high-PV plasticity (f, right). After day 8, D1/5 antagonist to dH suppressed dH high-PV plasticity and disrupted spatial memory (g). T, O: percentage time spent in target and opposite quadrant during spatial memory test in the absence of platform (stars refer to respective untreated controls). (h) D1/5 receptor antagonist to M1 at +12 h after training day 3 suppressed M1 low-PV plasticity and reset performance to pre-training levels.

Average values from 6 (except 24 h (5), 2 h, 4 h (4), control pERK (4), control pDARPP-32 (3)) mice and 60 PV neurons each; Student's t test or ANOVA, followed by Dunnett's post hoc; F/R2: 135/0.9642 (b), 69.33/0.942 (e); P = 0.00031, 0.00062 (a), 0.00011, 0.00015, 0.00022, 0.00020, 0.00011 (b), 0.00057, 0.0059, 0.018 (f), 0.00058 (e, left), 0.0056, 0.036 (e, right), 0.00035, 0.00069 (g). \*P < 0.05, \*\*P < 0.01, \*\*\*P < 0.001. Data

are presented as mean  $\pm$  s.e.m. Whisker plots: median, upper and lower quartile, and upper and lower extreme.

### **D1/5 signaling supports memory consolidation through PV plasticity**

To determine whether the requirement for endogenous local D1/5 receptor signaling at +12–14 h after acquisition for long-term memory consolidation reflects maintenance of long-lasting PV plasticity, we carried out experiments in which we combined imposition of PV plasticity and manipulation of D1/5 receptor signaling. In mice in which an additional high-PV shift was induced pharmacogenetically in vH at +3 h after acquisition of cFC, delivery of D1/5 receptor antagonist at +12 h only had a partial effect on high-PV levels and failed to suppress long-term consolidation of fear memory (Fig. 5a). Likewise, D1 receptor agonist delivered to vH at +12 h after acquisition failed to rescue long-term fear memory consolidation in mice in which a low-PV shift was imposed in vH via pharmacogenetic inhibition of PV neurons (Fig. 5b). In mice in which an additional low-PV plasticity signal (VIP to vH) was delivered at +11 h after 2 d of training in the MWM, D1/5 receptor antagonist delivered to vH at +12 h failed to disrupt the low-PV shift in vH at +13 h and at +24 h and to disrupt navigation memory on the next day (Fig. 5c).

Similarly, imposing a high-PV shift specifically in PV neurons of vH at +11 h via pharmacogenetic AC activation suppressed vH low-PV at +13 h and at +24 h, and navigation memory on the next day (Fig. 5d). Notably, local delivery of D1 receptor agonist to vH at +12 h failed to rescue the low-PV shift and navigation memory in this PV-specific DREADDs experiment (Fig. 5d).

Taken together, these results indicate that local D1/5 receptor signaling at +12–14 h is required to maintain learning-induced PV plasticity that is important for long-term memory consolidation.

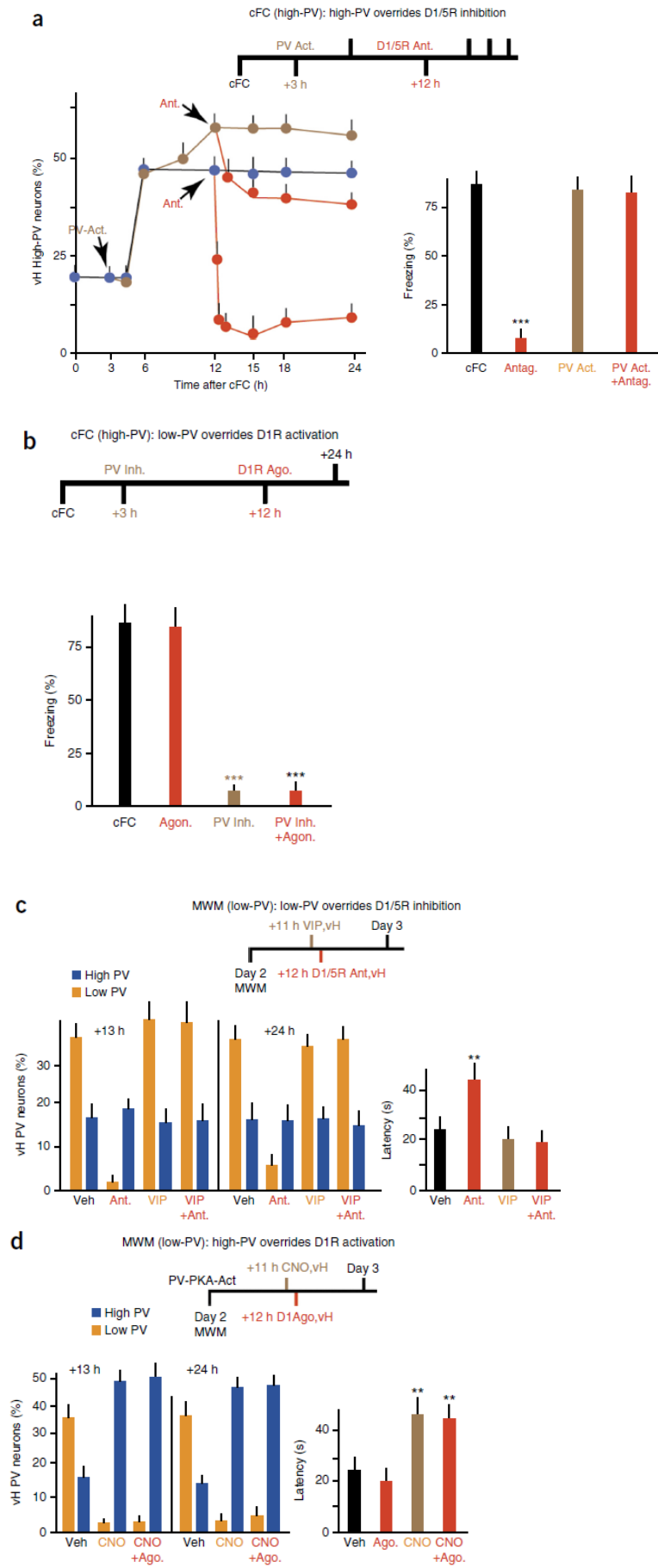


**Figure 5. D1/5 receptor signaling supports long-term memory consolidation through PV plasticity.**

**(a,b) D1/5 receptor signaling required for memory consolidation through sustainment of vH high-PV plasticity in cFC.** (a) Pharmacogenetic induction of high-PV plasticity in vH at +3 h after cFC led to further elevation of high-PV contents from +9 h on and to only partial loss of high-PV plasticity following D1/5 antagonist delivery at +12 h (left), and bypassed the requirement for D1/5 receptor signaling at +12 h for fear memory (right). (b) D1 agonist at +12 h after cFC failed to rescue fear memory when a low-PV shift was imposed pharmacogenetically at +3 h.

**(c,d) D1/5 receptor signaling required for memory consolidation through sustainment of low-PV plasticity in water maze learning.** (c) Potentiation of low-PV plasticity at +11 h with VIP prevented the loss of low-PV plasticity (left) and loss of training benefits induced by D1/5 antagonist to vH at +12 h. (d) D1 agonist at +12 h failed to rescue low-PV plasticity and loss of training benefits induced by DREADDs-mediated activation of PKA in vH PV neurons at +11 h.

Average values from 6 (except 3 h, 18 h (5), 24 h (4) (a), cFC (4) (b), vehicle 13h (5) vehicle 24h (4) (c,d)) mice and 60 PV neurons each; ANOVA, followed by Dunnett's post hoc; F/R2: 128/0.962 (b), 54.22/0.924 (d); P = 0.00029 (a), 0.00052, 0.00026 (b), 0.0054 (c), 0.0026, 0.0029 (d). \*\*P < 0.01, \*\*\*P < 0.001. Data are presented as mean  $\pm$  s.e.m.

**D1/5 signaling at +0–5 h modulates PV plasticity and memory**

To determine whether, similar to pharmacogenetic induction of PV plasticity in naive mice, the status of D1/5 receptor activation up to 5 h after acquisition might modulate the strength of PV plasticity and learning, we carried out experiments in mice that underwent a comparatively weak cFC protocol. A 2xUS (instead of 5xUS, two instead of five foot shocks) protocol resulted in a comparatively modest high-PV shift in vH at +12 h and +24 h after acquisition (Fig. 6a). In parallel, the 2xUS protocol produced a reduced freezing response at +24 h and strongly reduced freezing at +7 d (Fig. 6a). Local application of D1 receptor agonist to vH at +3 h or at +12 h after acquisition produced a sustained enhancement of vH high-PV contents (Fig. 6b). In parallel, D1 receptor agonist produced increased freezing to context at +24 h and at +7 d that was undistinguishable to fear memory following a 5xUS cFC protocol (Fig. 6b). By contrast, delivery of D1 agonist at +8 h failed to strengthen 2xUS fear memories (Fig. 6b). In control experiments, D1 agonist delivered 12 h after context exploration without foot shocks (no US) did not result in freezing to context on the

next day (Fig. 6b). Furthermore, pharmacogenetic induction of a high-PV shift in vH of non-fear conditioned mice failed to induce any freezing (Supplementary Fig. 4). These results suggest that enhancing local D1 signaling during an early sensitivity time window after acquisition potentiates PV plasticity and long-term memory consolidation.

We next determined whether D1/5 receptor interference during the early sensitivity time window might be rescued through D1 stimulation during the late time window. Delivery of D1/5 receptor antagonist to vH at +3 h in the 5xUS cFC protocol led to reduced high-PV values in vH at +6 h and +12 h, baseline high-PV values at +24 h, and reduced freezing at +24 h (Fig. 6c). Notably, and in contrast with D1/5 receptor inhibition at +12 h, the effect of D1/5 receptor inhibition at +3h could effectively be rescued by subsequent delivery of D1 receptor agonist to vH at +12 h (Fig. 6c).

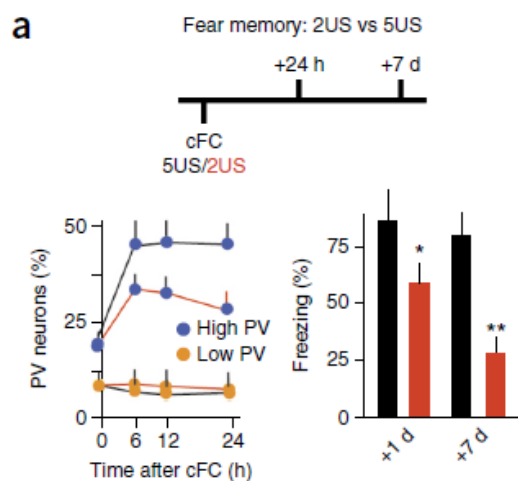
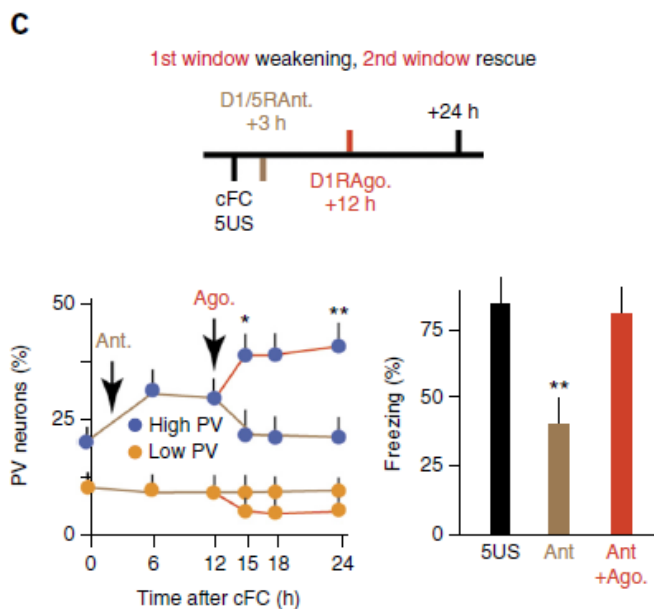
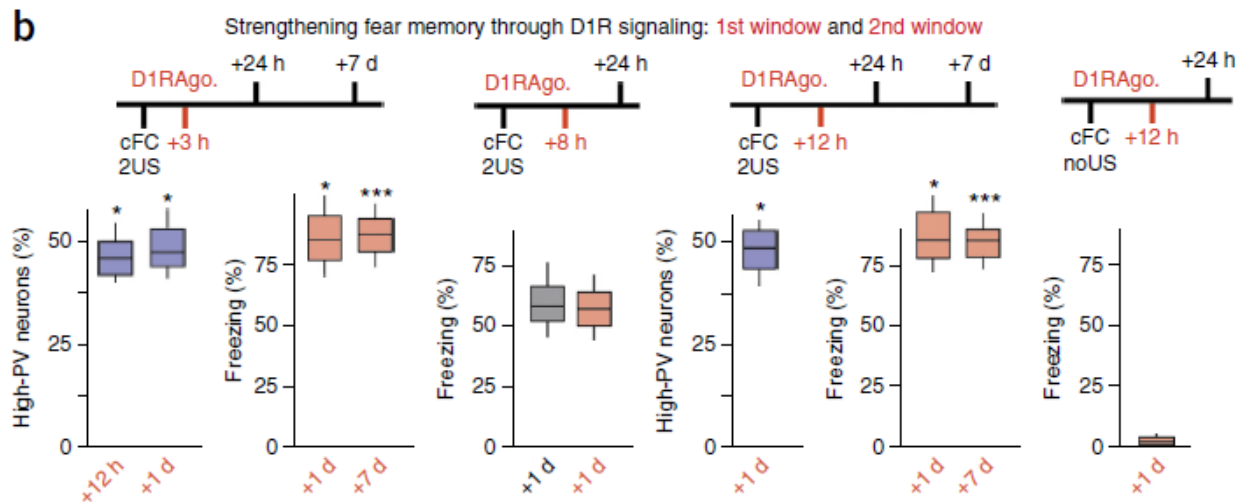


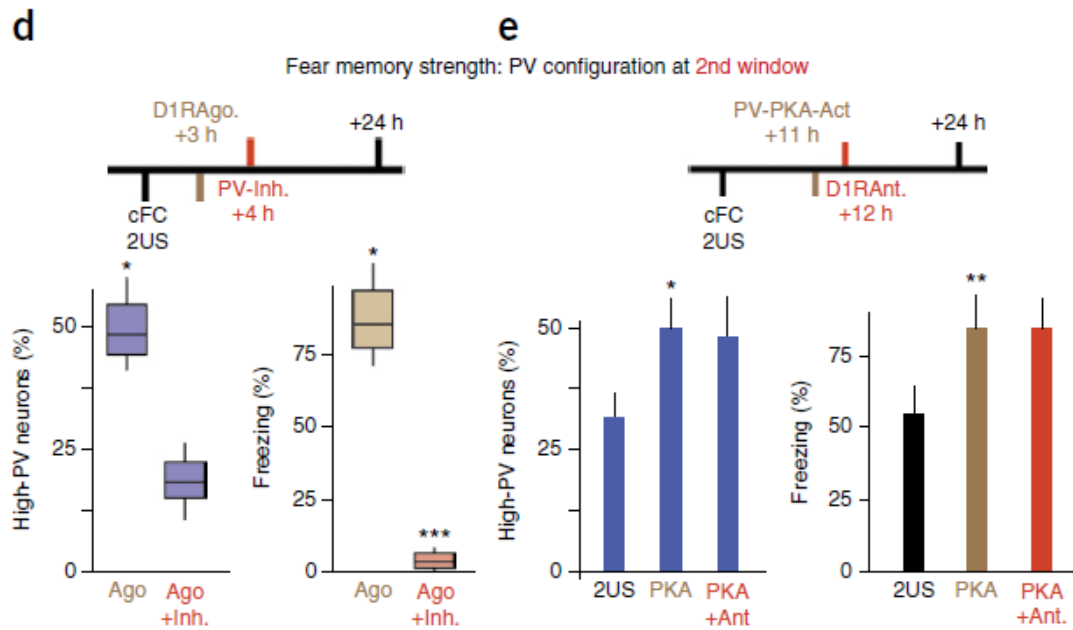
**Figure 6. D1/5 signaling at +0–5 h modulates PV plasticity strength and memory.**

**(a)** Reduced vH high-PV plasticity and fear memory following cFC with two US (2US, red) instead of five US (5US).



**(b) D1 receptor agonist delivery to vH at +3 h (first from left) or at +12 h (third from left), but not at +8 h (second from left), augmented two US cFC high-PV plasticity and fear memory to five US cFC values. D1 agonist in the absence of foot shocks failed to induce freezing (right).**

**(c) Analysis of PV plasticity and fear memory (five US) interference by D1/5 antagonist at +3 h. Note the reduced and transient high-PV shift rescued by delivery of D1 agonist at +12 h to vH (left), in parallel with rescue of fear memory (right).**



**(d,e) Fear memory strength determined by high-PV plasticity at +12–14-h time window.** (d) Potentiation of PV plasticity and fear memory by D1 agonist at +3 h disrupted by pharmacogenetic induction of low-PV plasticity at +4 h. (e) Disruption of PV plasticity and fear memory by D1/5 antagonist at +12 h neutralized by previous DREADDs-mediated activation of PV neuron PKA at +11 h.

Average values from 6 (except no US (5) (b), 24h (4) (a,c)) mice and 60 PV neurons each; ANOVA, followed by Dunnett's post hoc; F/R2: 148/0.972 (b);  $P = 0.022, 0.0077$  (a), 0.035, 0.028, 0.041, 0.00045, 0.00038 (b), 0.044, 0.0052, 0.0062 (c), 0.032, 0.026, 0.00055 (d), 0.0028, 0.018 (e). \* $P < 0.05$ , \*\* $P < 0.01$ , \*\*\* $P < 0.001$ . Data are presented as mean  $\pm$  s.e.m. Whisker plots: median, upper and lower quartile, and upper and lower extreme.

Finally, we determined whether fear memory modulation involves vH PV expression values at the +12–14 h consolidation time window. When delivery of D1 agonist at +3h was followed by pharmacogenetic inhibition of PV neurons at +4 h, both the high-PV shift and freezing to context were abolished on the next day (Fig. 6d).

Furthermore, DREADDs-mediated activation of AC specifically in PV neurons in the 2xUS cFC protocol at +11 h rescued high-PV values and freezing to 5xUS levels, and negated the effect of D1/5 receptor antagonist delivered 1 h after at +12 h (Fig. 6e).

Taken together, these results indicate that D1/5 receptor signaling during the +0–5-h time window after acquisition modulates the strength of PV plasticity and fear memories through its effect on PV expression values during the +12–14-h long-term memory consolidation time window.

### Ripple density at +12–14 h depends on PV plasticity

Under the assumption that induction of and requirement for PV neuron plasticity might reflect the involvement of local network activity processes, we monitored local field potential (LFP) activity in vH of awake head-fixed mice following cFC (Fig. 7a). In fear-conditioned mice, vH sharp-wave ripple densities at +12 h were about 2.5-fold higher than baseline values (Fig. 7b). Ripple event densities were partially elevated at +4 h and had returned to baseline values at +18 h, suggesting that they peaked around the long-term memory consolidation time window (Fig. 7b). No detectable differences were observed in vH ripple densities at different times of the day and night in mice that had explored a new environment not associated with foot shocks (Fig. 7c). In contrast with ripple densities, we did not detect alterations in the powers of  $\delta$ ,  $\tau$ ,  $\alpha$ - $\beta$  or  $\gamma$  oscillation in vH at +12 h (Fig. 7d).

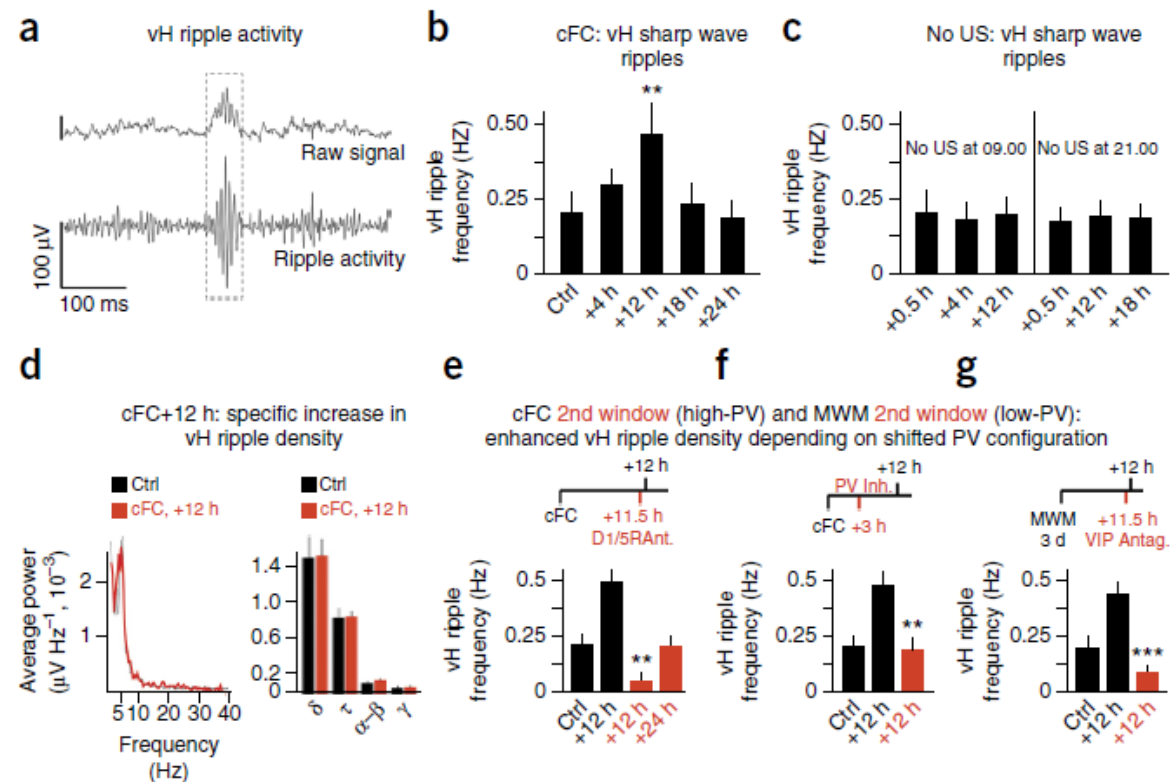




**Figure 7. Enhanced ripple density at +12–14 h depending on PV plasticity.**

**(a) Representative example of vH LFP trace and ripple event (cFC, +12 h).** Scale bar (top) represents 100  $\mu$ V.

**(b) Ripple event frequency in vH CA3 and CA1 following cFC.**

(c) vH ripple densities not affected by day-night cycle in control mice.

**(d) No alterations in power of local vH oscillation activities at +12 h following cFC.**

(e–g) Enhanced ripple event densities at +12 h in cFC (e,f) and MWM learning (g) depended on local D1/5 receptor signaling (e) and local PV plasticity (f, high PV; g, low PV).

Average values from 4 (except (c) (3), control (e,f) (2)) mice and 10 min each. ANOVA, followed by Dunnet's post hoc; F/R2: 132/0.967 (e), 146/0.971 (f); P = 0.0037 (b), 0.0028 (e), 0.0049 (f), 0.00036 (g). \*\*P < 0.01, \*\*\*P < 0.001. Data are presented as mean  $\pm$  s.e.m.

We next determined whether the sustained PV plasticity required for long-term memory consolidation might influence local ripple activity at +12 h. When D1/5 receptor antagonist was delivered to vH at +11.5 h following cFC, vH ripple densities dropped to below baseline values<sup>48</sup> at +12 h and recovered to baseline values at +24 h (Fig. 7e). Pharmacogenetic imposition of a low-PV shift to vH at +3 h following cFC suppressed enhanced ripple densities at +12 h (Fig. 7f). Enhanced ripple densities comparable to values following cFC were also detected in vH at +12 h following 3 d of MWM training (Fig. 7g). Specific interference with low-PV plasticity at +11.5 h through local delivery of VIP antagonist to vH suppressed the enhanced ripple activity at +12 h (Fig. 7g). Taken together, these results indicate that, during a +12–14-h time window that is critical for long-term fear memory consolidation, enhanced ripple activity in vH depends on sustained learning-induced PV plasticity.

**c-Fos expression peak at +12–14 h depends on PV plasticity**

To investigate whether a requirement for PV neuron plasticity at +12–14 h for long-term memory consolidation might be correlated to induction of plasticity in local principal neurons, we determined whether there is a second peak of c-Fos induction after cFC or water maze learning in the hippocampus. In addition to an early peak at about +90 min, fractions of c-Fos+ cells in vH CA3 peaked again at +15 h after acquisition (Fig. 8a). c-Fos+ neurons were mostly located in pyramidal

neuron layers in hippocampal CA3 and CA1, and no PV neurons with detectably elevated c-Fos signals could be detected (Supplementary Fig. 5). Consistent with the notion that sustained PV plasticity was necessary following cFC for plasticity involved in long-term memory consolidation, the c-Fos peak at +15 h was abolished by pharmacogenetic inhibition of PV neurons at +3 h (Fig. 8b). Likewise, D1/5 antagonist delivery at +12 h or at +14 h suppressed elevated c-Fos at +15 h (Fig. 8c). Consistent with its association with PV plasticity, a second c-Fos peak at +15 h was also detected in vH after 2 d of water maze training (Fig. 8d). Suppression of the low-PV shift by local delivery of VIP antagonist at +12 h abolished elevated c-Fos+ neuron levels at +15 h (Fig. 8d). Taken together, these results suggest that, during a +12–14-h time window that is critical for long-term fear memory consolidation, enhanced c-Fos expression in vH depends on sustained PV plasticity.

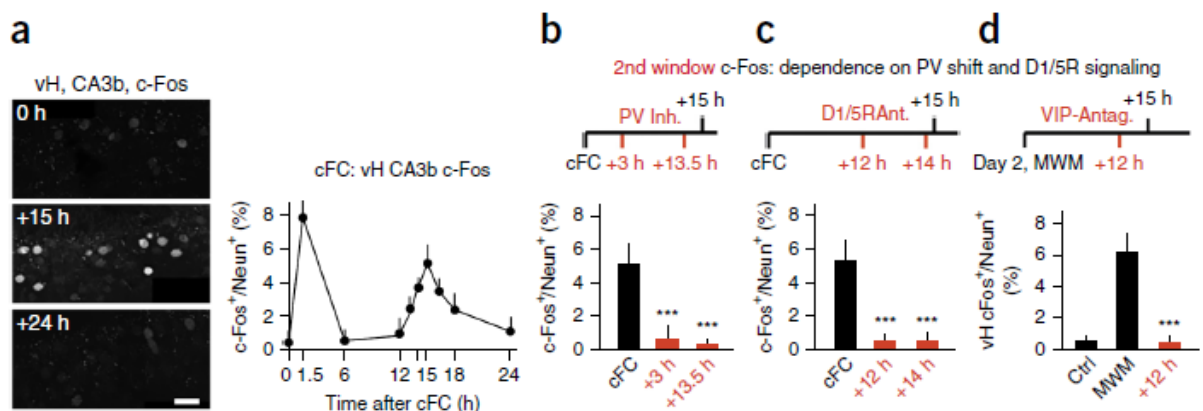


**Figure 8. c-Fos expression peak at +12h–14 h depending on PV plasticity.**

**(a) Time course of vH CA3b c-Fos expression following cFC.** Left, representative examples of c-Fos immunoreactivity. Scale bar represents 20  $\mu$ m.

**(b–d) Second peak of c-Fos induction in vH at +15 h** following cFC (b,c) or water maze training (d) suppressed by pharmacogenetic induction of low-PV plasticity at +3 h or +13.5 h (b), by local D1/5 antagonist delivery at +12 h or +14 h (c), or by local delivery of VIP antagonist at +12 h (d). Stars refer to corresponding untreated cFC or MWM values.

Average values from 6 (except 24h (4), 16h (5)) mice each; ANOVA, followed by Dunnett's post hoc; F/R2: 138/0.968 (b), 141/0.971 (d); P = 0.00021, 0.00028 (b), 0.00077, 0.00054 (c) 0.00051 (d). \*\*\*P < 0.001. Data are presented as mean  $\pm$  s.e.m.

## 2.2.4 Discussion

We investigated mechanisms of long-term memory consolidation and our results provide circuit-level insights into mechanisms specifically underlying the modulation and consolidation of long-term memories. Our findings specifically relate plasticity triggered at the time of acquisition to long-term, but not short/intermediate-term, memory consolidation processes, and suggest that features of PV basket cell plasticity define time windows in which long-term memory consolidation depends on local D1/5 receptor signaling. Our findings further reveal that, although incremental and definite learning induce PV plasticity of opposite sign, regulation of that plasticity by D1/5 receptor signaling and the roles of the plasticity for long-term consolidation of memories appear to be undistinguishable in the different types of learning.

### **Plasticity specifically required for late memory consolidation**

PV plasticity was triggered by learning protocols during a few minutes at the time of acquisition and became dependent on D1/5 signaling for maintenance through a +12–14-h time window, when it was required for long-term memory consolidation. The idea that plasticity specifically required for long-term memory consolidation involves large fractions of local PV basket cells is consistent with the notion that long-term memory consolidation might involve local network activity as well as system-wide synchronization processes.

Although alterations in PV levels only became detectable 6 h after acquisition, PV plasticity was already modulated during the first 5 h after acquisition through endogenous D1/5 receptor signaling, providing a potential mechanism by which events occurring subsequent to acquisition might influence long-term memory consolidation processes at +12–14 h. Notably, interventions that specifically suppressed detectable learning-induced PV plasticity from +6 h on did not affect intermediate memory tested, for example, at +6.5 h. These results suggest that short- and intermediate-term memories are consolidated through plasticity processes, which are distinct and partially independent from those underlying long-term memories.

Our findings are consistent with previous reports that D1/5 DA receptor signaling 12 h after acquisition is important for long-term consolidation and strengthening of fear memories<sup>7,8,35</sup>. However, we found that a requirement for local D1/5 receptor signaling at +12–14 h was a shared feature of learning involving PV plasticity. Notably, we found that D1/5 receptor signaling at +12–14 h was specifically required in PV neurons to ensure maintenance of learning-induced PV plasticity that is important for long-term memory consolidation. Consistent with this notion, incidental learning, such as familiar object recognition, which did not involve PV plasticity, was not affected by D1/5 receptor antagonist delivered at +12 h (data not shown).

The marked consistency of a long-term consolidation time window at +12–14 h in the different forms of learning might suggest a possible relationship with the daily wake-sleep rhythm. However, we found that the timing of the long-term consolidation window was not affected by the time at which learning had occurred.

Thus, although a role for sleep in long-term memory consolidation, possibly through sharp-wave ripple activity, is well established<sup>15,16,49,50</sup>, our findings argue against the possibility that the long-term consolidation time window might be defined by the wake-sleep cycle. Although our results indicate that PV plasticity at +12–14 h is important for enhanced ripple densities, for a c-Fos peak at +15 h, and for long-term memory consolidation, the mechanisms that specify the particular time-window of PV plasticity requirement at +12–14 h remain to be determined.

A further finding is that each learning process appeared to trigger its own late consolidation time window and its own PV plasticity process. The mechanisms involved remain to be determined, but, with respect to PV neurons, they might involve triggering of plasticity and its associated time constraints in subsets of PV basket cells during learning, followed by entrainment of larger groups of PV basket cells through local network mechanisms. Such a model might reconcile plasticity in large fractions of PV basket cells with sparse learning-related coding in hippocampal and cortical circuits.

## **Regulation of PV plasticity and long-term memory consolidation**

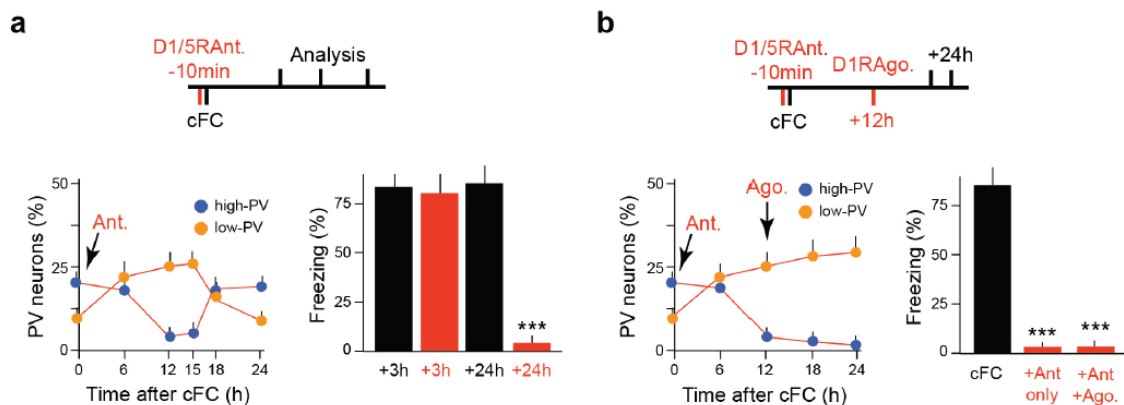
Our results point to cAMP metabolism in PV neurons as a key mechanism to regulate PV neuron plasticity. Enhancing AC activity specifically in PV neurons influenced long-term memory consolidation in incremental (inhibited; Fig. 5d) and definite learning (promoted; Fig. 6e), suggesting that cAMP levels in PV neurons influence both high- and low-PV plasticity. The finding that AC activation in naive mice resulted in comparable distributions of PV levels in early- and late-born PV neurons suggests that endogenous cAMP levels in late-born PV neurons with lower PV values under baseline conditions<sup>31</sup> might be comparatively low. This might, for example, involve high baseline cAMP hydrolyzing PDE activity conditions in late-born PV neurons, and high baseline cAMP synthesizing AC activity conditions in early-born PV neurons. Such distinct cAMP metabolism set points in early- and late-born PV neurons might be further potentiated following induction of plasticity. However, intracellular signaling networks involving cAMP can be particularly complex, and the actual molecular mechanisms underlying subpopulation-specific plasticity regulation remain to be determined.

Our findings suggest that D1/5 receptor signaling influences PV plasticity through mechanisms directly targeting PV neurons, and involving signal transduction pathways in PV neurons. In addition, D1/5 receptor signaling might influence local network activities such as sharp-wave ripples<sup>48</sup>, possibly again by targeting PV neurons, which might in turn support PV neuron plasticity through associated synaptic network processes. D1 DA receptors have been detected on PV neurons in prefrontal cortex, but precise information about cellular and subcellular expression sites of D1 and D5 receptors in hippocampus and neocortex PV neurons will be required to formulate more specific hypotheses as to how local D1/5 receptor signaling supports PV plasticity required for long-term memory consolidation.

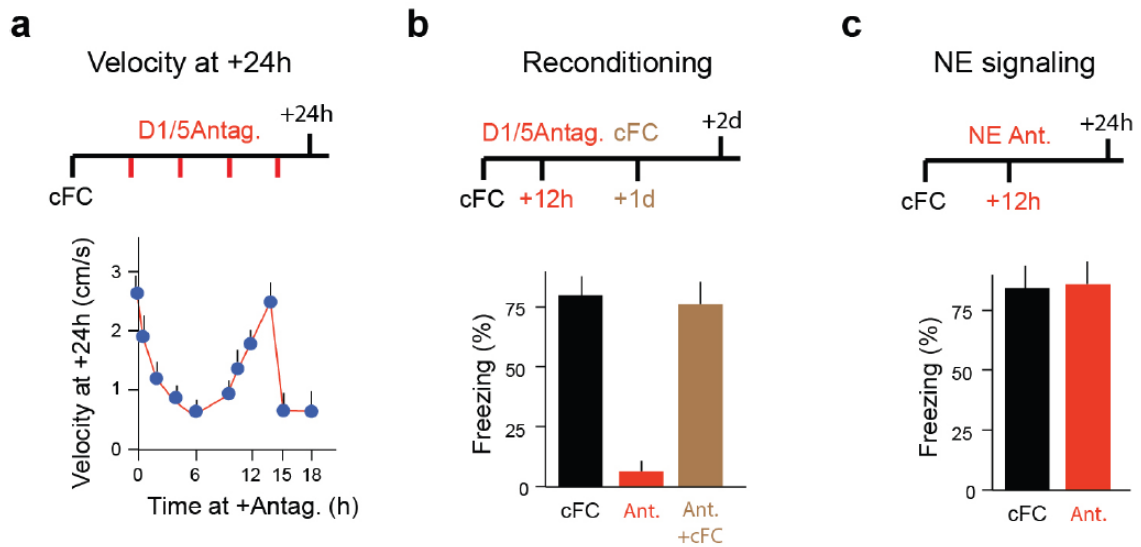
Finally, our findings, particularly the 2-h duration of the requirement for late D1/5 receptor signaling, are consistent with the notion that the configuration of local PV neurons late after acquisition might influence long-term memory consolidation through recurrent synaptic network processes leading to synaptic plasticity and strengthening of synapses involved in long-term memory traces. Local PV

networks have critical roles in fast oscillatory events such as sharp-wave ripples or spindles<sup>20–25</sup>, and the configuration of PV neurons might influence network activity by enhancing coherent activity of few strongly coupled neurons (high-PV configuration) or by facilitating binding of larger ensembles of weakly coupled neurons (low-PV configuration). The circuit mechanisms through which opposite-sign low- and high-PV plasticity specifically ensure long-term consolidation of provisional versus definite memories remain to be determined. However, because time course and regulation by D1/5 signaling were undistinguishable in learning involving low- or high-PV plasticity, our results indicate that regulation and role of PV plasticity reflect general mechanisms of long-term memory consolidation independent of the particular type of learning involved.

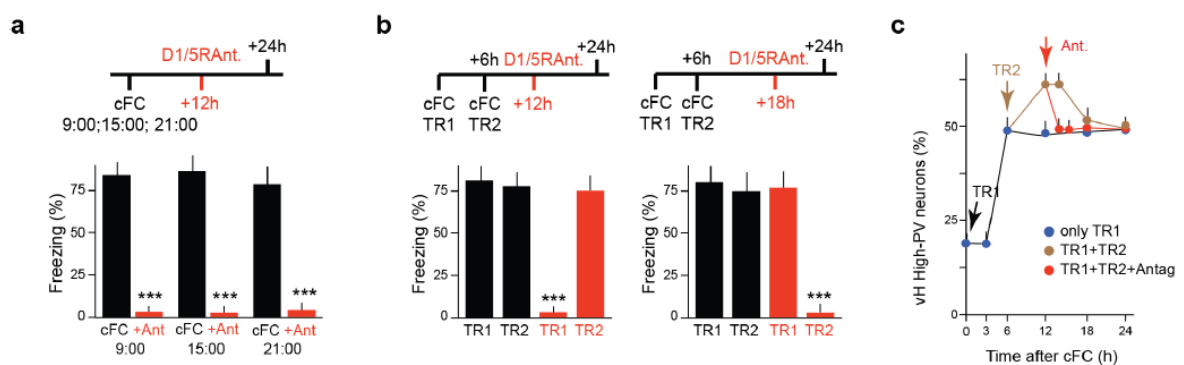
## 2.2.5 Supplementary Figures



**Suppl. Fig 1. D1/5 receptor signaling at acquisition required for PV plasticity and long-term fear memory consolidation.** a. Analysis of vH D1/5 signaling interference during fear memory acquisition. Note low-PV instead of high-PV shift induction (left), unaffected intermediate-term memory (+6.5h) and absence of long-term fear memory (+24h). b. No rescue of PV plasticity or fear memory by D1 agonist delivery at +12h in mice treated with D1/5 antagonist just before acquisition. Note sustainment of low-PV plasticity by D1 agonist at +12h (left), and absence of fear memory (right). Average values from 4-6 mice and 60 PV neurons each; ANOVA, followed by Dunnett's post-hoc;  $p < 0.001$  (\*\*\*)

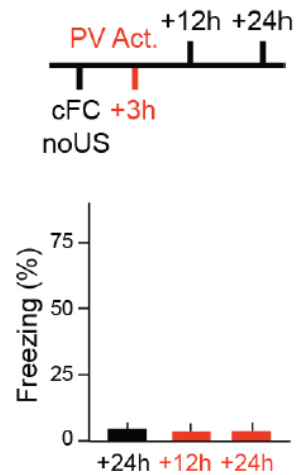


**Suppl. Fig 2. Specific suppression of long-term memory consolidation by D1/5 receptor antagonist at +12h.** a. Analysis of average center of mass movement (translocation) velocity in mice subjected to cFC, treated with D1/5 receptor antagonist at different times after acquisition (x-axis), and analyzed at +24h in training context. Note how mice with suppressed fear memory (e.g. +13h) do not move faster than untreated control mice (0h), arguing against loss of freezing due to hyper-locomotion. b. Mice that underwent cFC and were treated with D1/5 antagonist at +12h exhibit robust fear memory at +2d when reconditioned at +24h (orange), indicating that D1/5 antagonist at +12h specifically suppressed long-term consolidation of the fear memory induced 12h before (red). c. NE receptor antagonist delivered at +12h to vH does not interfere with long-term consolidation of fear memory. Average values from 4-6 mice.



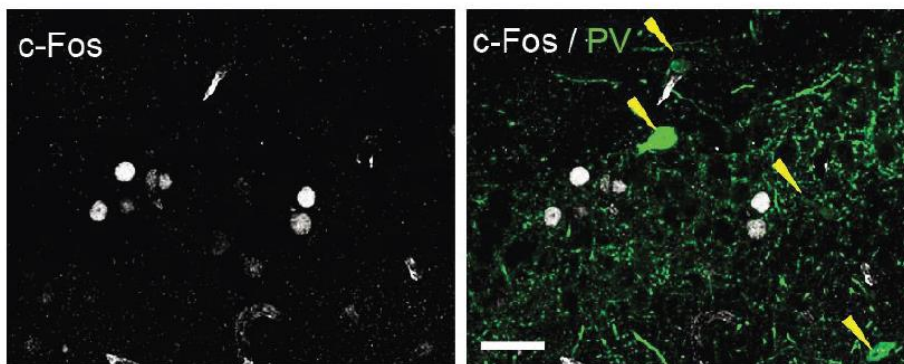
**Suppl. Fig 3. Specific suppression of individual long-term memories by D1/5 receptor antagonist at +12h.** a. Delivery of D1/5 receptor antagonist to vH at +12h suppresses fear memory consolidation regardless of whether acquisition occurred at 09:00, 15:00 or 21:00. b, c. Memory specific requirement for vH D1/5 receptor signaling at +12h for long-term memory consolidation. b: Specific suppression of TR1 or TR2 fear memory by D1/5 receptor antagonist at +12h after corresponding fear conditioning. c: Enhanced high-PV plasticity upon second cFC protocol, and reversal to high-PV levels comparable to those induced by one cFC protocol upon delivery of D1/5 receptor

antagonist at +12h. Average values from 4-6 mice and 60 PV neurons each; Student's t-test;  $p < 0.001$  (\*\*\*)



**Suppl. Fig 4. Pharmacogenetic induction of high-PV plasticity in naïve mice not sufficient to induce freezing.** Mice expressing pharmacogenetic activator virus in vH CA3 PV neurons explored context without foot shocks (no US), where treated with pharmacogenetic ligand at +3h, and tested for freezing in context at +12h or +24. Average values from 4-6 mice and 60 PV neurons each.

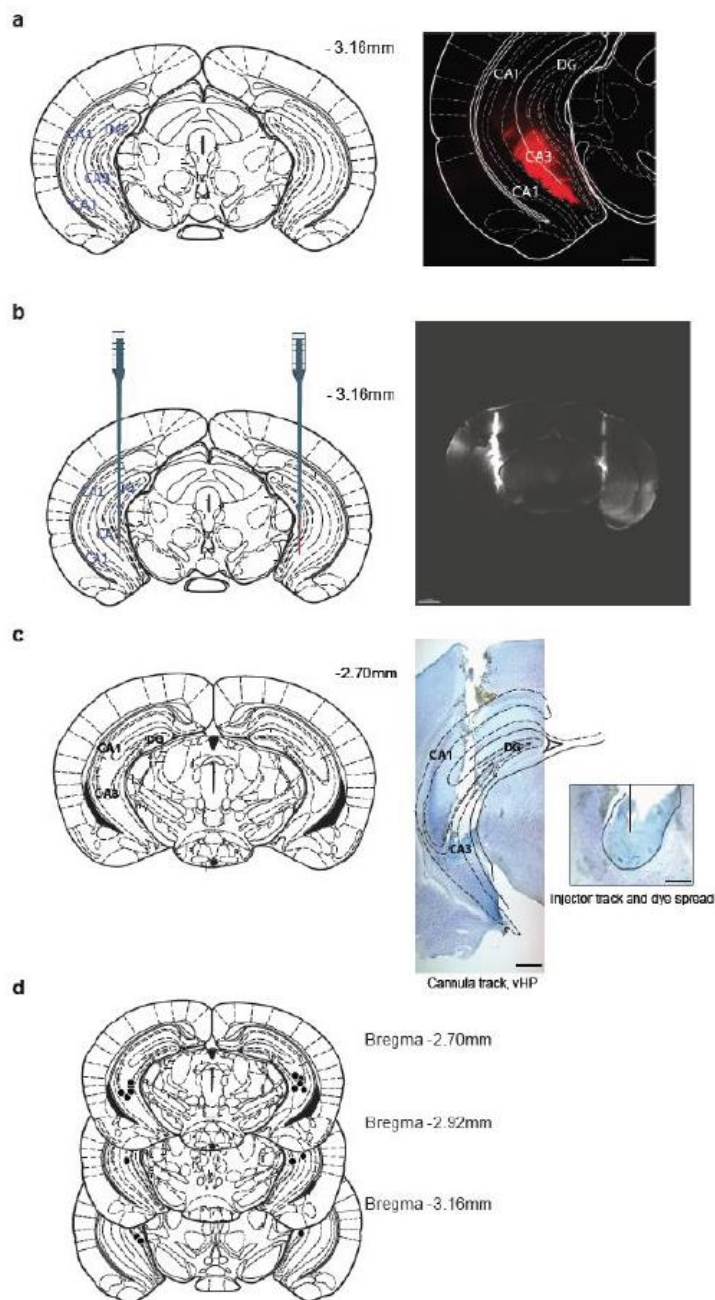
### cFC, +1.5h (vH, CA3b)



c-Fos+/NeuN+ : 5.7%  
c-Fos+/PV+ : < 1%

**Suppl. Fig 5. No detectable expression of cFos in vH CA3b PV neurons 90min after cFC.** Representative example of c-Fos/PV double-labeling experiment in vH CA3b 90min after cFC. Yellow arrows: PV+ neurons. Bar: 50  $\mu$ m. Average values from 3 mice and 80 PV neurons each.





**Suppl. Fig 6. Analysis of dye spread and electrode paths.** a. Left: Mouse brain coronal section with location of vH (DG, CA3, CA1). Numbers: antero-posterior coordinates caudal to bregma. Right: Representative image of Bodipy dye targeted at vH CA3 and its spread from the target site 6h after injection. Bar, 300 $\mu$ m. b. 16 channel Neuronexus probes (LFP experiments) inserted in both vH with 16 contacts covering 0.8mm length at the electrode tip. Example of electrode track position revealed with Dye I (right). Bar, 1500 $\mu$ m. c. Representative images of Nissl stained vH section (50  $\mu$ m) through the cannula track after dye injection (left). Bar: 200  $\mu$ m. Infusion site (dotted line) and injector track (black line) (right). Bar 100  $\mu$ m. d. Injection sites from 8 mice into CA3 region of vH.

### **2.2.6 Acknowledgments**

F. Carvalho (Friedrich Miescher Institut) found that PV plasticity was influenced by cAMP levels in PV neurons, and we acknowledge his contribution to this study. We thank S. Arber (FMI) for valuable comments on the manuscript. This work was supported in part by a Swiss National Fund grant to P.C. and by the NCCR Synapsy. The Friedrich Miescher Institut is part of the Novartis Research Foundation.

### **2.2.7 Author Contributions**

S.K. devised and carried out the local DA and PV interference and behavior experiments. A.C. carried out detailed time course analyses of hippocampal PV network plasticity following fear conditioning and maze learning, as well as experiments addressing signaling in PV neurons. F.D. carried out the initial pharmacogenetic and ChABC interference, as well as PV analysis experiments. C.Q. and C.M.M. carried out the LFP experiments. P.C. helped to devise the experiments and wrote the manuscript. All of the authors discussed the results and commented the manuscript.

### **2.2.8 References**

1. Kandel, E.R., Dudai, Y. & Mayford, M.R. The molecular and systems biology of memory. *Cell* 157, 163–186 (2014).
2. Dudai, Y. The restless engram: consolidations never end. *Annu. Rev. Neurosci.* 35, 227–247 (2012).
3. Redondo, R.L. & Morris, R.G. Making memories last: the synaptic tagging and capture hypothesis. *Nat. Rev. Neurosci.* 12, 17–30 (2011).
4. Bekinschtein, P. et al. Persistence of long-term memory storage requires a late protein synthesis- and BDNF- dependent phase in the hippocampus. *Neuron* 53, 261–277 (2007).
5. Caroni, P., Chowdhury, A. & Lahr, M. Synapse rearrangements upon learning: from divergent-sparse connectivity to dedicated sub-circuits. *Trends Neurosci.* 37, 604–614 (2014).
6. Katche, C. et al. Delayed wave of c-Fos expression in the dorsal hippocampus involved specifically in persistence of long-term memory storage. *Proc. Natl. Acad. Sci. USA* 107, 349–354 (2010).

7. Sekeres, M.J. et al. Increasing CRTC1 function in the dentate gyrus during memory formation or reactivation increases memory strength without compromising memory quality. *J. Neurosci.* 32, 17857–17868 (2012).
8. Katche, C., Cammarota, M. & Medina, J.H. Molecular signatures and mechanisms of long-lasting memory consolidation and storage. *Neurobiol. Learn. Mem.* 106, 40–47 (2013).
9. O'Neill, J., Pleydell-Bouverie, B., Dupret, D. & Csicsvari, J. Play it again: reactivation of waking experience and memory. *Trends Neurosci.* 33, 220–229 (2010).
10. Carr, M.F., Jadhav, S.P. & Frank, L.M. Hippocampal replay in the awake state: a potential substrate for memory consolidation and retrieval. *Nat. Neurosci.* 14, 147–153 (2011).
11. Singer, A.C. & Frank, L.M. Rewarded outcomes enhance reactivation of experience in the hippocampus. *Neuron* 64, 910–921 (2009).
12. Girardeau, G., Cei, A. & Zugaro, M. Learning-induced plasticity regulates hippocampal sharp wave-ripple drive. *J. Neurosci.* 34, 5176–5183 (2014).
13. Girardeau, G., Benchenane, K., Wiener, S.I., Buzsáki, G. & Zugaro, M.B. Selective suppression of hippocampal ripples impairs spatial memory. *Nat. Neurosci.* 12, 1222–1223 (2009).
14. Ego-Stengel, V. & Wilson, M.A. Disruption of ripple-associated hippocampal activity during rest impairs spatial learning in the rat. *Hippocampus* 20, 1–10 (2010).
15. Girardeau, G. & Zugaro, M. Hippocampal ripples and memory consolidation. *Curr. Opin. Neurobiol.* 21, 452–459 (2011).
16. Hsiang, H.L. et al. Manipulating a “cocaine engram” in mice. *J. Neurosci.* 34, 14115–14127 (2014).
17. Nakashiba, T., Buhl, D.L., McHugh, T.J. & Tonegawa, S. Hippocampal CA3 output is crucial for ripple-associated reactivation and consolidation of memory. *Neuron* 62, 781–787 (2009).
18. Jadhav, S.P., Kemere, C., German, P.W. & Frank, L.M. Awake hippocampal sharp-wave ripples support spatial memory. *Science* 336, 1454–1458 (2012).

19. Singer, A.C., Carr, M.F., Karlsson, M.P. & Frank, L.M. Hippocampal SWR activity predicts correct decisions during the initial learning of an alternation task. *Neuron* 77, 1163–1173 (2013).
20. Hu, H., Gan, J. & Jonas, P. Interneurons. Fast-spiking, parvalbumin GABAergic interneurons: from cellular design to microcircuit function. *Science* 345, 1255–1263 (2014).
21. Sullivan, D. et al. Relationships between hippocampal sharp waves, ripples, and fast gamma oscillation: influence of dentate and entorhinal cortical activity. *J. Neurosci.* 31, 8605–8616 (2011).
22. Ellender, T.J., Nissen, W., Colgin, L.L., Mann, E.O. & Paulsen, O. Priming of hippocampal population bursts by individual perisomatic-targeting interneurons. *J. Neurosci.* 30, 5979–5991 (2010).
23. Carr, M.F., Karlsson, M.P. & Frank, L.M. Transient slow gamma synchrony underlies hippocampal memory replay. *Neuron* 75, 700–713 (2012).
24. Hájos, N. et al. Input-output features of anatomically identified CA3 neurons during hippocampal sharp wave/ripple oscillation in vitro. *J. Neurosci.* 33, 11677–11691 (2013).
25. Stark, E. et al. Pyramidal cell-interneuron interactions underlie hippocampal ripple oscillations. *Neuron* 83, 467–480 (2014).
26. Chiovini, B. et al. Dendritic spikes induce ripples in parvalbumin interneurons during hippocampal sharp waves. *Neuron* 82, 908–924 (2014).
27. Korotkova, T., Fuchs, E.C., Ponomarenko, A., von Engelhardt, J. & Monyer, H. NMDA receptor ablation on parvalbumin-positive interneurons impairs hippocampal synchrony, spatial representations, and working memory. *Neuron* 68, 557–569 (2010).
28. Cardin, J.A. et al. Driving fast-spiking cells induces gamma rhythm and controls sensory responses. *Nature* 459, 663–667 (2009).
29. Hensch, T.K. Critical period plasticity in local cortical circuits. *Nat. Rev. Neurosci.* 6, 877–888 (2005).
30. Donato, F., Rompani, S.B. & Caroni, P. Parvalbumin-expressing basket-cell network plasticity induced by experience regulates adult learning. *Nature* 504, 272–276 (2013).

31. Donato, F., Chowdhury, A., Lahr, M. & Caroni, P. Early- and late-born parvalbumin basket cell subpopulations exhibiting distinct regulation and roles in learning. *Neuron* 85, 770–786 (2015).
32. Magnus, C.J. et al. Chemical and genetic engineering of selective ion channel-ligand interactions. *Science* 333, 1292–1296 (2011).
33. Zelikowsky, M., Bissiere, S. & Fanselow, M.S. Contextual fear memories formed in the absence of the dorsal hippocampus decay across time. *J. Neurosci.* 32, 3393–3397 (2012).
34. Lisman, J.E. & Grace, A.A. The hippocampal-VTA loop: controlling the entry of information into long-term memory. *Neuron* 46, 703–713 (2005).
35. Rossato, J.I., Bevilaqua, L.R., Izquierdo, I., Medina, J.H. & Cammarota, M. Dopamine controls persistence of long-term memory storage. *Science* 325, 1017–1020 (2009).
36. Shohamy, D. & Adcock, R.A. Dopamine and adaptive memory. *Trends Cogn. Sci.* 14, 464–472 (2010).
37. Huang, Y.Y. & Kandel, E.R. D1/D5 receptor agonists induce a protein synthesis-dependent late potentiation in the CA1 region of the hippocampus. *Proc. Natl. Acad. Sci. USA* 92, 2446–2450 (1995).
38. Hansen, N. & Manahan-Vaughan, D. Dopamine D1/D5 receptors mediate informational saliency that promotes persistent hippocampal long-term plasticity. *Cereb. Cortex* 24, 845–858 (2014).
39. Ortiz, O. et al. Associative learning and CA3-CA1 synaptic plasticity are impaired in D1R null, *Drd1a*<sup>-/-</sup> mice and in hippocampal siRNA silenced *Drd1a* mice. *J. Neurosci.* 30, 12288–12300 (2010).
40. Beaulieu, J.M. & Gainetdinov, R.R. The physiology, signaling, and pharmacology of dopamine receptors. *Pharmacol. Rev.* 63, 182–217 (2011).
41. Valjent, E. et al. Regulation of a protein phosphatase cascade allows convergent dopamine and glutamate signals to activate ERK in the striatum. *Proc. Natl. Acad. Sci. USA* 102, 491–496 (2005).
42. Sternson, S.M. & Roth, B.L. Chemogenetic tools to interrogate brain functions. *Annu. Rev. Neurosci.* 37, 387–407 (2014).

43. Lemon, N. & Manahan-Vaughan, D. Dopamine D1/D5 receptors gate the acquisition of novel information through hippocampal long-term potentiation and long-term depression. *J. Neurosci.* 26, 7723–7729 (2006).
44. Baudonnat, M., Huber, A., David, V. & Walton, M.E. Heads for learning, tails for memory: reward, reinforcement and a role of dopamine in determining behavioral relevance across multiple timescales. *Front. Neurosci.* 7, 175 (2013).
45. Kilts, C.D., Dew, K.L., Ely, T.D. & Mailman, R.B. Quantification of R-(+)-7-chloro-8-hydroxy-1-phenyl-2,3,4,5-tetrahydro-1H-3-methyl-3- benzazepine in brain and blood by use of reversed-phase high-performance liquid chromatography with electrochemical detection. *J. Chromatogr.* 342, 452–457 (1985).
46. Ruediger, S., Spirig, D., Donato, F. & Caroni, P. Goal-oriented searching mediated by ventral hippocampus early in trial-and-error learning. *Nat. Neurosci.* 15, 1563–1571 (2012).
47. Hosp, J.A., Pekanovic, A., Rioult-Pedotti, M.S. & Luft, A.R. Dopaminergic projections from midbrain to primary motor cortex mediate motor skill learning. *J. Neurosci.* 31, 2481–2487 (2011).
48. McNamara, C.G., Tejero-Cantero, Á., Trouche, S., Campo-Urriza, N. & Dupret, D. Dopaminergic neurons promote hippocampal reactivation and spatial memory persistence. *Nat. Neurosci.* 17, 1658–1660 (2014).
49. Rasch, B. & Born, J. About sleep's role in memory. *Physiol. Rev.* 93, 681–766 (2013).
50. Abel, T., Havekes, R., Saletin, J.M. & Walker, M.P. Sleep, plasticity and memory from molecules to whole-brain networks. *Curr. Biol.* 23, R774–R788 (2013).

2.3

**Early- and Late-Born Parvalbumin Basket  
Cell  
Subpopulations Exhibiting Distinct  
Regulation and Roles in Learning**

Flavio Donato\*, Ananya Chowdhury\*, Maria Lahr and Pico  
Caroni

Published: Neuron

Neuron 85, 770–786 (2015)

\* Equal contribution

### **2.3.1 Summary**

Brain networks can support learning by promoting acquisition of task-relevant information or by adhering to validated rules, but the mechanisms involved are poorly understood. Upon learning, local inhibitory parvalbumin (PV)-expressing Basket cell networks can switch to opposite configurations that either favor or interfere with further learning, but how this opposite plasticity is induced and relates to distinct learning requirements has remained unclear. Here, we show that PV Basket cells consist of hitherto unrecognized subpopulations, with distinct schedules of neurogenesis, input connectivities, output target neurons, and roles in learning. Plasticity of hippocampal early-born PV neurons was recruited in rule consolidation, whereas plasticity of late-born PV neurons was recruited in new information acquisition. This involved regulation of early-born neuron plasticity specifically through excitation, and of late-born neuron plasticity specifically through inhibition. Therefore, opposite learning requirements are implemented by distinct local networks involving PV Basket cell subpopulations specifically regulated through inhibition or excitation.

### **2.3.2 Introduction**

Brain plasticity enables individuals to flexibly produce adaptive behaviors, thereby learning from experience throughout life. Surprisingly, while molecular and cellular mechanisms underlying plasticity of individual synapses have been elucidated in substantial detail, how network and system level plasticity are adjusted to match requirements defined by experience has remained poorly understood. Reinforced trial-and-error learning tasks provide attractive experimental paradigms to investigate how plasticity is adjusted during learning. Thus, effective acquisition and flexible combination of potentially task-relevant information is essential during early phases of trial-and-error learning, whereas reliable application of validated routines dominates toward learning curve completion (Kaelbling et al., 1996). At the circuit level, these contrasting requirements are reflected by shifts in the configuration of local parvalbumin (PV)-expressing Basket cell networks, which exhibit pronounced plasticity induced by experience (Donato et al., 2013). Thus, PV network configurations enriched in neurons expressing low levels of PV and GAD67, and exhibiting high inhibitory



connectivity onto them are induced locally early during trial-and-error incremental learning, when they are required for effective learning. Such “low-PV configurations” promote acquisition and retention of new memories and structural synaptic plasticity (Donato et al., 2013). By contrast, configurations enriched in neurons expressing high levels of PV and GAD67, and exhibiting high excitatory connectivity onto them are induced toward completion of trial-and-error learning protocols. Such “high-PV configurations” interfere with the acquisition of new memories and structural synaptic plasticity (Donato et al., 2013). How induction of opposite PV network configurations is reliably and reversibly coupled to specific requirements during learning has remained unclear. The opposite configurations might emerge through learning-specific mechanisms sequentially shifting whole local PV neuron ensembles toward distinct network states. Alternatively, the opposite configurations might be induced through task-selective regulation of hitherto unknown PV neuron subpopulations.

PV-positive Basket cells are widely distributed and abundant GABAergic inhibitory interneurons that provide powerful local feedforward and feedback inhibition through perisomatic boutons onto principal excitatory neurons (Bartos et al., 2007; Klausberger and Somogyi, 2008; Hu et al., 2014). In addition, PV Basket cells inhibit each other reciprocally through perisomatic innervation and are dynamically coupled electrically through gap junctions (Bartos et al., 2007; Hu et al., 2014). As a result, PV Basket cells filter activation of principal neurons, and networks of PV Basket cells have major roles in regulating local ensemble activities, including theta and gamma oscillations (Fuchs et al., 2007; Cardin et al., 2009; Kuhlman et al., 2010; Isaacson and Scanziani, 2011; Lee et al., 2012; Hu et al., 2014). Synaptic regulation of PV Basket cells has been implicated in adult learning, and the maturation state of PV Basket cells has been implicated in critical period-type plasticity (Hensch et al., 1998; Hensch, 2005; Di Cristo et al., 2007; Southwell et al., 2010; Kuhlman et al., 2013; Wolff et al., 2014). The mechanisms through which PV neuron networks contribute to such a diverse range of functions have remained unclear.

The functions of GABAergic interneurons have been traditionally classified based on anatomical connectivities and physiological properties (Klausberger and

Somogyi, 2008). With the advent of methods for in vivo recording and genetic control of identified neurons in behaving animals, it became apparent that interneuron subtypes have distinct roles during behaviour and in learning by flexibly and selectively gating distinct information flows to principal neurons (Cardin et al., 2009; Isaacson and Scanziani, 2011; Pi et al., 2013; Wolff et al., 2014). These observations have led to new classifications of GABAergic neuron subtypes based on their specific circuit functions during behavior, complementing the original classifications based on anatomy and physiology (Kepecs and Fishell, 2014). In keeping with this emerging view of local GABAergic neuron functions, the induction of distinct PV network configurations upon learning might reflect specific and distinct roles of PV neuron subpopulations in different forms of learning.

Although PV Basket cells all share characteristic physiological and anatomical features, notable distinctions have been reported (Akgul and Wollmuth, 2013; Lee et al., 2014; Varga et al., 2014). A way through which neuronal subpopulations can be specified while maintaining many of their defining functional properties is through the acquisition of subfeatures during distinct developmental time windows of neurogenesis. For example, GABAergic interneurons differing in their schedule of neurogenesis tend to settle at different cortical layers in the adult (Rymar and Sadikot, 2007; Ciceri et al., 2013). Alternatively, closely comparable interneurons generated at different ganglionic eminence locations can have distinct functions (Chittajallu et al., 2013). PV Basket cells are generated in medial ganglionic eminence (MGE) during a protracted period of neurogenesis from embryonic day (E) 9.5 to E15.5 (Fishell, 2007). Accordingly, PV neurons generated at different times within this period might differ in connectivity/PV/GAD67 expression and/or in how they are regulated during experience-related plasticity.

Here, we investigated how plasticity of PV Basket cell networks leads to opposite configurations in response to specific learning requirements. We provide evidence that PV Basket cells consist of previously unrecognized subpopulations defined by their time schedule of neurogenesis, which exhibit plasticity upon distinct learning requirements and target distinct subpopulations of pyramidal

neurons in hippocampal cornus ammonis 1 (CA1). Learning depending on enhanced acquisition and combination of new information induces alterations in inhibitory connectivity specifically onto late-born PV Basket cells, whereas early-born cells are not affected. By contrast, learning that mainly relies on rule application induces alterations in excitatory connectivity onto early-born PV Basket cells, whereas late-born cells are not affected. We further show that early-born PV neuron cell plasticity is specifically regulated by excitation, whereas late-born PV neuron cell plasticity is specifically regulated by PV neuron inhibition. Late-born PV Basket cells specifically account for regulation of plasticity during critical periods of postnatal circuit maturation and upon environmental enrichment.

These results reveal how contrasting acquisition/exploitation requirements during learning are implemented through subpopulations of PV-expressing Basket cells, whose plasticity is regulated by distinct forms of learning specifically through excitation or inhibition. Because of their specific regulation properties, the two subpopulations of PV Basket cells might contribute to different mental health dysfunctions in conditions primarily affecting excitatory or inhibitory neurotransmission such as schizophrenia or autism (Chao et al., 2010; Curley et al., 2013; Han et al., 2014).

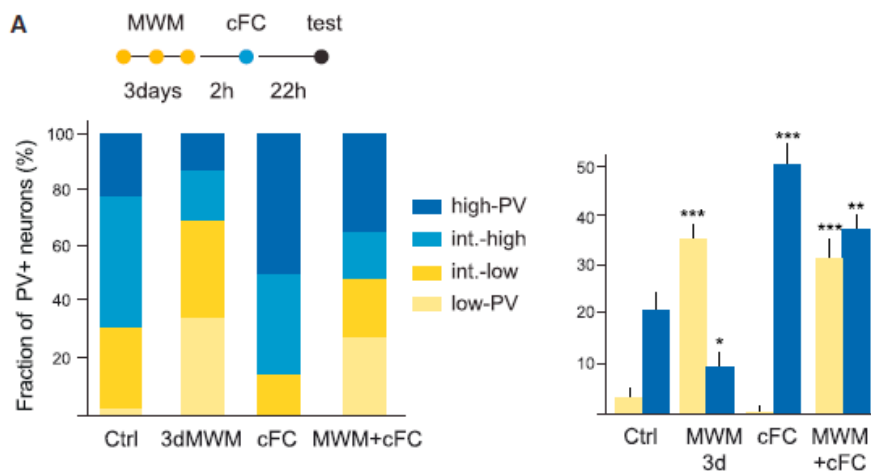
### **2.3.3 Results**

#### **Independent Regulation of High- and Low-PV Basket Cell Subnetworks upon Behavioral Learning**

To determine whether there might be PV Basket cell subnetworks that can be regulated independently by experience to reach high- and low-PV configurations, we sequentially subjected mice to learning protocols that induce opposite PV network configurations in the hippocampus. We trained mice in the Morris water maze during 3 days, thereby inducing a low-PV configuration in hippocampal CA3. Mice were subjected to contextual fear conditioning (cFC), a form of learning that induces a high-PV configuration in hippocampal CA3, two hours after the last maze training session (Donato et al., 2013). PV signal distributions were analyzed on day 4; i.e., 24 hr after maze training and 22 hr after cFC. Mice, only trained in the maze, exhibited the expected enrichment in low-PV neurons,

and mice, only subjected to cFC, exhibited a robust enrichment in high-PV neurons (Figure 1A). By contrast, mice, first trained in the water maze and then fear conditioned, exhibited elevated contents of both low and high-PV neurons, suggesting that low- and high-PV subnetworks can be induced in parallel upon learning (Figure 1A; one-way ANOVA correlation among all groups,  $p < 0.01$ ).

To further explore regulation of PV neuron subsets upon different forms of learning, we subjected mice to 3 weeks of environmental enrichment (EE), a protocol that induces a low-PV network configuration that persists for more than 8 weeks upon returning mice to control non-enriched conditions (Figure 1B). At the end of the 3 weeks of EE, mice were returned to their home cages and subjected 2 days later to cFC, a protocol that induces a high-PV configuration that persists for less than 2 weeks (Figure 1B). Again, 1 day after, cFC enriched mice exhibited both enhanced low- and high-PV neuron contents in hippocampal CA3 (Figure 1B; one-way ANOVA correlation among all groups,  $p < 0.01$ ; Student t test: EE versus EE 8 weeks not significant [n.s.], control versus cFC 2 weeks n.s.). Notably, 2 weeks after fear conditioning, the hippocampal PV network in these mice returned to its enriched low-PV configuration, not the baseline configuration (Figure 1B). By providing evidence for long-term memory of a low-PV network configuration in spite of the more transient high-PV arrangement induced upon cFC, these results suggested that independent PV neuron subsets can undergo plasticity upon enrichment and upon cFC.



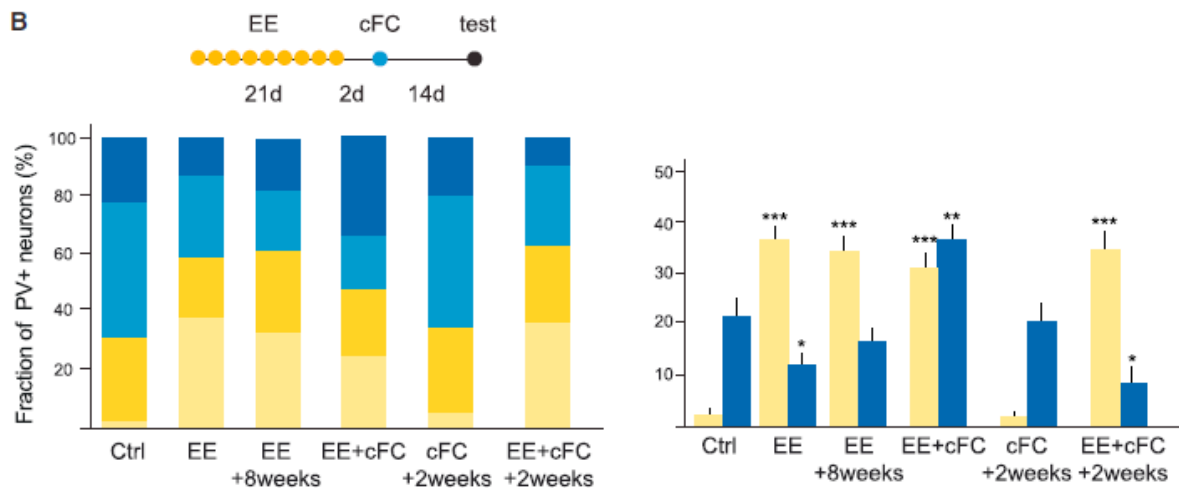


**Figure 1. Independent Regulation of High- and Low-PV Basket Cell Subnetworks upon Behavioral Learning**

(A) Three days of MWM learning followed by fear conditioning produce both low- and high-PV shifts in hippocampal CA3b. PV expression levels defined as described in Experimental Procedures.

(B) Long-term memory of low-PV network configuration in mice first enriched during 3 weeks and then fear conditioned. Average values (means  $\pm$  SEM) from five mice and 60 PV neurons each;  $p < 0.001$  (\*\*\*) and  $< 0.01$  (\*\*).

### Developmental Neurogenesis Schedule Predicts Baseline PV and Connectivity Levels in the Adult

PV neuron subsets could be selected from homogeneous pools of PV neurons through regulation by experience or might reflect the existence of PV neuron subpopulations with distinct regulatory properties. To investigate the possible existence of PV Basket cell subpopulations, we labeled proliferating cells at distinct stages of embryonic development with bromodeoxyuridine (BrdU) and analyzed BrdU/PV double-positive cells in hippocampal CA3 of 2–3 months old (adult) mice. We found that hippocampal PV neurons generated at E9.5 or E11.5 were predominantly high- and intermediate-high PV (Figure 2A). By contrast, neurons generated at E13.5 or E15.5 were predominantly intermediate-low- and low-PV (Figure 2A; one-way ANOVA,  $p < 0.0001$ ). Undistinguishable relationships were detected between time schedules of neurogenesis and PV or GAD-67 levels in PV neurons (Figure 2A). After neurogenesis, PV Basket cells migrate from MGE to populate most brain regions (Fishell, 2007; Marin, 2012). To

determine whether the dramatic bias in adult PV levels as a function of birthdate might apply generally to MGE-derived PV neurons, we analyzed BrdU/PV double-positive cells in hippocampal CA1, primary somatosensory whisker cortex, and dorsal striatum. In these different brain regions PV levels were again consistently correlated to birthdate, with intermediate-high/high-PV levels in E9.5- and E11.5-born cells and intermediate-low/low-PV levels in E13.5- and E15.5-born cells (Figure 2B).

Basket cells with high, respectively low PV/GAD67 levels exhibit major differences in excitatory and inhibitory synaptic puncta densities in the adult (Donato et al., 2013). Specifically, excitatory (Bassoon/PSD95-positive) to inhibitory (Gephyrin/VGAT-positive) synaptic puncta ratios vary as a function of PV signal levels, and are up to 4:1 in the most high-PV neurons and 1:2 in the most low-PV neurons (Figure 2C). This striking relationship between excitatory/inhibitory synaptic puncta ratios and PV levels was matched by a corresponding relationship between PV cell birthdate and synapse densities (Figure 2C; Student's t test, E9.5 and E11.5 differ from E13.5 and E15.5,  $p < 0.001$  [Bassoon] and  $p < 0.01$  [Gephyrin]; no significant difference between E9.5 and E11.5 or between E13.5 and E15.5). Notably, at comparable PV levels, early-born PV neurons tended to exhibit higher excitatory synaptic puncta densities, whereas late-born neurons exhibited higher inhibitory synaptic puncta densities, suggesting that early- and late-born PV neurons might differ in how they receive excitatory, respectively inhibitory synapses (Figure 2D). Therefore, PV neurons generated during the first half of subpallium neurogenesis (early-born) mainly exhibit high PV and GAD-67 level distributions and high excitatory synaptic puncta densities in the adult, whereas PV neurons generated during the second half of subpallium neurogenesis (late-born) predominantly exhibit low PV and GAD-67 levels and higher inhibitory synaptic puncta densities in the adult (Figure 2E).

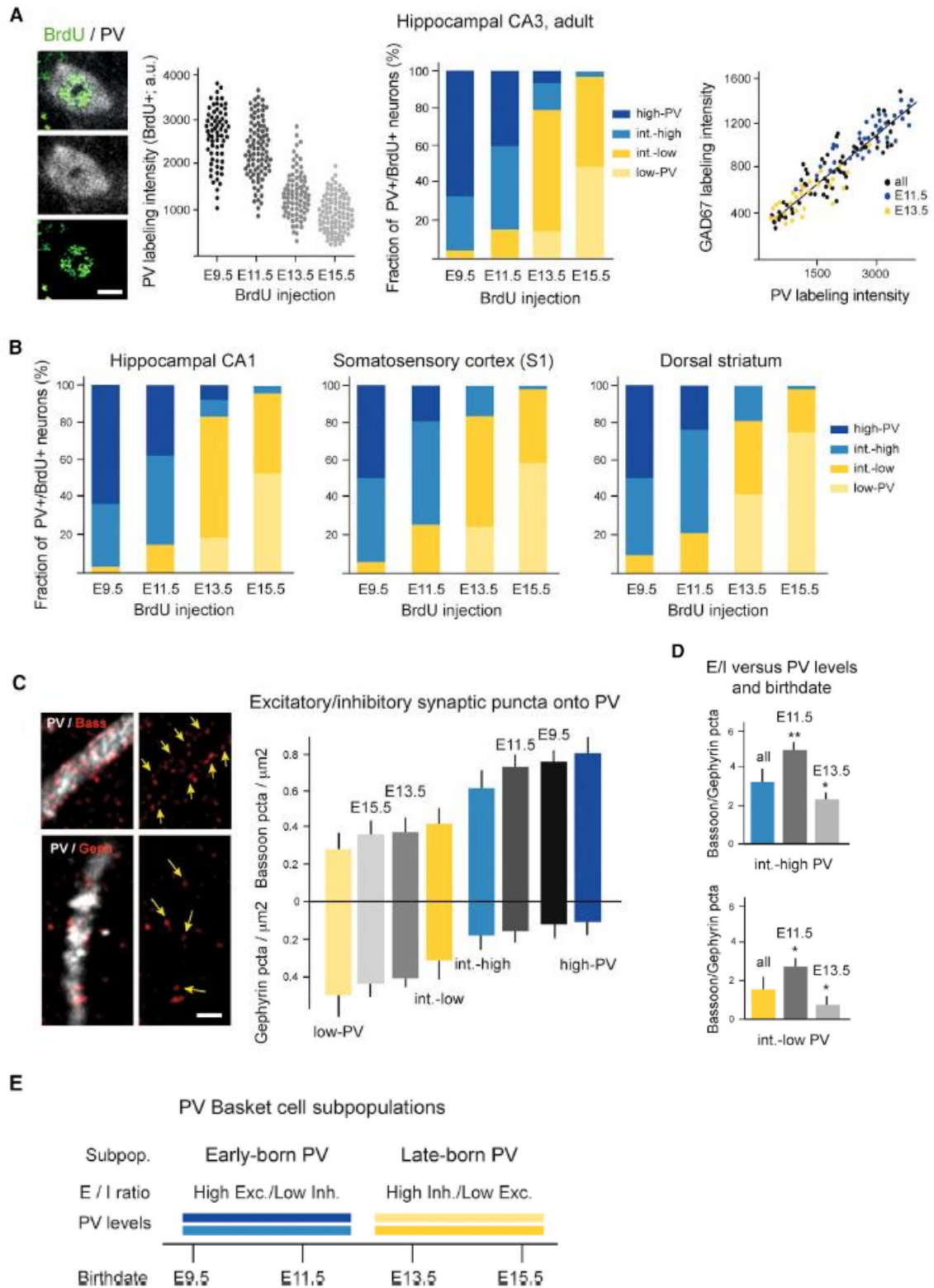


**Figure 2. Developmental Schedule of Neurogenesis Predicts Baseline PV Levels in the Adult.**

(A) Relationship between schedule of neurogenesis (BrdU labeling time) and PV/GAD67 levels in adult hippocampal CA3b. Left, representative example of PV neuron in adult hippocampal CA3b labeled with BrdU and scatter plot of PV labeling

values for cells (individual dots) labeled at E9.5, E11.5, E13.5, and E15.5. Center, labeling value distributions as a function of birthdate. Right, relationship between PV and GAD67 labeling signals in individual PV cells labeled at E11.5 or at E13.5 and comparison with random collection of PV cells.

**(B)** Relationship between schedule of neurogenesis (BrdU labeling time) and PV levels in adult hippocampal CA1, primary somatosensory (barrel) cortex, and dorsal striatum.

**(C) Relationship between schedule of neurogenesis and average values of excitatory (Bassoon) and inhibitory (Gephyrin) synaptic puncta densities onto PV dendrites in CA3b.** Left, representative examples of PV+ dendrites counterstained for Bassoon or Gephyrin (single confocal sections; arrows, individual synaptic puncta). Right, comparison of excitatory and inhibitory synaptic puncta densities for PV neurons identified by their PV labeling intensities or their birthdates.

**(D)** Relationship between PV labeling values and excitatory/inhibitory synaptic puncta densities for whole PV population (all), early-born PV neurons (labeled at E11.5), and late-born PV neurons (labeled at E13.5).

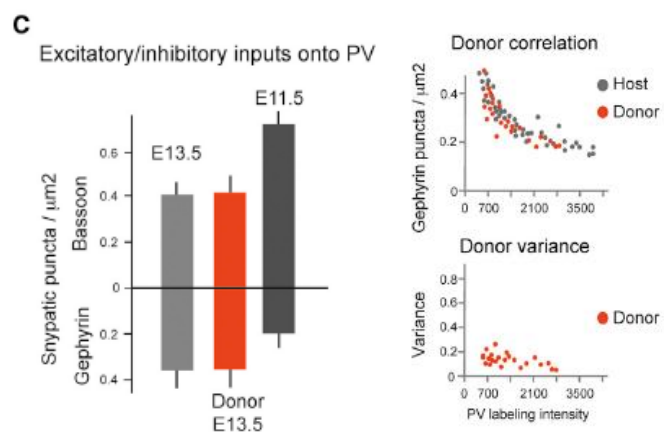
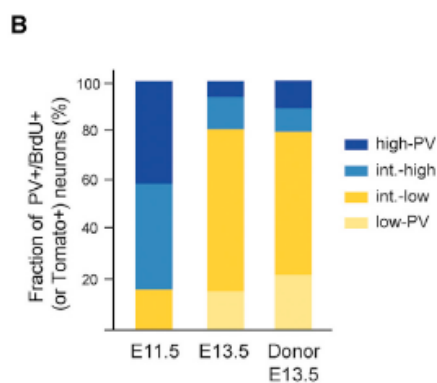
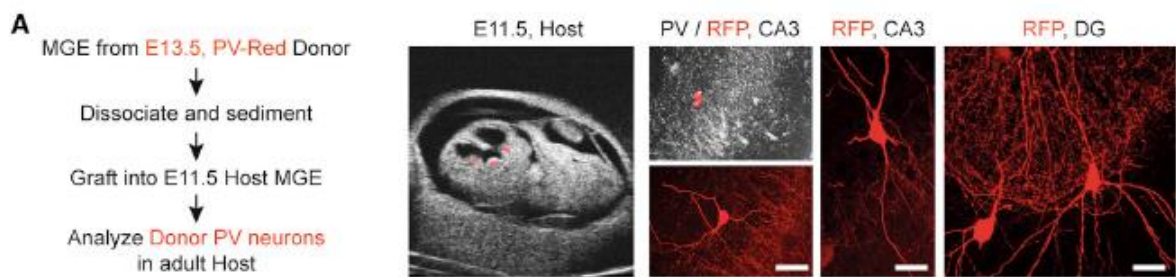
**(E) Schematic of how early- and late-born PV neurons exhibit distinct PV labeling intensities and excitation-inhibition connectivity in the adult.** (A–D) Average values (means  $\pm$  SEM) from five mice and 60 PV neurons each. Scale bars, 7 (A) and 2.5 (C) mm.

### **Adult PV/Connectivity Values Reflect Intrinsic Properties of Early- and Late-Born PV Neurons**

To determine whether the relationship between developmental time of neurogenesis and PV-excitatory/inhibitory values under baseline adult conditions reflects intrinsic properties of PVneurons and/or distinct signals from the environment during their migration and local network incorporation, we carried out donor-host graft experiments in embryonic mice. In a first series of experiments, donor PV neurons were dissected from the MGE of E13.5 PV-Cre:Rosa-flex-tdTomato embryos in which PV-expressing neurons are fated to express tdTomato, dissociated in vitro, concentrated, and injected under ultrasound guidance into E11.5 non-transgenic host MGE (Figure 3A). We determined whether, in the adult, the relatively older donor PV neurons had assumed an early, host-related fate, or whether they had maintained a late donor-related fate. We found that tdTomato-positive donor PV neurons exhibited predominantly low-PV neuron values characteristic of their birthdate in the donor embryo (Figures 3A and 3B; Mann-Whitney test, E11.5 versus E.13.5 or versus donor,  $p < 0.0001$



and E13.5 versus donor, n.s.). In parallel, late-born donor neurons exhibited low excitatory/inhibitory synaptic puncta ratio distributions (absolute values and variances) characteristic of late-born low-PV neurons (Figure 3C). In complementary experiments, we delivered neurons from the MGE of E11.5 PV-Cre: Rosa-flex-tdTomato embryos into E13.5 non-transgenic host MGE. We found that tdTomato-positive donor PV neurons exhibited high- and intermediate-high PV neuron values characteristic of their birthdate in the donor E11.5 embryo (Figure 3D). Therefore, PV and excitation/inhibition connectivity profiles of early- and late-born PV neurons in the adult reflect distinct intrinsic properties of these neurons determined at the time of neurogenesis. These results are consistent with the possibility that PV Basket cells generated during early and late developmental windows of neurogenesis might represent distinct subpopulations of PV neurons.



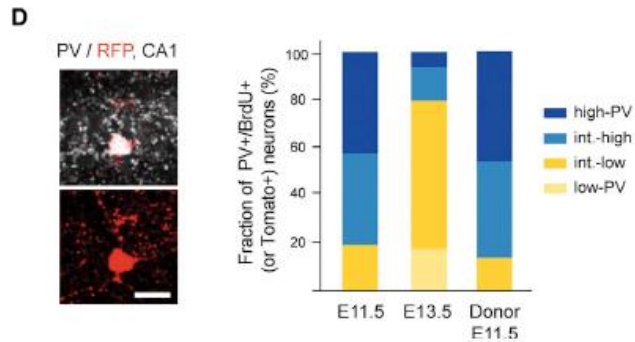


**Figure 3. PV and Connectivity Values in the Adult Reflect Intrinsic Properties of Early- and Late-Born PV Neurons.**

**(A) Grafting late-born (E13.5) MGE neurons into E11.5 MGE.** Left, schematic of experimental protocol. Center, ultrasound image of E11.5 host, with GE indicated by red dots. Right, examples of tomato-labeled donor PV neurons in adult CA3 and DG.

**(B) Distribution of PV labeling intensities in donor neurons closely matched to late-born PV neurons of host.** Average values (means  $\pm$  SEM) from five mice and 15–40 PV neurons each.

**(C) Densities of excitatory and inhibitory synaptic puncta along dendrites of donor PV neurons.** Graphs on the right, Gephyrin puncta densities along E13.5-born PV neurons and donor PV neurons (E13.5 donor) exhibit closely comparable distributions as a function of PV labeling intensities (correlation and variance). Dots represent individual PV neurons.

**(D) Grafting early-born (E11.5) MGE neurons into E13.5 MGE.** Left, example of tomato-labeled donor PV neuron in adult CA1. Right, distribution of PV labelling intensities in donor neurons closely matched to early-born PV neurons of host. Average values (means  $\pm$  SEM) from three mice and 20–30 PV neurons each. Scale bars, 30  $\mu$ m.

## Non-Overlapping Regulation of Cell-Plasticity in Early- and Late-Born PV Neurons

To determine whether intrinsic properties of PV neurons generated at early and late embryonic developmental time points might influence how these neurons are affected by learning in the adult, we subjected BrdU-labeled 2–3-month-old mice to either cFC or EE. cFC had a major impact on PV value distributions in hippocampal CA3 cells labeled at E9.5 or E11.5 (Figure 4A). By contrast, PV value distributions in cells labeled at E13.5 or E15.5 were not noticeably affected by cFC (Figure 4A). Conversely, EE affected PV value distributions of

hippocampal CA3 cells labeled at E13.5 or E15.5, but cells labeled at E9.5 or E11.5 exhibited no noticeable changes in PV value distributions upon EE (Figure 4A). Estimated fractions of PV neurons generated at the various time windows against the total of BrdU labeled PV neurons were 18.5% (E9.5), 32% (E11.5), 35.5% (E13.5), and 14% (E15.5). Combining these estimates with the values in Figures 1A, 2A, and 4A, we predict 48.7% high-PV neurons upon cFC (versus about 49.8% in Figure 1A) and 34.7% low-PV neurons upon EE (versus 35% in Figure 1A). In parallel, excitatory/inhibitory synaptic puncta ratios were affected by cFC selectively in cells labeled at E9.5 and E11.5 (excitatory puncta densities further enhanced), and by EE selectively in cells labeled at E13.5 or E15.5 (inhibitory puncta densities further enhanced; Figure 4B).

To search for molecular counterparts of excitatory versus inhibitory experience-dependent connectivity regulation onto early- versus late-born PV neurons, we focused on Mef2a, an activity-regulated transcription factor that has been linked to learning-related plasticity and that negatively regulates excitatory synapse numbers (Flavell et al., 2006). Under baseline conditions, PV and Mef2a levels in PV neurons were positively correlated, with highest Mef2a signals in early-born high-PV neurons and lowest Mef2a signals in late-born low-PV neurons (Figure 4C). Upon cFC, Mef2a levels decreased specifically in early-born PV neurons in parallel with increased excitatory puncta densities (Figure 4C). Furthermore, upon EE, Mef2a levels increased specifically in late-born PV neurons in parallel with increased inhibitory puncta densities (Figure 4C). Notably, regardless of endpoint PV values, Mef2a values of early-born neurons (>95%,  $p < 0.01$ ) were regulated by cFC, but not EE, whereas Mef2a values of late-born neurons were regulated by EE, but not cFC (Figure 4D). In control experiments, baseline and learning-induced changes in PV network configurations of BrdU-labeled mice were undistinguishable from those in non-labeled mice (data not shown).

To investigate whether subpopulation specific regulation of PV neurons during learning is a general phenomenon not restricted to cFC and EE, we analyzed PV and Mef2a level regulation in BrdU-labeled cells of mice subjected to water maze training. In this trial and error incremental learning protocol, hippocampal CA3 PV neurons first shift to a low-PV network configuration (days 2–6) and then to a

high-PV network configuration (>day 7) (Donato et al., 2013). Late-born PV neurons were selectively regulated during early phases of maze learning, when they reversibly shifted to low-PV/high-Mef2a values (Figure 4E). By contrast, early-born PV neurons were selectively regulated during late phases of maze learning, when they shifted to high-PV/low-Mef2a values (Figure 4E). The subpopulation specificity of learning-induced PV neuron regulation was thus undistinguishable for PV, Mef2a, and connectivity, but the signs of subpopulation specific Mef2a shifts were opposite to those induced in excitatory/inhibitory connectivity (Figure 4F). In the following, we designate these concerted alterations in PV/Mef2a/connectivity as PV neuron cell-plasticity.

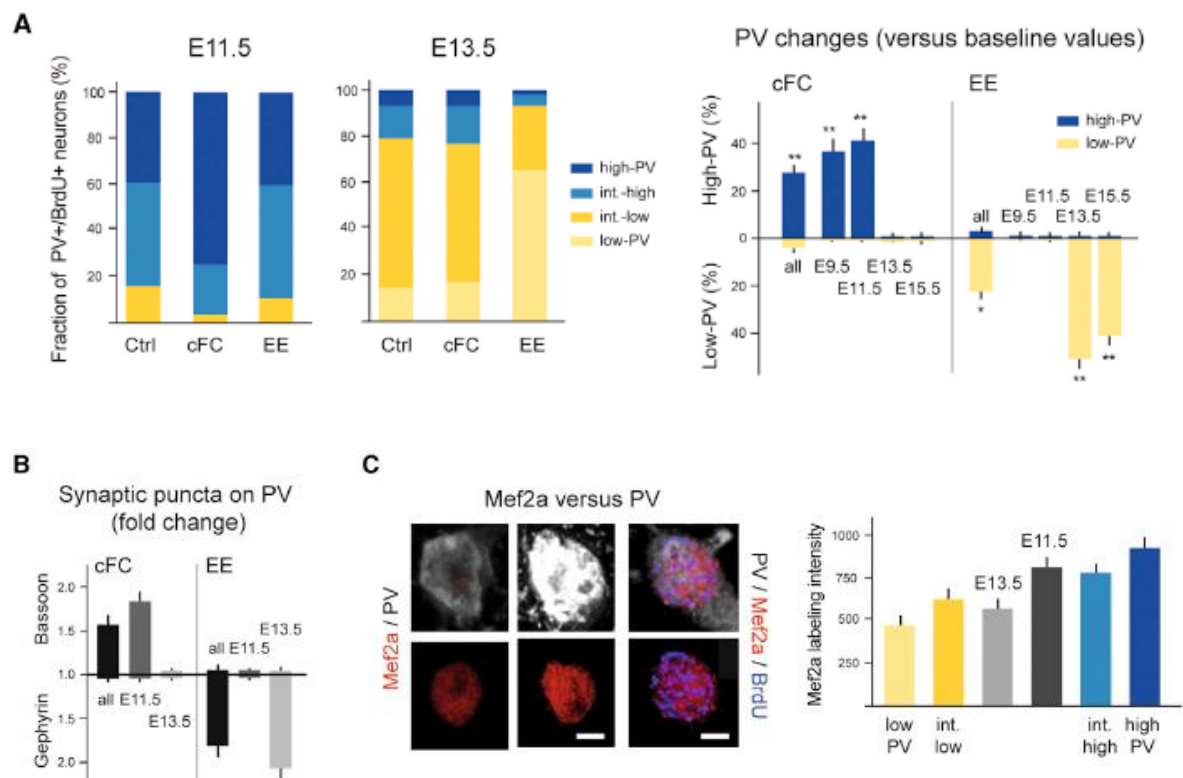


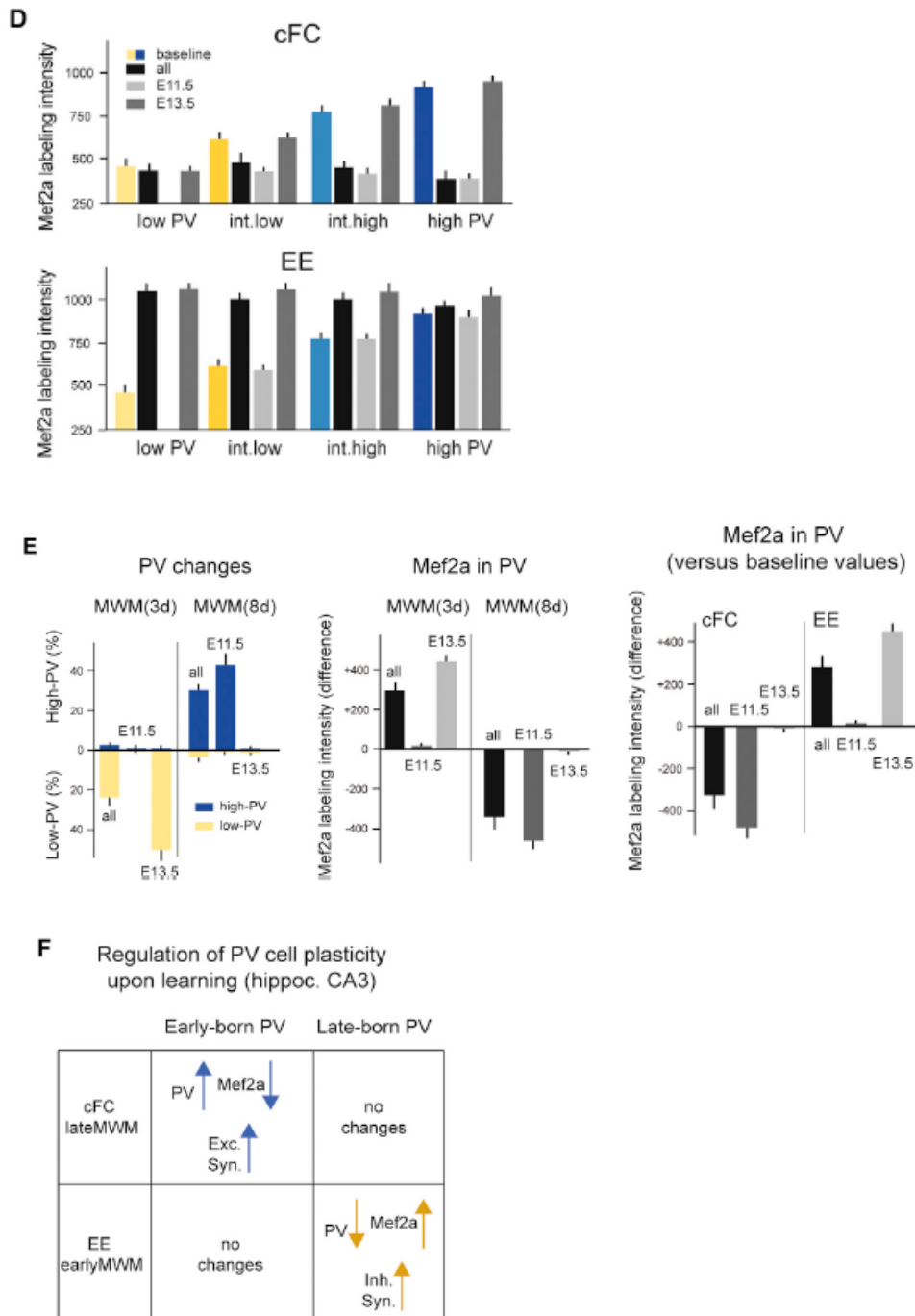
**Figure 4. Non-Overlapping Regulation of Cell-Plasticity upon Learning in Early- and Late-Born PV Neurons.**

**(A) Time schedule of neurogenesis versus regulation of PV levels upon cFC or EE.** PV changes (graph on the right) are indicated as differences of high- and low-PV contents in cFC or EE versus baseline values.

**(B) Time schedule of neurogenesis versus regulation of excitatory and inhibitory synaptic puncta densities onto PV neurons upon cFC or EE.**

**(C) Mef2a labeling levels in PV neurons under baseline conditions and upon cFC or EE.** Upper left, representative examples of Mef2a and PV labeling intensities. Upper

right, Mef2a versus PV levels or birthdate in adult hippocampal CA3b under baseline conditions. Lower panel, time schedule of neurogenesis versus regulation of Mef2a labeling intensities in PV neurons upon cFC or EE. Scale bars, 4 mm.



(D) Mef2a values as a function of endpoint PV values and PV neuron birthdate in cFC and EE experiments.

(E) Time schedule of neurogenesis versus regulation of PV or Mef2a levels PV early (3 days) and late (8 days) in MWM learning. Changes are against corresponding baseline values.

(F) Schematic of how early-born PV neurons undergo plasticity upon cFC and late in MWM learning, whereas late-born PV neurons undergo plasticity upon EE and early in maze learning.

(A–E) Average values (means  $\pm$  SEM) from five mice and 60 PV neurons each; Mann-Whitney,  $p < 0.01$  (\*\*), and  $p < 0.05$  (\*).

### **Early- and Late-Born PV Basket Cells Target Distinct Subpopulations of Pyramidal Neurons in CA1**

To determine whether early- and late-born PV Basket cell subpopulations exhibiting plasticity upon distinct learning requirements might in turn control distinct subpopulations of local excitatory neurons, we focused on their pyramidal neuron targets in hippocampal CA1. Deep cells in CA1 stratum pyramidale are generated 1–2 days before superficial cells during embryonic neurogenesis (Slomianka et al., 2011). When compared to superficial cells, deep cells exhibit distinct firing and gene expression properties (Mizuseki et al., 2011; Slomianka et al., 2011), receive stronger innervation from PV neurons (Lee et al., 2014), and exhibit distinct extra-hippocampal projection targets (Slomianka et al., 2011; Lee et al., 2014). Because PV levels at soma and presynaptic boutons of individual Basket cells are closely comparable (Donato et al., 2013), we analyzed distributions of PV labelling intensities at pyramidal layer presynaptic boutons as an estimate of PV neuron inputs. We found that in mice housed under control conditions, presynaptic boutons targeting deep layer pyramidal cells predominantly exhibited high- and intermediate-high PV signals, whereas presynaptic boutons targeting superficial cells predominantly exhibited low- and intermediate-low PV signals (Figure 5A). Bouton PV level distributions at deep layer pyramidal cells resembled those of early-born neuron somas, whereas those at superficial pyramidal cells resembled those at late-born neuron somas (Figure 5A). These distinctions were not majorly affected when the outer 20% or 40% of the pyramidal cell layer in dorsal hippocampus CA1 was compared, suggesting that the differences did not reflect a continuous gradient distribution (Figure 5A). Notably, a high-PV shift upon cFC was specifically restricted to terminals onto deep cells, whereas a low-PV shift upon EE was specifically restricted to terminals targeting superficial cells (Figure 5B). These results

suggested that early-born PV Basket cells preferentially target deep cells within the pyramidal cell layer in CA1, whereas late-born PV Basket cells preferentially target superficial cells.

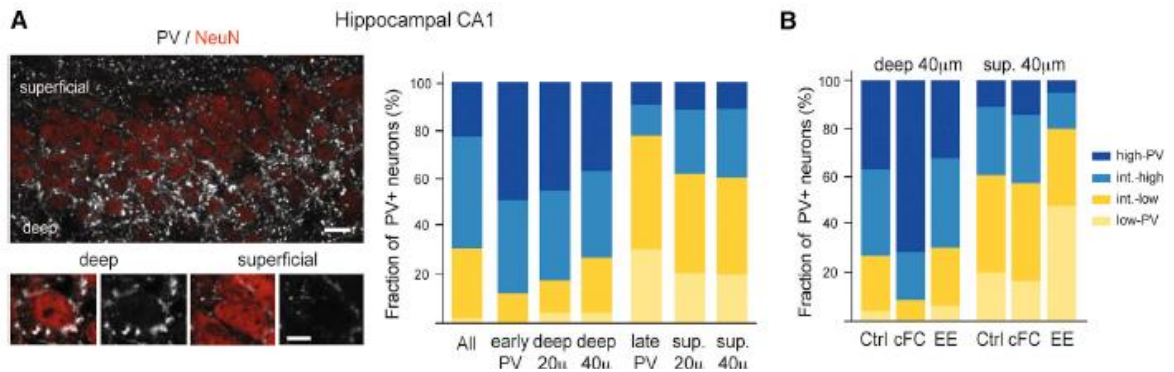


**Figure 5. Early- and Late-Born PV Neurons Preferentially Target Distinct Subpopulations of Principal Neurons in Hippocampal CA1.**

**(A) PV signals of perisomatic boutons at deep- and superficial-layer CA1 pyramidal cells.** Left, representative examples of bouton signal distributions at deep- and superficial-layer pyramidal neurons. Scale bars, 15 (top) and 5 mm. Right, PV level distributions of PV perisomatic boutons in hippocampal CA1. Weighted values at somas of E9.5 (18.5% of total BrdU-labeled PV neurons) and E11.5 (32% of total), early-PV, and weighted values at somas of E13.5 (35.5% of total) and E15.5 (14% of total), late-PV. Deep/superficial 20 m, first 20 mm from oriens or radiatum; deep/superficial 40 m, first 40 mm from oriens or radiatum.

**(B) PV level distributions of perisomatic boutons at deep- and superficial-layer CA1 pyramidal cells upon cFC or EE.** (A and B) Average values (means  $\pm$  SEM) from five mice and 300 boutons each. Scale bars, 30 mm.

### Early- and Late-Born PV Cell-Plasticity Specifically Associated with Distinct Learning Requirements

To determine whether subpopulation specific regulation involves the sign of PV/connectivity shifts or rather the specific type of learning requirement, we searched for systems where cFC, EE, and Morris water maze (MWM) might induce PV network shifts differing from those in hippocampal CA3. We found that in stark contrast to hippocampal CA3 and CA1, the PV cell network in hippocampal dentate gyrus (DG) shifted to a low-PV configuration upon cFC and at the end of MWM learning, and to a high-PV configuration upon EE and during MWM learning (Figure 6A). Like in CA3/CA1, PV baseline levels in DG PV cells

were positively correlated to developmental schedules of neurogenesis, with early-born cells predominantly exhibiting high and intermediate-high PV values and late-born cells exhibiting intermediate low and low PV values (Figure 6B). Notably, and again like in CA3/CA1, only early-born cells shifted PV levels upon cFC, or at the end of MWM learning, although in DG the shift was toward low-PV values (Figure 6C). Likewise, upon EE, or early in MWM learning, only late-born cells shifted their PV levels, but the shift in DG was toward high-PV values (Figure 6C). Mef2a levels again shifted opposite to PV levels; i.e., toward higher values upon cFC in early-born cells and toward lower values in late-born cells upon EE (Figure 6C). Therefore, although the signs of learning induced PV/Mef2a shifts were opposite in hippocampal CA3/CA1 and DG, early-born neurons were specifically regulated by cFC and at the end of MWM learning, whereas late-born neurons were specifically regulated by EE and early in MWM learning in all three hippocampal subdivisions.

We next determined whether shifts in excitation/inhibition synaptic puncta densities in DG adjust to the sign of PV changes; i.e., more inhibitory synaptic puncta upon a shift to low-PV and more excitatory synaptic puncta upon a shift to high-PV, or whether they adjust according to PV neuron subpopulation; i.e., changes in excitatory puncta for early-born cells and in inhibitory puncta for late-born cells. We found that in DG, cFC specifically induced a reduction in excitatory synaptic puncta onto early-born PV cells, and that EE specifically induced a reduction in inhibitory synaptic puncta onto late-born PV cells (Figure 6C). Therefore, both in CA3/CA1 and in DG, early-born PV neuron cell-plasticity specifically involved changes in excitatory connectivity onto PV neurons, whereas late-born cell-plasticity specifically involved changes in inhibitory connectivity onto PV neurons (Figure 6D).



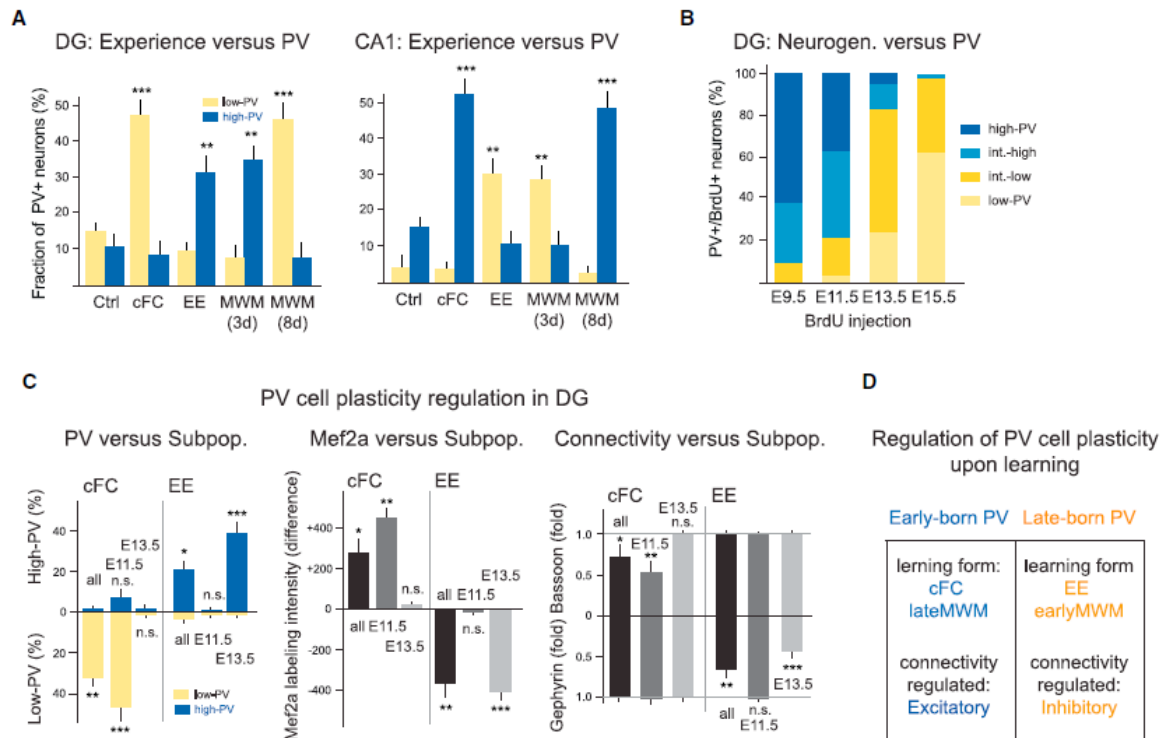


**Figure 6. Early- and Late-Born PV Cell-Plasticity Specifically Associated with Distinct Learning Paradigms.**

(A) Learning-related PV network shifts in hippocampal CA1 and DG.

(B) Baseline PV level distributions as a function of neurogenesis schedule in DG.

(C) PV neuron cell plasticity upon cFC or EE as a function of neurogenesis schedule in DG.

(D) Schematic of how cell plasticity in early-born PV neurons specifically involves changes in excitatory connectivity upon cFC or late in MWM learning, whereas plasticity in late-born neurons specifically involves changes in inhibitory connectivity upon EE or early in maze learning.

(A–C) Average values (means  $\pm$  SEM) from five mice and 60 PV neurons each;  $p < 0.001$  (\*\*\*) and  $< 0.01$  (\*\*).

### Subpopulation Cell-Plasticity Specifically Regulated through Excitation or Inhibition

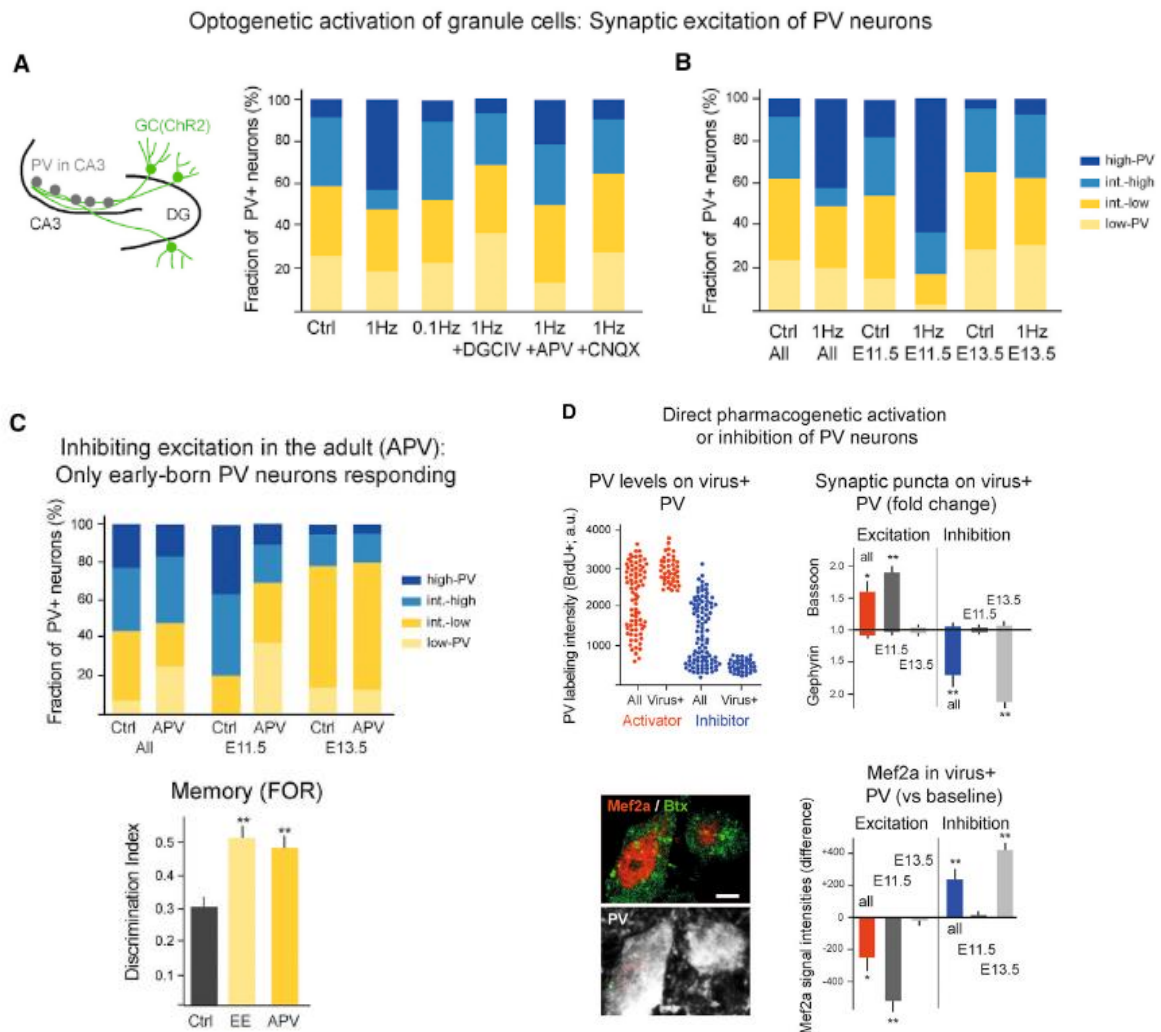
To investigate whether early-born PV neuron cell-plasticity might be specifically regulated through synaptic excitation, we took an optogenetic approach. Channel rhodopsin (Chr2) was expressed in DG granule cells in hippocampal slice cultures using an adeno-associated virus (AAV) viral construct. Light activation of granule cells (500 milliseconds pulses at 1 Hz during 3 min) induced a robust

increase in PV signals in Basket cells in CA3, consistent with the notion that excitatory synaptic stimulation of PV neurons can induce a high-PV shift (Figure 7A). The high-PV shift in CA3 was suppressed by an  $\alpha$ -amino-3-hydroxy-5-methyl-4-isoxazolepropionic acid or an N-methyl-D-aspartate (NMDA) receptor antagonist, and by an mGluR2 agonist, consistent with the notion that it involved plasticity-inducing mossy fiber-mediated synaptic transmission in CA3 (Figure 7A). Notably, early-born PV neurons exhibited markedly higher PV values upon optogenetic granule cell stimulation, whereas late-born PV neurons did not (Figure 7B). Since mossy fiber terminal filopodia contacted both early- and late-born PV neurons (data not shown), these results suggested that early-born, but not late-born PV neuron cell-plasticity, is regulated by excitation.

To investigate whether early-born PV neurons specifically respond to changes in synaptic excitation in situ, we treated adult mice pharmacologically with the competitive inhibitor of NMDA receptors, AP5. Delivery of AP5 during 3 days induced lower contents of high-PV and higher contents of low-PV neurons in hippocampal CA3 (Figure 7C). Notably, AP5 specifically affected PV levels in early-born neurons, whereas late-born neurons were not affected (Figure 7C). When AP5 treated mice were tested for hippocampal memory in the familiar object recognition (FOR) test, they exhibited enhanced memory comparable to EE mice (Figure 7C), suggesting that when a low-PV configuration is induced pharmacologically, it can enhance formation of new memories regardless of whether it involved plasticity in late- or in early-born PV neurons.

To further investigate specific regulation of PV subpopulation cell-plasticity by excitation or inhibition, we induced PV shifts in vivo using a direct pharmacogenetic approach (Magnus et al., 2011) in BrdU-labeled adult PV-Cre mice. In >98% of virus-transduced PV neurons, pharmacogenetic activation of PV neurons induced a high-PV shift, whereas pharmacogenetic inhibition induced a low-PV shift (Figure 7D; one-way ANOVA or post hoc Bartlett and Brown-Forsythe,  $p < 0.0001$ ). Notably, however, only early-born neurons exhibited a corresponding shift in Mef2a levels and excitatory synaptic puncta densities upon pharmacogenetic activation, whereas the high-PV shift in late-born cells did not involve a corresponding Mef2a/connectivity shift (Figure 7D). Likewise, only late-

born cells exhibited a corresponding Mef2a/inhibitory connectivity shift upon pharmacogenetic inhibition, whereas the low-PV shift was not accompanied by a corresponding Mef2a/connectivity shift in early-born neurons (Figure 7D). These results provided evidence that persistent direct non-synaptic excitation (through depolarization) or inhibition (through hyperpolarization) of PV neurons can shift PV expression values in all PV cells, but only early-born neurons exhibit Mef2a/connectivity plasticity upon excitation, and only late-born neurons exhibit Mef2a/connectivity plasticity upon inhibition (Figure 7E).



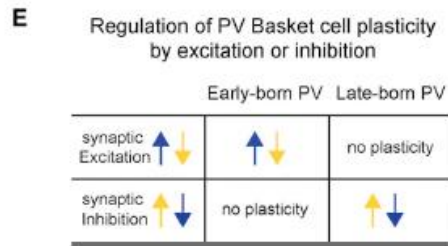


**Figure 7. Subpopulation Cell-Plasticity Specifically Regulated through Excitation, Respectively Inhibition.**

(A and B) Synaptic excitation of PV neurons in CA3 upon optogenetic activation of DG granule cells in hippocampal slice cultures.

(A) Schematic of experimental protocol (left) and experimental conditions producing a high-PV network configuration shift in CA3.

(B) High-PV shift upon granule cell activation in early-born PV neurons, but not in late-born PV neurons. Average values (means ± SEM) from three mice, six slice cultures, and 60 PV neurons each.

(C) Pharmacological inhibition of NMDA receptors in adult hippocampus specifically induces a low-PV configuration shift in early-born PV neurons, but not in late-born PV neurons. Top, average values from five mice and 60 PV neurons each. Bottom, enhanced FOR memory upon APV treatment; average values (means ± SEM) from four mice each.

**(D) Direct pharmacogenetic excitation or inhibition of PV neurons in adult hippocampal CA3.** Activator virus-positive PV neurons are all shifted to high-PV values (upper left, red), but only early-born PV neurons exhibit enhanced excitatory connectivity densities (upper right, red) and reduced Mef2a labeling values (lower panel, red). Average values (means ± SEM) from five mice and 60 PV neurons each; Mann-Whitney test,  $p < 0.05$  (\*), and  $p < 0.01$  (\*\*). Lower left, representative example of two PV neurons co-labeled for Mef2a and virus expression (Bungarotoxin [Btx]). Scale bar, 4 mm.

(E) Schematic of how early-born PV neurons specifically exhibit cell plasticity upon changes in their synaptic excitation, whereas late-born PV neurons specifically exhibit cell plasticity upon changes in their synaptic inhibition.

**Enhancing New Learning during Development and in the Adult Involves Late-Born PV Regulation**

Given that task-related requirements leading to enhanced new learning specifically involved inhibitory connectivity regulation on late-born PV neurons, we wondered whether this subpopulation of PV Basket cells might generally account for regulation enhancing new learning. Indeed, the opening of critical

period plasticity during circuit maturation depends on growing PV neuron inhibition (Hensch, 2005; Levelt and Hu bener, 2012). Furthermore, dissolving local perineuronal nets onto PV neurons, a procedure that induces a low-PV shift in the hippocampus, can prevent critical period closing and promotes adult plasticity (Pizzorusso et al., 2002). Accordingly, we investigated whether such critical period-type plasticity specifically involves late-born PV neuron regulation.

To investigate PV regulation by inhibition during circuit maturation, we analyzed the timing of PV neuron differentiation in developing mouse hippocampal CA3b. Following the establishment of a first mossy fiber bouton from postnatal day (P) 6–P7 on, large mossy fiber terminals went through a dramatic phase of filopodial growth (P7–P11), which was followed by expansion of the large core terminal and loss of most filopodia (Figure 8A) (Wilke et al., 2013). The filopodia contacted PV neurons and established putative presynaptic terminals onto these cells (Figure 8A). In parallel, we observed a gradual increase in PV positive cells in CA3 from P8 to P16, when PV-positive neuron densities reached >85% of adult levels (Figure 8A; one-way ANOVA,  $p < 0.05$ ). Interfering with mossy fiber transmission using an mGluR2 receptor agonist between P8 and P10 interfered with PV neuron maturation in CA3 and CA1, suggesting that this process is promoted by DG granule cell activity (data not shown). Mimicking increasing inhibition by delivery of the GABA-A receptor agonist Diazepam between P8 and P10 strongly increased low-PV neuron contents and total PV-positive (differentiated) neuron densities in hippocampal CA3 at P11 (Figure 8B). Notably, delivery of Diazepam during PV neuron maturation selectively enhanced PV-positive neuron numbers and low-PV contents among late-born PV neurons at P11, whereas early-born PV neurons were not affected by the treatment (Figure 8B).

To determine whether interventions that reinduce critical period-like plasticity in the adult also selectively target late-born PV neurons, we dissolved perineuronal nets in adult CA3b by locally applying Chondroitinase ABC (ChABC) (Pizzorusso et al., 2002). In hippocampal CA3 Wisteria floribunda lectin (WFA)-positive perineuronal nets were not restricted to cells with high PV levels and also surrounded cells with low-PV signals (Figure 8C). As expected, ChABC induced a robust low-PV shift in hippocampal CA3, although many cells exhibiting high-PV

signals were still detected (Figure 8C). Notably, ChABC specifically affected PV levels in late-born cells, whereas early-born cells were not affected (Figure 8C). Consistent with specific regulation of late-born PV neurons through inhibition, the low-PV shift upon ChABC was accompanied by a specific increase in inhibitory puncta densities onto late-born cells, whereas excitatory puncta were not affected (Figure 8C).

In further experiments aiming at relating induction of plasticity in the adult to late-PV neuron regulation, we determined whether delivery of Diazepam in the adult, a treatment that can induce critical period-like plasticity (Hensch, 2005), might again selectively affect late-born PV neurons. Delivery of Diazepam during 3 days induced higher contents of low-PV neurons in hippocampal CA3 (Figure 8D). Notably, Diazepam specifically affected PV levels in late-born PV neurons, whereas early-born neurons were not affected (Figure 8D).

Finally, to determine whether plasticity in late-born PV neurons is causally related to enhanced learning in the adult, we specifically interfered with learning-related inhibition of PV neurons during the first 3 days of water maze training by delivering vasointestinal peptide (VIP) antagonist to ventral hippocampus (Donato et al., 2013). As expected, VIP antagonist prevented a learning-related low-PV shift in ventral hippocampus (Figure 8E). Notably, the antagonist specifically affected learning-related plasticity in late-born PV neurons, whereas early-born PV neurons were not affected (Figure 8F). In parallel, the antagonist suppressed maze learning (Figure 8E), supporting the notion that plasticity in late-born PV neurons early during maze training is required for learning.

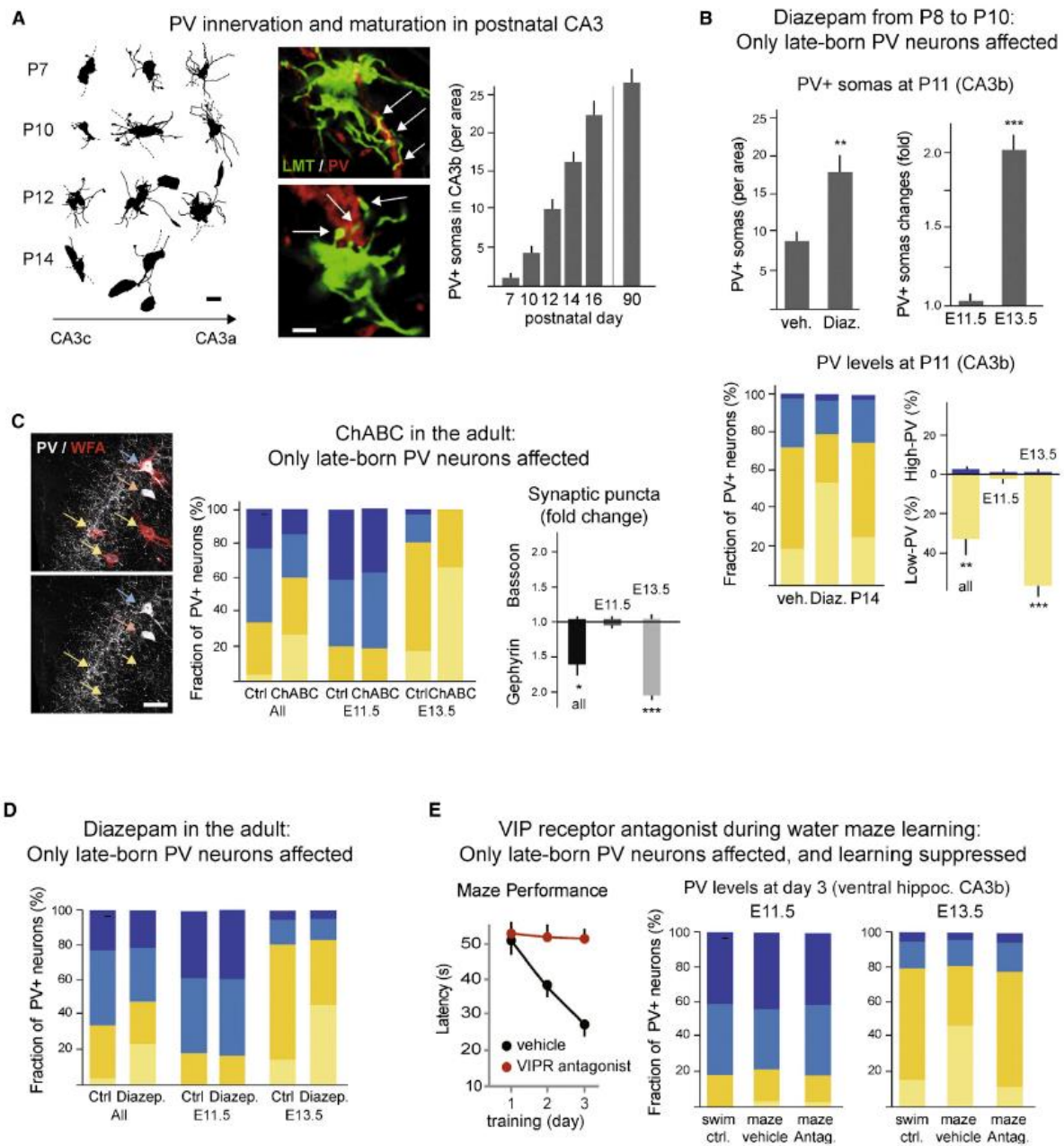


**Figure 8. Enhancing Plasticity during Development and in the Adult Involves Late-Born PV Regulation.**

**(A) Innervation and maturation of PV neurons in hippocampal CA3.** Left, representative camera lucida of large mossy fiber terminals with their filopodia along the CA3 axis (CA3c matures last). Center, representative examples of large mossy fiber terminals (LMT) in CA3b at P10, with filopodial varicosities contacting PV neuron dendrites (arrows). Right, average densities of PV+ neurons in CA3b as a function of age. Average values (means  $\pm$  SEM) from three mice and 15 areas each.

**(B) Enhancing inhibition with Diazepam between P8 and P10 specifically augments numbers of late-born PV+ low-PV neurons in CA3b at P11.** Left, PV+ soma densities.

Right, PV levels distributions. Average values (means  $\pm$  SEM) from five mice and 15 areas (or 40 PV neurons) each.

**(C) ChABC treatment in adult hippocampal CA3 specifically targets late-born PV neurons.** Left, representative example of PV/PNN (WFA) double labeling in CA3b. Some PNN+ neurons exhibit low PV levels (yellow arrows), some PNN+ neurons exhibit high PV levels (blue arrow), and some high-PV neurons exhibit no detectable PNNs (orange arrow). Center, PV level distributions in PV+ neurons upon ChABC as a function of PV neuron birthdate. Right, Synaptic puncta density changes upon ChABC (versus baseline values) onto PV+ neuron dendrites as a function of PV neuron birthdate. Average values (means  $\pm$  SEM) from five mice and 60 PV neurons each (C–E).

(D) Enhancing inhibition with Diazepam in adult CA3 specifically induces a low-PV shift in late-born PV neurons.

**(E) Interfering with plasticity specifically in late-born PV neurons prevents new learning in water maze training.** Left, learning curve during first 3 days of training, with and without interference with VIP receptor signaling in ventral hippocampus CA3. Right, specific low-PV shift in late-born PV neurons and interference by VIP receptor antagonist; analysis after third day of training. Scale bars, 3 (A) and 20 (C) mm.

### 2.3.4 Discussion

We have investigated how local PV network plasticity is regulated upon learning and provide evidence that PV Basket cells consist of two previously unrecognized subpopulations, which are specified during the first and second half of neurogenesis in mouse subpallium, and differ in their connectivities and plasticity regulation. Early-born PV Basket cells generated during the first half of neurogenesis exhibit comparatively high PV/ GAD-67 levels and excitation/inhibition connectivity ratios under baseline conditions, which in most cases further increase upon learning-induced plasticity. Furthermore, early-born PV neurons exhibit plasticity upon cFC and at the end of maze learning, but not upon EE or during maze learning. By contrast, late-born PV Basket cells specified during the second half of neurogenesis exhibit low PV/GAD-67 levels and excitation/inhibition connectivity ratios under baseline conditions, which in most cases further decrease upon learning-induced plasticity. Furthermore, late-born PV neurons exhibit plasticity upon EE, during maze learning, and when critical period-type plasticity is induced. Notably, early-born PV neuron cell plasticity is specifically regulated by excitation, whereas late-born PV neuron cell plasticity is specifically regulated by PV neuron inhibition. Furthermore, early- and late-born PV Basket cells preferentially target distinct subpopulations of pyramidal neurons



in hippocampal CA1. In the following sections, we discuss main implications of these findings, and how they relate to those of previous studies on the regulation of plasticity upon learning.

### **Two Subpopulations of PV Basket Cells**

Our results provide evidence for the existence of two subpopulations of PV Basket cells defined by their distinct schedules of neurogenesis. E13.5-derived PV neurons transplanted into the MGE of an E11.5 host embryo or E11.5-derived PV neurons transplanted into the MGE of an E13.5 host embryo exhibited characteristic features of donor PV neurons in the adult, providing evidence that PV/GAD-67 levels and excitatory/inhibitory connectivity ratios reflect intrinsic properties of PV neurons specified around the time of neurogenesis. Notably, regardless of their final PV levels, early-born neurons specifically exhibited excitatory connectivity and Mef2a regulation upon cFC, but not EE, and late-born neurons specifically exhibited inhibitory connectivity and Mef2a plasticity upon EE, but not cFC. Baseline Mef2a values in early- and late-born PV neurons were opposite than might have been predicted based on excitatory-inhibitory synaptic puncta densities in the two subpopulations, whereas Mef2a regulation upon plasticity was as might have been predicted (Flavell et al., 2006; i.e., toward lower-Mef2a and higher-excitatory puncta and toward higher-Mef2a and higher inhibitory puncta). While subpopulation specific Mef2a baseline values might provide for effective regulation of synaptic density changes in the two subpopulations upon induction of plasticity, whether the Mef2a shifts upon plasticity do mediate changes in synapse densities onto PV neurons remains to be determined.

Taken together, these results suggest that PV Basket cells generated up to E11.5 exhibit closely comparable early-born PV neuron properties, whereas Basket cells generated from E13.5 on exhibit closely comparable late-born PV neuron properties. Together, these time windows account for 80%–85% of total PV Basket cell neurogenesis in the MGE (data not shown). While our results are consistent with the notion that with respect to experience-related cell plasticity, PV Basket cells can all be assigned to one of two opposite subpopulations, our analysis cannot address subpopulation distributions at the time of early/late-born

PV neurogenesis overlap. Furthermore, our results do not exclude the existence of further distinctions among PV Basket cells (see Varga et al., 2014).

The consistent experience-related plasticity regulation of the two subpopulations of PV Basket cells raised the issue of whether these might also exhibit distinct output targets related to behavioral function (Kepecs and Fishell, 2014; Lee et al., 2014). While PV Basket cells exhibit high probabilities of connectivity to local principal neurons, early-born PV neurons are more abundant in deep cortical layers of neocortex, whereas late-born neurons are more abundant in upper layers (Ciceri et al., 2013), suggesting that early- and late-born PV neurons might directly control different ensembles of excitatory cortical neurons. Indeed, we found that early-born PV neurons preferentially target deep cells in the pyramidal layer of hippocampal CA1, whereas late-born PV neurons preferentially target superficial cells. The selective connectivity between early/late-born PV neurons and early/late-born pyramidal cells is reminiscent of selective connectivity among principal neuron subpopulations in hippocampal DG, CA3, and CA1, suggesting that it might reflect circuit assembly principles based on relative schedules of neurogenesis and neuronal maturation (Deguchi et al., 2011). While the functional implications of the selective output connectivity of PV neuron subpopulations remain to be determined, our findings would be consistent with the notion that the distinct excitation/inhibition input ratios onto early- and late-born PV neurons and the specific regulation upon learning might reflect information flow through functionally distinct microcircuits (see Larkin et al., 2014).

### **Convergent Network and Plasticity Regulation through Excitation or Inhibition in Learning**

A key finding of our study is that early-born PV neuron plasticity is regulated through excitation and late-born PV neuron plasticity is regulated through inhibition. Furthermore, cell plasticity in early-born neurons involved alterations in the densities of excitatory, but not inhibitory synaptic puncta, and cell plasticity in late-born neurons involved alterations in inhibitory, but not excitatory synaptic puncta densities onto PV neuron dendrites. These matched specificities of regulation were particularly striking in comparisons of how cFC or EE induced PV

cell plasticity in CA3/CA1 versus DG. Thus, while cFC consistently involved early-born neuron plasticity and EE consistently involved late-born neuron plasticity, the signs of PV and Mef2a changes were opposite in the hippocampal subdivisions, and this was reflected in opposite signs of excitatory, respectively inhibitory connectivity regulation in the two subpopulations. The functional significance of opposite PV level regulation upon learning in CA3/CA1 versus DG is currently unclear, but it is reminiscent of reports that perisomatic inhibition can have opposite effects on principal neurons in CA1 and DG (Sauer et al., 2012). Taken together, our results suggest that PV neuron regulation specifically through excitation provides a mechanism to match implementation of validated rules in learning to early-born PV neuron cell plasticity. Likewise, regulation of PV neurons specifically through inhibition matches enhanced plasticity and learning to late-born PV neuron cell plasticity. While the circuit mechanisms linking the opposite requirements in behavioral learning to plasticity of specific PV Basket cell subpopulations remain to be determined, they might involve specific learning-related gating mechanisms, as revealed in recent studies of Pavlovian conditioning (Lovett-Barron et al., 2014).

Concerning the mechanisms underlying specific regulation of PV Basket cell subpopulations through excitation or inhibition, our findings suggest that early- and late-born PV neurons exhibit distinct cellular regulatory networks. Thus, pharmacogenetic depolarization (excitation) induced enhanced PV levels in all transgene-expressing neurons, but only early-born neurons exhibited corresponding cell plasticity regulation, including reduced Mef2a levels and enhanced excitatory connectivity. Likewise, only late-born PV neurons exhibited cell plasticity regulation upon pharmacogenetic hyperpolarization (inhibition). Furthermore, while ChABC dissolved perineuronal nets surrounding all PV neurons, only late-born PV neurons exhibited reduced PV levels and enhanced inhibitory connectivity upon this pharmacological treatment. Early-born Lsi1 mossy fiber terminal filopodia (Deguchi et al., 2011; Ruediger et al., 2011) did not appear to preferentially contact dendrites of high- and intermediate-high PV neurons in stratum lucidum, and VIP boutons were not obviously enriched among the GABAergic boutons contacting low and intermediate-low PV neuron dendrites in CA3 stratum radiatum (data not shown), suggesting that specific learning-

related regulation of PV neuron plasticity might not reflect specific patterns of input connectivity onto early- and late-born PV neurons, but resolving this important issue will require more detailed studies. Taken together, our results suggest that distinct intracellular signaling features (Spiegel et al., 2014) in early- and late-born PV neurons might be sufficient to ensure control of early-born PV neurons selectively through excitation and of late-born PV neurons selectively through inhibition.

### **Distinct Functional Roles of PV Basket Cell Subpopulations**

Our results establish late-born PV Basket cells as the subpopulation that specifically accounts for positive regulation of plasticity during learning, upon EE, and during critical period-like plasticity. These results provide a unifying framework to account for how apparently unrelated phenomena produce closely comparable consequences on learning and plasticity in the adult. Our results are consistent with previous findings that a reduced excitation-inhibition balance specifically involving enhanced inhibition promotes plasticity in the adult (Hensch, 2005; Di Cristo et al., 2007; Levelt and Hubener, 2012). Furthermore, our results are consistent with the notion that ChABC treatments enhance plasticity and learning through mechanisms related to those involved in EE and critical period plasticity (Pizzorusso et al., 2002; Hensch, 2005). Interestingly, the Serotonin reuptake inhibitor Fluoxetine can promote critical period-like plasticity (Maya Vetencourt et al., 2008). Serotonin might enhance inhibition onto late-born PV neurons by enhancing VIP neuron activity through 5HT<sub>3</sub> ionotropic receptors expressed at high levels on these PV controlling neurons (Pi et al., 2013). Enhancing inhibitory connectivity and reducing PV and GAD-67 levels in late-born PV neurons might enhance further learning by reducing PV-mediated inhibition of principal neuron subpopulations (Volman et al., 2011; Lazarus et al., 2013) under acquisition regimes involving local circuit disinhibition. However, the specific circuit mechanisms relating late-born PV neuron networks to learning and plasticity remain to be determined.

Early-born PV Basket cells appear to account for characteristic features of mature fast-spiking PV neuron networks such as narrow synchronization windows and learning-related theta gamma entrainment within and among brain systems

(Bartos et al., 2007). Thus, high PV and GAD-67 levels enhance fast and high frequency firing properties of PV neuron networks important for gamma band network activity (Doischer et al., 2008; Fuchs et al., 2007; Cardin et al., 2009; Kuhlman et al., 2010; Goldberg et al., 2011). Enhanced functionality of early-born PV neuron networks upon validated learning might promote consolidation of strong memories within and between brain systems. Such a mechanism might account for the enhanced gamma-phase coupling between entorhinal cortex and hippocampal CA1 that was detected during late phases of hippocampal learning (Igarashi et al., 2014).

In summary, and reflecting specific regulation through inhibition or excitation, late-born PV neuron network plasticity might promote learning through reduced functional recruitment of PV neurons, whereas early-born PV neuron network plasticity might promote consolidation of validated learning through enhanced PV neuron function and network coherence. Deficits in the strength of inhibitory transmission might impair late-born PV neuron plasticity in mental retardation and autism (Gogolla et al., 2009; Chao et al., 2010; Han et al., 2014). By contrast, deficits in the strength of excitatory transmission might lead to reduced PV and GAD-67 levels in early-born Basket cells, accounting for greatly reduced gamma band activity and impaired prefrontal working memory support, as found in schizophrenia (Curley et al., 2013).

### **2.3.5 Acknowledgements**

We are grateful to S. Arber (FMI and Biozentrum, Basel) for critically reading the manuscript, to S.B. Rompani (FMI) for the Channel rhodospin construct, to P. Capelli (FMI) for assistance with the in utero transplantation experiments, and to S. Sternson (Janelia Farms) for the pharmacogenetic reagents. The Friedrich Miescher Institute for Biomedical Research is supported by the Novartis Research Foundation. F.D. was supported by the National Competence Center Research Synapsy (Swiss National Fund).

### 2.3.6 Author Contributions

F.D. and A.C. devised and carried out most of the experiments; M.L. devised and carried out the optogenetics experiments; P.C. devised the experiments and wrote the manuscript.

### 2.3.7 References

Akgul, G., and Wollmuth, L.P. (2013). Synapse-associated protein 97 regulates themembrane properties of fast-spiking parvalbumin interneurons in the visual cortex. *J. Neurosci.* 33, 12739–12750.

Bartos, M., Vida, I., and Jonas, P. (2007). Synaptic mechanisms of synchronized gamma oscillations in inhibitory interneuron networks. *Nat. Rev. Neurosci.* 8, 45–56.

Cardin, J.A., Carlen, M., Meletis, K., Knoblich, U., Zhang, F., Deisseroth, K., Tsai, L.H., and Moore, C.I. (2009). Driving fast-spiking cells induces gamma rhythm and controls sensory responses. *Nature* 459, 663–667.

Chao, H.T., Chen, H., Samaco, R.C., Xue, M., Chahrour, M., Yoo, J., Neul, J.L., Gong, S., Lu, H.C., Heintz, N., et al. (2010). Dysfunction in GABA signalling mediates autism-like stereotypies and Rett syndrome phenotypes. *Nature* 468, 263–269.

Chittajallu, R., Craig, M.T., McFarland, A., Yuan, X., Gerfen, S., Tricoire, L., Erkkila, B., Barron, S.C., Lopez, C.M., Liang, B.J., et al. (2013). Dual origins of functionally distinct O-LM interneurons revealed by differential 5-HT(3A)R expression. *Nat. Neurosci.* 16, 1598–1607.

Ciceri, G., Dehorter, N., Sols, I., Huang, Z.J., Maravall, M., and Marin, O. (2013). Lineage-specific laminar organization of cortical GABAergic interneurons. *Nat. Neurosci.* 16, 1199–1210.

Curley, A.A., Eggan, S.M., Lazarus, M.S., Huang, Z.J., Volk, D.W., and Lewis, D.A. (2013). Role of glutamic acid decarboxylase 67 in regulating cortical parvalbumin and GABA membrane transporter 1 expression: implications for schizophrenia. *Neurobiol. Dis.* 50, 179–186.

Deguchi, Y., Donato, F., Galimberti, I., Cabuy, E., and Caroni, P. (2011). Temporally matched subpopulations of selectively interconnected principal neurons in the hippocampus. *Nat. Neurosci.* 14, 495–504.

Di Cristo, G., Chattopadhyaya, B., Kuhlman, S.J., Fu, Y., Belanger, M.C., Wu, C.Z., Rutishauser, U., Maffei, L., and Huang, Z.J. (2007). Activity-dependent PSA expression regulates inhibitory maturation and onset of critical period plasticity. *Nat. Neurosci.* 10, 1569–1577.

Doischer, D., Hosp, J.A., Yanagawa, Y., Obata, K., Jonas, P., Vida, I., and Bartos, M. (2008). Postnatal differentiation of basket cells from slow to fast signaling devices. *J. Neurosci.* 28, 12956–12968.

Donato, F., Rompani, S.B., and Caroni, P. (2013). Parvalbumin-expressing basket-cell network plasticity induced by experience regulates adult learning. *Nature* 504, 272–276.

Fishell, G. (2007). Perspectives on the developmental origins of cortical interneuron diversity. *Novartis Found. Symp.* 288, 21–35, discussion 35–44, 96–98.

Flavell, S.W., Cowan, C.W., Kim, T.K., Greer, P.L., Lin, Y., Paradis, S., Griffith, E.C., Hu, L.S., Chen, C., and Greenberg, M.E. (2006). Activity-dependent regulation of MEF2 transcription factors suppresses excitatory synapse number. *Science* 311, 1008–1012.

Fuchs, E.C., Zivkovic, A.R., Cunningham, M.O., Middleton, S., Lebeau, F.E., Bannerman, D.M., Rozov, A., Whittington, M.A., Traub, R.D., Rawlins, J.N., and Monyer, H. (2007). Recruitment of parvalbumin-positive interneurons determines hippocampal function and associated behavior. *Neuron* 53, 591–604.

Gogolla, N., Leblanc, J.J., Quast, K.B., Sudhof, T.C., Fagiolini, M., and Hensch, T.K. (2009). Common circuit defect of excitatory-inhibitory balance in mouse models of autism. *J. Neurodev. Disord.* 1, 172–181.

Goldberg, E.M., Jeong, H.Y., Kruglikov, I., Tremblay, R., Lazarenko, R.M., and Rudy, B. (2011). Rapid developmental maturation of neocortical FS cell intrinsic excitability. *Cereb. Cortex* 21, 666–682.

- Han, S., Tai, C., Jones, C.J., Scheuer, T., and Catterall, W.A. (2014). Enhancement of inhibitory neurotransmission by GABA<sub>A</sub> receptors having  $\alpha$ -2,3-subunits ameliorates behavioral deficits in a mouse model of autism. *Neuron* 81, 1282–1289.
- Hensch, T.K. (2005). Critical period plasticity in local cortical circuits. *Nat. Rev. Neurosci.* 6, 877–888.
- Hensch, T.K., Fagiolini, M., Mataga, N., Stryker, M.P., Baekkeskov, S., and Kash, S.F. (1998). Local GABA circuit control of experience-dependent plasticity in developing visual cortex. *Science* 282, 1504–1508.
- Hu, H., Gan, J., and Jonas, P. (2014). Interneurons. Fast-spiking, parvalbumin<sup>+</sup> GABAergic interneurons: from cellular design to microcircuit function. *Science* 345, 1255263, <http://dx.doi.org/10.1126/science>.
- Igarashi, K.M., Lu, L., Colgin, L.L., Moser, M.B., and Moser, E.I. (2014). Coordination of entorhinal-hippocampal ensemble activity during associative learning. *Nature* 510, 143–147.
- Isaacson, J.S., and Scanziani, M. (2011). How inhibition shapes cortical activity. *Neuron* 72, 231–243.
- Kaelbling, L.P., Littman, M.L., and Moore, A.W. (1996). Reinforcement learning: a survey. *J. Artif. Intell. Res.* 4, 237–285.
- Kepecs, A., and Fishell, G. (2014). Interneuron cell types are fit to function. *Nature* 505, 318–326.
- Klausberger, T., and Somogyi, P. (2008). Neuronal diversity and temporal dynamics: the unity of hippocampal circuit operations. *Science* 321, 53–57.
- Kuhlman, S.J., Lu, J., Lazarus, M.S., and Huang, Z.J. (2010). Maturation of GABAergic inhibition promotes strengthening of temporally coherent inputs among convergent pathways. *PLoS Comput. Biol.* 6, e1000797.
- Kuhlman, S.J., Olivas, N.D., Tring, E., Ikrar, T., Xu, X., and Trachtenberg, J.T. (2013). A disinhibitory microcircuit initiates critical-period plasticity in the visual cortex. *Nature* 501, 543–546.



- Larkin, M.C., Lykken, C., Tye, L.D., Wickelgren, J.G., and Frank, L.M. (2014). Hippocampal output area CA1 broadcasts a generalized novelty signal during an object-place recognition task. *Hippocampus* 24, 773–783.
- Lazarus, M.S., Krishnan, K., and Huang, Z.J. (2013). GAD67 deficiency in parvalbumin interneurons produces deficits in inhibitory transmission and network disinhibition in mouse prefrontal cortex. *Cereb. Cortex*. Published online November 24, 2013. <http://dx.doi.org/10.1093/cercor/bht322>.
- Lee, S.H., Kwan, A.C., Zhang, S., Phoumthippavong, V., Flannery, J.G., Masmanidis, S.C., Taniguchi, H., Huang, Z.J., Zhang, F., Boyden, E.S., et al. (2012). Activation of specific interneurons improves V1 feature selectivity and visual perception. *Nature* 488, 379–383.
- Lee, S.H., Marchionni, I., Bezaire, M., Varga, C., Danielson, N., Lovett-Barron, M., Losonczy, A., and Soltesz, I. (2014). Parvalbumin-positive basket cells differentiate among hippocampal pyramidal cells. *Neuron* 82, 1129–1144.
- Levelt, C.N., and Hubener, M. (2012). Critical-period plasticity in the visual cortex. *Annu. Rev. Neurosci.* 35, 309–330.
- Lovett-Barron, M., Kaifosh, P., Kheirbek, M.A., Danielson, N., Zaremba, J.D., Reardon, T.R., Turi, G.F., Hen, R., Zemelman, B.V., and Losonczy, A. (2014). Dendritic inhibition in the hippocampus supports fear learning. *Science* 343, 857–863.
- Magnus, C.J., Lee, P.H., Atasoy, D., Su, H.H., Looger, L.L., and Sternson, S.M. (2011). Chemical and genetic engineering of selective ion channel-ligand interactions. *Science* 333, 1292–1296.
- Marin, O. (2012). Interneuron dysfunction in psychiatric disorders. *Nat. Rev. Neurosci.* 13, 107–120.
- Maya Vetencourt, J.F., Sale, A., Viegi, A., Baroncelli, L., De Pasquale, R., O’Leary, O.F., Castreñón, E., and Maffei, L. (2008). The antidepressant fluoxetine restores plasticity in the adult visual cortex. *Science* 320, 385–388.

- Mizuseki, K., Diba, K., Pastalkova, E., and Buzsaki, G. (2011). Hippocampal CA1 pyramidal cells form functionally distinct sublayers. *Nat. Neurosci.* 14, 1174–1181.
- Pi, H.J., Hangya, B., Kvitsiani, D., Sanders, J.I., Huang, Z.J., and Kepecs, A. (2013). Cortical interneurons that specialize in disinhibitory control. *Nature* 503, 521–524.
- Pizzorusso, T., Medini, P., Berardi, N., Chierzi, S., Fawcett, J.W., and Maffei, L. (2002). Reactivation of ocular dominance plasticity in the adult visual cortex. *Science* 298, 1248–1251.
- Ruediger, S., Vittori, C., Bednarek, E., Genoud, C., Strata, P., Sacchetti, B., and Caroni, P. (2011). Learning-related feedforward inhibitory connectivity growth required for memory precision. *Nature* 473, 514–518.
- Rymar, V.V., and Sadikot, A.F. (2007). Laminar fate of cortical GABAergic interneurons is dependent on both birthdate and phenotype. *J. Comp. Neurol.* 501, 369–380.
- Sauer, J.F., Struber, M., and Bartos, M. (2012). Interneurons provide circuit specific depolarization and hyperpolarization. *J. Neurosci.* 32, 4224–4229.
- Slomianka, L., Amrein, I., Knuesel, I., Sørensen, J.C., and Wolfer, D.P. (2011). Hippocampal pyramidal cells: the reemergence of cortical lamination. *Brain Struct. Funct.* 216, 301–317.
- Southwell, D.G., Froemke, R.C., Alvarez-Buylla, A., Stryker, M.P., and Gandhi, S.P. (2010). Cortical plasticity induced by inhibitory neuron transplantation. *Science* 327, 1145–1148.
- Spiegel, I., Mardinly, A.R., Gabel, H.W., Bazinet, J.E., Couch, C.H., Tzeng, C.P., Harmin, D.A., and Greenberg, M.E. (2014). Npas4 regulates excitatory inhibitory balance within neural circuits through cell-type-specific gene programs. *Cell* 157, 1216–1229.

Varga, C., Oijala, M., Lish, J., Szabo, G.G., Bezaire, M., Marchionni, I., Golshani, P., and Soltesz, I. (2014). Functional fission of parvalbumin interneuron classes during fast network events. *eLife*. <http://dx.doi.org/10.7554/eLife.04006>.

Volman, V., Behrens, M.M., and Sejnowski, T.J. (2011). Downregulation of parvalbumin at cortical GABA synapses reduces network gamma oscillatory activity. *J. Neurosci.* 31, 18137–18148.

Wilke, S.A., Antonios, J.K., Bushong, E.A., Badkoobehi, A., Malek, E., Hwang, M., Terada, M., Ellisman, M.H., and Ghosh, A. (2013). Deconstructing complexity: serial block-face electron microscopic analysis of the hippocampal mossy fiber synapse. *J. Neurosci.* 33, 507–522.

Wojtowicz, J.M., and Kee, N. (2006). BrdU assay for neurogenesis in rodents. *Nat. Protoc.* 1, 1399–1405.

Wolff, S.B., Grundemann, J., Tovote, P., Krabbe, S., Jacobson, G.A.A., Müller, C., Herry, C., Ehrlich, I., Friedrich, R.W., Letzkus, J.J., and Luthi, A. (2014). Amygdala interneuron subtypes control fear learning through disinhibition. *Nature* 509, 453–458.

### 3. General Discussion

Understanding the mechanisms and rules underlying learning and memory formation has intrigued neurobiologists for decades. Memories are part of our day-to-day existence, and yet, not everything we experience becomes a long-term memory. This means that learning itself could be one important checkpoint that determine if something ought to be retained. Though there have been several studies to understand the consolidation of memories from their short-term to long-term form, how learning is successfully transformed into memory and how the microcircuits as well as the distributed networks ensure formation of that memory has remained unclear. In this thesis, I have focused on investigating some of these questions using different learning paradigms and different transgenic mouse-lines to probe into how relevant information is acquired and how memories are formed in time, in the scale of a day.

### **Time-units of Learning and Role of cFos+ neuronal ensembles**

My work demonstrates the existence of dedicated temporal units for learning. While the entire block of learning can be completed within a short time which has been the norm for behavioural paradigms used in laboratories, I show that there is a window of 5h from the first acquisition during which related information or trials can be added. The related information can be confirmatory or contradictory or even additional to what was acquired initially. While this provides the opportunity to ascertain that necessary associations do not get lost by linking them together into meaningful memory, it also shows high sensitivity to contradictory information by interfering with effective learning. This time-unit demarcates the boundary that defines learning, thereby serving as an important checkpoint for memory formation.

Recent findings have indicated that memories can be linked in time, within a few hours of each other, by virtue of shared neuronal ensemble in different brain areas (Cai, Aharoni et al. 2016, Rashid, Yan et al. 2016). Previously unrelated memories can also be associated together by artificially activating the independent ensembles of one experience during the other, creating false or synthetic memories (Garner, Rowland et al. 2012, Ramirez, Liu et al. 2013, Ohkawa, Saitoh et al. 2015, Trouche, Perestenko et al. 2016). These findings do

bring forth the possibility that events can be connected together into one memory if they were acquired or artificially reactivated in temporal proximity.

My findings provide the first evidence that the temporal window of 5h might be important to decide whether to learn and what is learnt. While individual memories can be connected into a hybrid or composite memory, this window can also connect pieces of information or repeated trials into one memory. If a relevant association did not happen at the moment of the first acquisition, there is a grace period of 5h during which it can be added. Furthermore, I show that network activity play a key role in the function of this time-unit, in a cFos-dependent manner. cFos expression remains elevated in neuronal assemblies across the brain areas involved in learning during the 5h after the initial acquisition and is required to be functionally active during the time-unit for successful learning to happen. Inhibition of network activity in one system can potentially suppress the entire distributed network and the function of time-unit. On the other hand, reactivating the cFos ensemble for a particular memory or recalling the memory can reopen a new time-unit of similar temporal span to specifically allow related information to be further linked to that memory. Reactivation of learning-related cFos ensemble in one brain area re-induces cFos in the distant areas originally used for that learning and BDNF might be one of the long-range neuromodulators that serves to reassert the cFos ensemble in the entire network. This is in line with the findings that reactivation of cFos ensemble in critical brain areas can retrieve memory (Tonegawa, Liu et al. 2015) and the retrieval of memory reactivates the memory trace in multiple brain areas involved (Reijmers, Perkins et al. 2007, Tanaka, Pevzner et al. 2014). I show that, indeed, time-units of learning can also be reinstated by reactivation of specific learning-related cFos+ ensemble and it requires cFos and BDNF activity for functional time-units.

Understanding the role of functionally interconnected memory-specific neuronal assemblies in distant brain areas participating in a learning would give a huge momentum in the direction of studying their contributions to learning and memory. Permanent lesions or transient silencing of brain areas, in past and at current times as well, has been highly informative in our understanding of memory consolidation but it lacks the precision that the neuronal connections display. Our

work show that a very small percentage of cFos+ neurons in different brain areas that originally involve in the learning process become functionally connected; possibly, incorporating a new and strengthened sub-network specific to the learning. This subnetwork would ensure more efficient retrieval with partial cue and keep memories (that involve the same or some of the same brain regions) from being intertwined without good reason (shared element). Furthermore, the cFos+ ensembles in different brain areas might have different roles in learning as well as hierarchy of contribution. Using optogenetic and pharmacogenetic activation and silencing tools, one can methodically dissect the subnetwork into more defined nodes. With calcium imaging, one can hope to study the online formation of these dedicated subnetworks distributed across the brain structures. As Karl Lashley (Lashley, 1950) had realized long ago, engram is not localized but distributed, making it very difficult to manipulate in its entirety. So, by mapping the distributed components of functionally connected learning subnetwork and then by targeting different nodes of the subnetwork, we might be able to study the memory trace that endures time and know the differential roles of the brain areas with a higher degree of precision.

### **Late Time Window for Memory Consolidation and Role of PV plasticity**

The moment of acquisition marks the beginning of several plasticity related processes that ensure memory consolidation; however, those processes do not end after a few hours when short-term memory is supposedly converted into the long-lasting long-term memory. Studies have shown the existence of a late-window of consolidation around 9-12h after acquisition when several of the signalling and molecular cascades that were engaged during the initial hours are active again (Trifilieff, Herry et al. 2006, Bekinschtein, Cammarota et al. 2007, Katche, Bekinschtein et al. 2010) as well as the sequences of learned events through neuronal replay during quite rest and sleep (Atherton, Dupret et al. 2015, Genzel and Robertson 2015).

One of the plasticity processes that are initiated upon learning was shown to be reversible and highly dynamic shifts in PV+ basket population. Depending on the type of learning (definite vs incremental), the percentage of PV+ basket cells with either high or low levels of PV and GAD67 would become predominant in the

population (Donato, Rompani et al. 2013); this plasticity is detectable from 6h onwards, coming back to baseline levels around 36-48h later. In our work, we provide evidence that the PV plasticity needs to be maintained during the late-window of consolidation for the long-term memory formation. PV plasticity is sustained through the dopamine D1D5 receptor signalling via cAMP-dependent pathway. Even if the acquired memory is weak or artificially weakened during the early window (0-5h), it can be strengthened during the late-window by supplying exogenous D1 dopamine agonist, while inhibiting the dopamine D1D5 receptor signalling during that window resulted in complete loss of memory. We show that enforcing PV plasticity with pharmacogenetic ligands could bypass the dopamine signalling, suggesting that PV plasticity is downstream of the dopamine D1D5 receptor signalling cascade. Furthermore, the PV plasticity and dopamine receptor signalling was shown to be essential for the increased sharp-wave ripple density and second peak of cFos expression in neuronal assemblies during the late-window.

Together, this gives us an insight into the fine-tuned checkpoint connecting neuromodulator signalling, PV+ interneurons and neuronal ensembles, which exists late in the consolidation process, occurring 'offline' hours after learning is completed and determines which memories would endure and which get lost in time.

However, this study brings forth several questions in understanding the offline consolidation mechanism. Without any sensory input that initiates the onset of learning and the early consolidation process, what demarcates the second late window of consolidation? How does the network reiterates the learning events in activity (sharp-wave ripples, replay), in molecular cascade (pERK, Arc, cFos etc.) and finally in maintaining PV+ interneuron and cFos+ ensembles? Dopamine signalling is a major player in initiating some of the events mentioned before but it does not explain the temporally specific and controlled dopamine upregulation. Could VTA-NAc pathway be involved in setting the clock for the dopaminergic bursts during the second consolidation window? With DAT-cre mouse-lines to tag and manipulate the dopaminergic neuronal populations, one could interrogate how and when dopamine sets the second window, if at all. Understanding the mechanisms that demarcates the hours that constitute as the dopamine-



dependent second window could help us study the memory formation and retention. Furthermore, it would be important to investigate the networks that might be specifically involved at the second window (not at the early learning window of 0-5h as discussed above) and their roles in regulating the maintenance of memories.

### **Distinct sub-populations of PV+ interneurons and Role in Learning**

PV+ interneurons have been found to play a distinctive role in learning and memory. As mentioned in the previous section of discussion, they are shown to exhibit plasticity upon learning which is crucial for long-term memory. However, there are two possible directions for the PV+ population to shift in their expression levels of PV (and GAD67). In certain types and phases of learning, like contextual fear conditioning and completion of incremental learning, there is an increase in the fraction of PV+ basket cells expressing high levels of PV (and GAD67) while in other experiences, like environmental enrichment or early days of incremental learning, the PV+ population shift towards increased fraction of low PV and GAD67 expressing cells. The 'high PV configuration' or 'low PV configuration' is accompanied with a concomitant increase or decrease in the ratio of excitatory-inhibitory inputs on the PV+ basket cells, respectively and has been shown to either inhibit or favour further learning (Donato, Rompani et al. 2013). The bi-directional shifts in PV-states raise the possibility that there might be different sub-populations of PV+ baskets yet unidentified.

Fast-spiking PV+ interneurons (both basket and chandelier cells) are known to originate from medial ganglionic eminence (MGE) between embryonic day E 9.5 to E 15.5 (Fishell 2007, Tricoire, Pelkey et al. 2011). We demonstrate that depending on their day of neurogenesis, the PV+ basket cells can be functionally divided into 'early-born' and 'late-born' cells with distinctive roles in learning in the adults and exhibit specific regulation that determines their subsequent plasticity. We show that early-born PV+ cells (E9.5 to E11.5) already exhibit higher levels of PV and GAD67 and increased excitatory/inhibitory balance onto them at baseline, which are shown to further increase in response to high-PV-dependent learning like contextual fear conditioning and later days of Morris water maze. The late-born PV+ cells (E13.5 to E15.5), on the other hand, have reduced levels of PV

and GAD67 and decreased excitatory/inhibitory synaptic puncta density onto them, which are further reduced in response to low-PV-dependent forms of learning like early days of Morris water maze. Furthermore, the early-born PV+ cells are selectively regulated by increase or decrease of excitation while the late-born PV+ cells specifically respond to increase or decrease of inhibitory drive.

As we know from an earlier study that the high-PV configuration of network limited further learning while low-PV configuration was permissive to learning (Donato, Rompani et al. 2013), the specificity in regulation of the different subpopulations of PV+ cells according to their birth date and selectivity towards excitation and inhibition provides insights into how the PV+ basket cells could be acting as another checkpoint of learning and memory.

Additional studies could be performed to investigate which subpopulations of PV+ basket cells might be impaired in different neuropsychiatric disorders like Schizophrenia, Autism models (unpublished work from Arghya Mukherjee, Komal Bhandari and Sebastian Kruettner in the lab) as well as neurological disorders like Alzheimer's disease, Post-traumatic Stress Disorders. This could help to better understand the network dysregulation underlying the symptoms developed by the patients and provide opportunity to devise more targeted approach towards the therapeutic strategies. Furthermore, with single-cell RNA seq, one could investigate the genetic markers for the PV+ early-born and late-born subpopulations and gain access to the two subpopulations for future manipulations (unpublished work from Matteo Tripodi in the lab). This would be a powerful tool to study in further details the differential role and specific connectivity of these subpopulations in learning and memory and possibility of manipulating the individual PV+ subpopulations would support the therapeutic approaches discussed before.

## 4. Perspective

More than a century ago the term 'consolidation' was coined by Muller and Pilzecker (Muller and Pilzecker, 1900); the study of memory formation has moved forward in leaps and bounds since then. From the brain structures involved in different functional domains of memory consolidation and retrieval to the neuronal networks and manipulating memory at will, the field of learning and memory has progressed with our understanding and technological tool-box. With the advent of genetic tools, one can develop transgenic mouse lines for specific neuronal markers (whether principal neurons or interneurons, or different subtypes of interneurons or different neurons expressing different IEGs). Combining the genetic approaches with the advancement of imaging facilities, one can study the neurons in animals fixed post-mortem upon behavior with high precision using confocal microscopy or visualize the active neurons with calcium imaging and 2-photon microscopy in a head-fixed or freely behaving animal. With the myriad and still growing optogenetic and pharmacogenetic toolbox, one can manipulate the neuronal populations, activating or silencing them, and study diverse aspects of learning and memory formation. With electrophysiological techniques, one can study single-cell or population properties of neurons upon and during behavior. Nevertheless, there is a long way to go as the understanding of learning and memory is still barely the tip of the iceberg.

In this thesis, I study the cellular and network basis of learning and memory. For one to learn, the information has to be behaviorally relevant (salience and confirmation), leading to molecular cascades (pERK, pCREB, cFos, BDNF) that not only would define the time-window for learning but also ensure its consolidation into long-term memory. Taking advantage of some of the tools described above, I show that the cFos+ ensembles upon a task can be tagged and reactivated to reopen the learning window anytime in future, ensuring further learning. While behavioral retrieval can restart the learning window as well, it fails to do so upon silencing of the cFos+ neuronal ensemble for that specific learning. Furthermore, the cFos+ ensemble reactivated from one region can reinstate the cFos-expressing neurons in distant brain areas that were involved in that learning. So, how the cFos+ neuronal ensemble are connected between distant brain areas so faithfully for each learning? Are the cFos+ subnetworks formed in different areas separately during acquisition and then functionally connected

during the offline post-acquisition replay or are they already established together at acquisition? Using brain-wide  $\text{Ca}^{2+}$  imaging, one could try to study in time lapse the emergence of learning related neuronal population in distant brain areas and the impact of one area on the establishment of engram in other (Grewe, Grundemann et al. 2017, Wagner, Kim et al. 2017). With optogenetics and  $\text{Ca}^{2+}$  imaging in freely behaving animal, it could be possible to ask the relative roles of the different nodes of engram during the behavior itself, connecting the ongoing behavior in various learning paradigms with the active neuronal populations (Packer, Russell et al. 2015). Furthermore, cFos neuronal population has been a proxy for engram in several recent studies ((Reijmers, Perkins et al. 2007, Garner, Rowland et al. 2012, Liu, Ramirez et al. 2012, Ryan, Roy et al. 2015); however, the downstream target genes of cFos transcription factor and their role in establishing the titular 'engram' are yet unknown. With more detailed knowledge about the targets of cFos protein, the molecular and signaling cascades underlying the formation of engram could be understood in further depth.

A couple of recent studies (Cai, Aharoni et al. 2016, Rashid, Yan et al. 2016) introduce the idea that memories get linked together through shared neural ensemble within a time window of 5h. My study shows that not only completely formed memories, but pieces of information (individual trials or evidence) can be linked during this 5h window that together becomes a behaviorally relevant memory. The mechanism behind the linking of the memories or trials still need to be studied to understand how the neuronal ensemble modifies itself to incorporate the linked memories or informations. Several possible mechanisms could be behind this phenomenon: synaptic tagging and capture (Frey and Morris 1998, Rogerson, Cai et al. 2014) of first memory trace by the second one and spine clustering on the dendrites of overlapping neuronal population of shared memories (Kastellakis, Cai et al. 2015, Kastellakis, Silva et al. 2016) are just two of them. Taking the earlier considerations, since memory traces are established throughout a distributed network across several brain areas, the question would remain if the linking of memories is also function of this distributed neuronal ensemble or only formation of the composite long-term memory is represented as such? If so, how is the information coded in the ensembles?

Finally, as I discussed the necessity of studying the networks in more distributed frame, we should not disregard the study of microcircuits in specific subnetworks. One needs to tease apart how the 'ensemble' is established in a particular subnetwork (e.g- dorsal or ventral hippocampus, BLA or NAcc, PreLimbic Cortex or Retrosplenial cortex). Are the ensembles that respond to a learning event homogenous with the same neurons expressing the different IEGs at different temporal range or is it an assembly of different ensembles expressing different IEGs? How do the different representatives of 'engram' like cFos and Arc interact with each other and contribute to assembly formation and function? Furthermore, how do the inhibitory interneurons fit in defining the ensembles? My thesis discusses how PV+ interneurons are critical for making the network permissive for further learning (Donato, Rompani et al. 2013, Letzkus, Wolff et al. 2015) and are necessary for late window of memory consolidation. Recent studies have shown the importance of PV+ and SOM+ interneurons for neuronal allocation to specific memories (Morrison, Rashid et al. 2016, Stefanelli, Bertollini et al. 2016). However, further studies need to be done to address how the different subtypes of interneurons interact with the IEG+ neuronal ensembles for learning, memory linking and memory consolidation.

Learning and memory is such an integral part of our existence that understanding the process would help in deciphering the different cognitive dysfunctions associated with several psychiatric, neurological and developmental disorders. The more we unravel the mysteries of memory formation, the more we can help in treating the mnemonic dysregulations in different forms of dementia or post-traumatic stress disorders. There are several questions that wait to be answered with the increasingly sophisticated arsenal of techniques and tools Neuroscience now has at its disposal.

## 5. Materials and Methods

## **Mice**

PV-Cre and cFos-CreERT2 mice were from Jackson laboratories. Mice were kept in temperature-controlled rooms on a constant 12h light-dark cycle. Before the behavioral experiment, mice were housed individually for 3-4d and provided with food and water ad libitum. All animal procedures were approved and performed in accordance with the Veterinary Department of the Kanton of Basel-Stadt.

## **Behavioral procedures**

All behavioral experiments were carried out with male mice that were 60–75d old at the onset of the experiment. For cFC, mice were placed in the training context (Habitest Unit, Coulbourn Instruments, Allentown, PA), were allowed to explore the apparatus for 3min, and then received five foot shocks (1s and 0.8mA each, inter-trial interval: 30s). The conditioning chamber was cleaned with 70% ethanol before and after each session, and specific odor (odor A, 2% acetic acid) was used to identify the conditioning context. Training context 1 (TR1) was rectangular and TR2 was cylindrical in shape. Identities of the contexts were maintained with the presence of two distinct odors, odor A (2% acetic acid: TR1) or B (0.25% benzaldehyde: TR2). Control mice were subjected to the same procedure without receiving foot shocks. We assessed contextual fear memory by returning mice to the training chamber after fear conditioning during 5min, and analyzed freezing during a test period of 4min (first min excluded to avoid stress related responses). Freezing was defined as complete absence of somatic mobility other than respiratory movements. For object binding, a falcon tube smeared with the odor corresponding to that used at conditioning or as otherwise specified was introduced during 30min into the home cage. Freezing and avoidance behavior to the falcon tube were assessed on the next day for 5min in a neutral context (no odor associated) that had been cleaned with water before and after testing.

In MWM training, a 140cm pool filled with milky water was surrounded by 3 different objects placed as reference cues onto black curtains. A circular escape platform (10cm diameter) was submerged 0.5cm below the water surface. Mice were trained to find the platform during four trials a day or as otherwise specified, with inter-trial intervals of 5min (or as otherwise specified) spent in their home



cage. During training, mice were released from pseudo-randomly assigned start locations; they were allowed to swim for up to 60s. At the end of each trial, mice were allowed to sit on the platform for 15s; when trials were unsuccessful, mice were manually guided to the platform (only on the visible platform day, i.e. day 1). Performance was scored as latency to find the platform in each trial, and as the average of the four consecutive trials each day. Swim controls were age-matched mice, which were allowed to swim in the pool without escape platform, in a comparable training regime. For swim controls, trial durations for each day were adjusted to average values of training animals. Data were collected and analyzed using Viewer2 Software (Biobserve, Bonn, Germany).

For rotarod learning, mice were trained on an accelerating rotating rod (Ugo Basile srl; four trials per day and inter-trial intervals of 5min in home cage, or as otherwise specified). A smooth scotch tape was used to enhance the level of difficulty. For each trial, mice were placed on the rod before the rotation was initiated, ensuring that they were able to sit on it for 5s without falling. The training phase began only after the mice could successfully position themselves on the rod. Speed was increased in a step-wise fashion from 5 to 50rpm over 5min (maximal duration of each trial). Performance was scored as latency to fall in each trial, and as the average of the four consecutive trials each day. Activity controls were age-matched mice that were allowed to run on a rod at a fixed speed (10rpm) in a comparable training regime.

In the FOR (familiar object recognition) test, mice explored two objects (A/A or A/B) placed in an open arena for 10 min on day one, and returned to their home cage immediately after training. Next day, they were placed back into the original context for 5min and tested for object recognition, when one of the two familiar objects had been replaced with a novel one (A/B or B/C). Discrimination indices were calculated as  $(t_{\text{novel}} - t_{\text{familiar}})/(t_{\text{novel}} + t_{\text{familiar}})$ . To avoid discrimination of the objects based on odor, both the arena and the objects were thoroughly wiped with 70% ethanol before and after each trial.

### **Immunohistochemistry**

Antibodies use for different experiments were as follows: rabbit anti-cFos (Santa Cruz biotechnology, sc-253) 1:10000; mouse anti-NeuN (Millipore, MAB377),

1:1000; goat anti-PV (PVG-214, Swant biotechnologies) 1:5000;  $\alpha$ -Bungarotoxin, Alexa 488 Conjugate (Molecular Probes, Life Technologies, B-13422) 1:200; rat anti-BrdU (abcam, ab6326), 1:500; rabbit anti-RFP (abcam, ab62341), 1:500; rabbit anti-phospho-p44/42 MAPK (Erk1/2) (Thr202/Thr204) (Cell Signaling-9101), 1:500; rabbit anti-phospho-DARPP-32 (Thr34)-R (Santa Cruz sc-21601), 1:500; mouse anti-GAD-67 (Chemicon), 1:500; rabbit anti-Mef2 (Santa Cruz Biotechnology, sc-313) 1:1,000; mouse anti-Bassoon (Molecular Probes) 1:200; mouse anti-Gephyrin (Molecular Probes) 1:500; biotinylated WFA (Vector laboratories), 1:500. Secondary antibodies were Alexa Fluor 488 (Molecular Probes; A150077), 568 (Molecular Probes; A10037), or 647 (Molecular Probes; A31571, A21469); 1:500. dH and vH were analyzed at -1.82 to -1.94mm and -2.80 to -3.16mm from bregma respectively; BLA was at -1.22mm to -1.58mm, M1 was at +1.58 to +1.8mm from bregma and PreLC was at +1.8 to +1.98mm from bregma.

Mice were perfused at the indicated time point after the training session, or as indicated (transcardially with 4% PFA in PBS, pH 7.4). Brains were kept in fixation solution overnight at 4°C, then transferred to 30% sucrose solution for 24h, sectioned (40  $\mu$ m thickness) on a cryostat and stained while free-floating. The sections were blocked for 1h at room temperature in 0.2% Triton-X100 in PBS and 10% BSA solution. The subsequent primary and secondary antibodies were diluted in 0.2% Triton-X100 in PBS and 3% BSA solution. The primary antibody incubation was overnight (~21h) at 4°C and the secondary antibody incubation was 2h at room temperature, both with constant shaking.

For c-Fos analysis, samples belonging to the same experiment (for example, from the mice of a given time point, with their respective controls) were acquired in parallel and with the same settings (laser power, 6%; Master gain, 585 units, Optical Slice, 1  $\mu$ m for cFos) on an LSM700 confocal microscope (Zeiss) using an EC Plan-Neofluar 40X/1.3 oil-immersion. All c-Fos and NeuN immunopositive cells were quantified using an automatic spot-detection algorithm (Imaris 8.2.0, Bitplane AG; expected radius, 10mm; quality level, 7), and their fraction expressed as a percentage of the total neuronal population.

For PV related analysis (intensity and synaptic puncta), samples belonging to the same experiment (e.g. the mice of a given time point, with their controls) were acquired in parallel and with the same settings (laser power: 2%; Optical Slice: 1.28-1.35 air units; GaAsP detectors implemented) on an LSM710 confocal microscope (Zeiss) using an EC Plan-Neofluar x40/1.3 oil-immersion or x63/1.4 oil immersion objective (Zeiss). For the PV, GAD-67 and MEF2A intensity analysis, the dynamic range was set during the acquisition of adult (P60) cage control samples. PV neurons whose soma was included within the tissue sections with optimal staining (dampening of intensity between the first and last confocal plane <15%) were isolated in 3D (Imaris 7.0.0, Bitplane AG). 3D isosurfaces were created around each PV neuron soma (smoothness: 0.5  $\mu\text{m}$ ; quality level: 5) and labeling intensities were quantified automatically in arbitrary units as the mean of all isolated pixels. We set the zero value at CA3 pyramidal neurons somas, and the highest threshold so that <20% of the pixels belonging to the brightest PV cells were saturated (ZEN2010 acquisition software, Zeiss). Normalization and recalibration across different experiments was achieved by using internal control animals, which were included in each experiment, and were processed using the same criteria mentioned above. For synapse densities and correlation analyses, dendritic and somatic surfaces (all objects within a visual field) were visualized using Imaris software. 3D isosurfaces were created for each object, and automatic spot detection algorithms were implemented for synapse detection based on 3D colocalization. PV neuron dendritic stretches included in the analysis were between 15 and 50  $\mu\text{m}$  in length and between 45 and 200  $\mu\text{m}^2$  in area. PV Neurons numbers were quantified on oversaturated images, and normalized to CA3 areas (ImageJ, NIH).

A comparative analysis revealed a cluster of low PV intensities (threshold, 800 arbitrary confocal units [au]) that were present early during development (P15), absent in adult control samples (P60), and induced upon EE. The 800 au threshold was adopted to classify PV neurons into four subclasses as follows; low-PV, 0–800 au; intermediate-low, 800–1,600 au; intermediate-high, 1,600–2,400 au; high-PV, >2,400 au (for further details, read Donato, Rompani et al. 2013) .

For BrdU labelling, mice were injected with BrdU at defined times during embryonic development, and hippocampal sections were analyzed for BrdU labeling in the adult. Only strongly BrdU-labeled cells that did not undergo further rounds of DNA replication and cell division subsequent to BrdU incorporation were included in the analysis.

For LFP electrode or injection site experiments, brains were collected at the end of the experiments for histological analysis. Serial slices including vH were imaged at 10x or at 4x to locate the injection site and the extent of volume spread. Serial slices were also labeled with 0.5% cresyl violet (vol/vol) for Nissl substance to demarcate cannula placements and syringe tip locations. Virus infection and spread were determined by staining with identifiers like GFP, mCherry or  $\alpha$ -Bungarotoxin as applied.

### **Pharmacogenetics and Pharmacology in vivo**

All surgeries were conducted under aseptic conditions using a small animal stereotaxic instrument (David Kopf Instruments). Mice were anaesthetized with isoflurane (4% for induction, followed by 1.5–2.0%) in the stereotaxic frame during the entire surgery procedure and body temperature was maintained with a heating pad. Local virus delivery and drug treatments were carried out with a 33-gauge needle coupled to a 5ul syringe (Hamilton, Reno, NV) or delivered using glass pipettes (tip diameter 10–20  $\mu$ m) connected to a Picospritzer (Parker Hannifin Corporation). Coordinates relative to bregma were as follows: PreLC (anteroposterior (AP) +2.0mm, mediolateral (ML) +0.5mm, dorsoventral (DV, relative to dura) -2.1mm; dH (AP -1.58/-1.8mm, ML 1.65/2.0mm, DV -1.5/-2.1mm) and vH (AP -3.0mm, ML +2.9mm, DV -3.5mm). Drugs were injected at the rate of 100nl/min to a final maximum volume of ~300nl. After completion of injection the needle was left in its place for 5 min to allow for diffusion of the drug, and then slowly withdrawn. For virus injections, ~500nl of the virus preparation was slowly injected using Picospritzer or Hamilton over a period of 10min. After the end of the injection the pipette or needle was left in its place for further 10min to allow for diffusion of the virus. All drugs and viruses were injected bilaterally.

For acute silencing, we delivered floxed PSAM-carrying AAV9 (excitation: rAAV9-CAG-flox-PSAM(Leu41Phe,Tyr116Phe)5HT3-WPRE) in PV-Cre mice. For

activation or inhibition of c-Fos ensembles or PV interneurons, floxed PSAM-carrying AAV9 (excitation: rAAV9-CAG-flox-PSAM(Leu41Phe, Tyr116Phe)5HT3-WPRE; or (inhibition: rAAV9-CBA-flox-PSAM(Leu141Phe, Tyr116Phe)GlyR-WPRE) were delivered locally in cFos-CreERT2 or PV-Cre mice respectively. To allow for transgene expression, mice were kept under home cage conditions for 10d before any behavioral experiment. 4-Hydroxy Tamoxifen (H6278, Sigma) dissolved in sunflower seed oil (Sigma) was injected i.p at the dose of 50mg/kg to activate Cre recombinase activity for cFos-CreERT2 mice. PSAM agonist PSEM308 was injected i.p. at 5mg/kg to activate PSAM channels.

To activate Gs, AC and cAMP signaling in vH PV neurons, PV-Cre mice received local microinjections of Gs-coupled DREADD virus (B. Roth, UNC gene therapy center vector core, rAAV8-hSyn-DIO-rM3D (Gs)-mCherry; Gs-DREADDs). Selective chemogenetic activation of the Gs-DREADD receptor was achieved by administering the selective DREADD agonist designer drug clozapine-N-oxide (CNO; 5 mg per kg, intraperitoneal, Tocris).

Drugs used were as follows: T-5224 (1.5ug/side, in 20% PVP and 10% DMSO, MedChemExpress, Inhibitor of cFos-AP1 transcription complex); Anisomycin (i.p, 50mg/kg, in 10% DMSO, Applichem); MG-132 (100µM, in 1% DMSO, Calbiochem); BDNF (0.5µg/µl, in saline, 0.25µg/side, Peprotech); ANA-12 (2µg/µl, in 1% DMSO, 1µg/side, Sigma, TrkB antagonist); SCH23390 (0.15 µg per side, Sigma; D1/5R antagonist); SK38393 (12.5 µg per side, Sigma; D1R agonist); VIP (1 nM, Tocris); [Ac-Tyr1,D-Phe2]-GRF 1-29 (300 nM, Tocris; VIP antagonist); quinpirole hydrochloride (1 µg per side, Sigma; D2R agonist); eticlopride hydrochloride (5 µg per side, Tocris; D2R antagonist); D-AP5 (i.p, 10 mg per kg in saline, Tocris), Rolipram (7.5 µg per side, in saline with 20% DMSO (vol/vol), Tocris; PDE-4 inhibitor); SQ22536 (30 ng per 60 nl, Tocris, AC inhibitor); Diazepam (i.p, 3 mg/kg in saline, Roche); ChABC (0.08 units, Sigma), BrdU (i.p, 0.1mg/g in saline).

### **Local Field Potential Recordings**

All in vivo recordings were performed in awake head fixed mice. A small custom stainless-steel head post was attached to the skull of the animals under isoflurane anesthesia. For head-post surgery, mice were mounted in a stereotaxic

frame (Narishige). The scalp was anesthetized with bupivacain (0.25% (vol/vol), 30  $\mu$ l; Carbostesin, AstraZeneca, CH), the skull bones were widely exposed and a layer of cyanoacrylate adhesive (Loctite) was applied to the skull preventing its dehydration and fixing the reclined scalp. The head post was then fixed to the occipital and nasal bones using ultraviolet curable dental cement (Miris 2 dentin, Coltene AG, CH). The central part of the head post ring, which allows access to the skull surface is then filled with a removable silicone elastomer (Kwik-Cast, World Precision Instruments). Mice were allowed at least 3 d of postoperative recovery. After the recovery period, mice were accustomed to the head fixed position (two daily sessions for 3 d with progressively longer periods of head fixation from 10 min to 35 min for the two last sessions).

Bilateral ventral hippocampal recordings were made using two linear multi-electrode probes (iridium-based, 177  $\mu$ m<sup>2</sup>; NeuroNexus Technologies) inserted perpendicularly to the skull surface bilaterally to vH (3.0 mm posterior and 2.6 mm lateral from bregma) and referenced to the skull bone. Each probe was lowered to 3.1-mm depth and recorded from 16 channels with 100- $\mu$ m inter-channel distance; recordings spanned a 1.6-mm height, between 1.5-mm and 3.1-mm depth. For the first recording session, immediately after placing of the animal in the head fixed system and under light isoflurane anesthesia, two small craniotomies (<500  $\mu$ m<sup>2</sup>) were applied above the recording locations and the probes were inserted. After a 5-min recovery period to ensure complete awakening of the mice, LFP activity was recorded for 30 min. During all recordings mice were neither moving nor sleeping. Differential potentials were amplified, bandpass-filtered online between 1 and 4,000 Hz and sampled at 8 kHz using a Digital Lynx Sx acquisition system (Neuralynx). At the end of the recording session, mice were anesthetized with isoflurane, the electrodes were removed, and silicon elastomer was applied above the skull. For the last recording session, probes were painted with a fluorescent marker (Dye I; Invitrogen) to determine their positions through histology. Recordings were further filtered offline for LFP analyses between 150–250 bandpass and 50-Hz notch filter. Analyses were performed using Cartool software by Denis Brunet (<http://brainmapping.unige.ch/cartool>), and Matlab toolboxes (MathWorks). Ripples were detected as events with at least eight peaks (one cycle = 2 peaks),

not longer than ~100 ms, and with an amplitude at least 2.5-fold larger than average local noise.

### **Embryonic and developmental analysis**

The ventricular and subventricular layers of the medial ganglionic eminence (MGE) or lateral ganglionic eminence (LGE) were dissected from embryonic day 13.5 (E13.5) or E11.5 donor embryo (mouse line: PV-cre:Rosa-flexed-tdTomato). Multiple donor neuroblasts were pooled together to increase cell density. Embryonic day 0.5 was defined as the time when the sperm plug was detected. Embryonic MGE explants were dissected in Leibovitz L-15 medium containing DNaseI (100 µg/ml), and mechanically dissociated into a single cell suspension by repeated pipetting. The dissociated cells were then concentrated by centrifugation (3 min, 3000 r/min) and suspended in L-15 medium. Progenitor injections were conducted under ultrasound guidance (Fujifilm Visualsonic Inc, VeVo 770 imaging station). Concentrated cell suspensions were loaded in a beveled glass micropipette mounted on an injection pump (Fujifilm visualsonic Inc). Pregnant females were anesthetized with isoflurane, and uterine horn exposed to injection in a sterile environment. Embryos were exposed and stabilized in a dissection micro chamber filled with warm sterile PBS; the target region was visualized using an RMV scanhead (RMV-704, Visualsonic inc), and injected under visual guidance (Imaging: B-Mode; Frequency: 40 MHz; Power: 100%; Sound speed: 1540 m/s; Frame rate: 34 Hz. Fujifilm Visualsonics, Inc). After injection, embryos were carefully placed in the maternal womb; recovery was monitored until delivery on day E18.5.

### **Statistical analysis**

Statistical analyses were performed using GraphPad Prism version 6.00 (GraphPad Software, La Jolla, California, USA). As mentioned in the figure legends, depending on data-set, unpaired Student's t-test or one-way ANOVA followed by Dunnett's posthoc test with additional validation through the Brown-Forsythe and Bartlett's test were performed;  $P < 0.05$  in post hoc comparisons. Results are presented as mean  $\pm$  s.e.m. All tests were two-tailed. Data distributions were assumed to be normal but not formally tested. The variance was comparable between groups for all metrics measured. The sample size per

group (total number of animals collected over multiple repetitions of each experiment) is mentioned in the respective figure legends and was chosen and validated on the basis of previous studies performed in the laboratory. No statistical methods were applied to predetermine sample size. Male mice of closely comparable age were assigned randomly to experimental groups. Intensity analysis and freezing data were verified by investigators blinded to experimental conditions.



## 6. Abbreviations

AAV: Adeno-associated Virus

AC: Adenylyl Cyclase

ACC: Anterior Cingulate Cortex

Act.: Activation

Ago.: Agonist

AMPA:  $\alpha$ -amino-3-hydroxy-5-methyl-4-isoxazolepropionic receptor

Antag./Ant.: Antagonist

AS-PaRac1: Activated synapse targeting photoactivatable Rac1

AU: Arbitrary Units

BDNF: Brain-derived neurotrophic factor

BLA: Basolateral Amygdala

BrdU: Bromo-deoxyuridine

BSA: Bovine Serum Albumin

CA1/3: Cornu Ammonis 1/3

Ca<sup>2+</sup>: Calcium 2+ ion

CAMKII: calcium/calmodulin-regulated kinase II

cAMP: cyclic adenosine monophosphate

cFC: contextual Fear Conditioning

ChABC: Chondroitinase

ChR2: Channelrhodopsin 2

CNO: clozapine-N-oxide

CREB: cAMP response element binding protein

DA: Dopamine

DAT: Dopamine Transporters

DARPP-32: Dopamine- and cAMP-regulated phosphoprotein, Mr 32

DG: dentate gyrus

dH: dorsal Hippocampus

DMSO: Dimethyl sulfoxide

DREADD: Designer Receptors Exclusively Activated by Designer Drugs

E/I : Excitatory/Inhibitory

E: Embryonic

EE: Environmental Enrichment

ER: Estrogen Receptor

ERK: Extracellular-signal regulated Kinase

FOR: Familiar Object Recognition

Gs: Stimulatory G protein

IEG: Immediate Early Gene

Inh: Inhibition

LFP: Local field potentials

LGE: Lateral Ganglionic Eminence

LTD: Long-term Depression

LTP: Long-term Potentiation

M1: Primary Motor Cortex

MAPK: Mitogen-activated Protein Kinase

MGE: Medial Ganglionic Eminence

mGluR: metabotropic glutamate receptor

MWM: Morris Water Maze

NAcc: Nuclear Accumbens

NeuN: Neuronal Nuclei

NC: Neutral context

NMDAR: N-methyl-D-aspartate-type receptors

P: Postnatal

PBS: Phosphate Buffer Saline

pCREB: phosphorylated CREB

PDE-4: Phospho Diesterase-4

PFA: Paraformaldehyde

PKA: Protein Kinase A

PKC: Protein Kinase C

PNN: Perineuronal nets

PreLC: Prelimbic Cortex

PSAM: pharmacologically selective actuator molecule

PSEM: pharmacologically selective effector molecule

PV+: Parvalbumin-positive

PVP: Polyvinylpyrrolidone

Refr.: Refractory

RR: Rotarod

Seq. : Sequencing

Silen.: Silencing

SOM+: Somatostatin positive

TetTag: TETRacycline transactivator controlled genetic TAGging of active neural circuits

TR: Training context

TRAP: Targeted Recombination in Active Populations

TRE: tetracycline-responsive promoter element

TrKB: tyrosine receptor kinase B

tTA: tetracycline transactivator

US: Unconditioned Stimulus

VGAT: vesicular GABA transporter

vH: ventral Hippocampus

VIP: Vasoactive intestinal peptide

WFA: Wisteria floribunda agglutinin

## 7. References

Abel, T. and K. M. Lattal (2001). "Molecular mechanisms of memory acquisition, consolidation and retrieval." *Curr Opin Neurobiol* 11(2): 180-187.

Abrams, T. W., K. A. Karl and E. R. Kandel (1991). "Biochemical studies of stimulus convergence during classical conditioning in *Aplysia*: dual regulation of adenylate cyclase by Ca<sup>2+</sup>/calmodulin and transmitter." *J Neurosci* 11(9): 2655-2665.

Alberini, C. M. (2009). "Transcription factors in long-term memory and synaptic plasticity." *Physiol Rev* 89(1): 121-145.

Amilhon, B., C. Y. Huh, F. Manseau, G. Ducharme, H. Nichol, A. Adamantidis and S. Williams (2015). "Parvalbumin Interneurons of Hippocampus Tune Population Activity at Theta Frequency." *Neuron* 86(5): 1277-1289.

Atherton, L. A., D. Dupret and J. R. Mellor (2015). "Memory trace replay: the shaping of memory consolidation by neuromodulation." *Trends Neurosci* 38(9): 560-570.

Bekinschtein, P., M. Cammarota, L. M. Igaz, L. R. Bevilacqua, I. Izquierdo and J. H. Medina (2007). "Persistence of long-term memory storage requires a late protein synthesis- and BDNF- dependent phase in the hippocampus." *Neuron* 53(2): 261-277.

Bliss, T. V. and G. L. Collingridge (2013). "Expression of NMDA receptor-dependent LTP in the hippocampus: bridging the divide." *Mol Brain* 6: 5.

Bourtchouladze, R., T. Abel, N. Berman, R. Gordon, K. Lapidus and E. R. Kandel (1998). "Different training procedures recruit either one or two critical periods for contextual memory consolidation, each of which requires protein synthesis and PKA." *Learn Mem* 5(4-5): 365-374.

Bourtchouladze, R., B. Frenguelli, J. Blendy, D. Cioffi, G. Schutz and A. J. Silva (1994). "Deficient long-term memory in mice with a targeted mutation of the cAMP-responsive element-binding protein." *Cell* 79(1): 59-68.

Cai, D. J., D. Aharoni, T. Shuman, J. Shobe, J. Biane, W. Song, B. Wei, M. Veshkini, M. La-Vu, J. Lou, S. E. Flores, I. Kim, Y. Sano, M. Zhou, K.

Baumgaertel, A. Lavi, M. Kamata, M. Tuszynski, M. Mayford, P. Golshani and A. J. Silva (2016). "A shared neural ensemble links distinct contextual memories encoded close in time." *Nature* 534(7605): 115-118.

Cardin, J. A., M. Carlen, K. Meletis, U. Knoblich, F. Zhang, K. Deisseroth, L. H. Tsai and C. I. Moore (2009). "Driving fast-spiking cells induces gamma rhythm and controls sensory responses." *Nature* 459(7247): 663-667.

Caroni, P., A. Chowdhury and M. Lahr (2014). "Synapse rearrangements upon learning: from divergent-sparse connectivity to dedicated sub-circuits." *Trends Neurosci* 37(10): 604-614.

Choi, G. B., D. D. Stettler, B. R. Kallman, S. T. Bhaskar, A. Fleischmann and R. Axel (2011). "Driving opposing behaviors with ensembles of piriform neurons." *Cell* 146(6): 1004-1015.

Cowansage, K. K., T. Shuman, B. C. Dillingham, A. Chang, P. Golshani and M. Mayford (2014). "Direct reactivation of a coherent neocortical memory of context." *Neuron* 84(2): 432-441.

Dash, P. K., A. E. Hebert and J. D. Runyan (2004). "A unified theory for systems and cellular memory consolidation." *Brain Res Brain Res Rev* 45(1): 30-37.

Dash, P. K., B. Hochner and E. R. Kandel (1990). "Injection of the cAMP-responsive element into the nucleus of Aplysia sensory neurons blocks long-term facilitation." *Nature* 345(6277): 718-721.

Davis, H. P. and L. R. Squire (1984). "Protein synthesis and memory: a review." *Psychol Bull* 96(3): 518-559.

Davis, S., P. Vanhoutte, C. Pages, J. Caboche and S. Laroche (2000). "The MAPK/ERK cascade targets both Elk-1 and cAMP response element-binding protein to control long-term potentiation-dependent gene expression in the dentate gyrus in vivo." *J Neurosci* 20(12): 4563-4572.

Deng, W., M. Mayford and F. H. Gage (2013). "Selection of distinct populations of dentate granule cells in response to inputs as a mechanism for pattern separation in mice." *Elife* 2: e00312.



Denny, C. A., M. A. Kheirbek, E. L. Alba, K. F. Tanaka, R. A. Brachman, K. B. Laughman, N. K. Tomm, G. F. Turi, A. Losonczy and R. Hen (2014). "Hippocampal memory traces are differentially modulated by experience, time, and adult neurogenesis." *Neuron* 83(1): 189-201.

Descalzi, G., X. Y. Li, T. Chen, V. Mercaldo, K. Koga and M. Zhuo (2012). "Rapid synaptic potentiation within the anterior cingulate cortex mediates trace fear learning." *Mol Brain* 5: 6.

Donato, F., S. B. Rompani and P. Caroni (2013). "Parvalbumin-expressing basket-cell network plasticity induced by experience regulates adult learning." *Nature* 504(7479): 272-276.

Dudai, Y. (2004). "The neurobiology of consolidations, or, how stable is the engram?" *Annu Rev Psychol* 55: 51-86.

Dudai, Y., Y. N. Jan, D. Byers, W. G. Quinn and S. Benzer (1976). "dunce, a mutant of *Drosophila* deficient in learning." *Proc Natl Acad Sci U S A* 73(5): 1684-1688.

Fanselow, M. S. and A. M. Poulos (2005). "The neuroscience of mammalian associative learning." *Annu Rev Psychol* 56: 207-234.

Fishell, G. (2007). "Perspectives on the developmental origins of cortical interneuron diversity." *Novartis Found Symp* 288: 21-35; discussion 35-44, 96-28.

Flavell, S. W. and M. E. Greenberg (2008). "Signaling mechanisms linking neuronal activity to gene expression and plasticity of the nervous system." *Annu Rev Neurosci* 31: 563-590.

Fonseca, R., U. V. Nagerl and T. Bonhoeffer (2006). "Neuronal activity determines the protein synthesis dependence of long-term potentiation." *Nat Neurosci* 9(4): 478-480.

Frey, U. and R. G. Morris (1998). "Synaptic tagging: implications for late maintenance of hippocampal long-term potentiation." *Trends Neurosci* **21**(5): 181-188.

Garner, A. R., D. C. Rowland, S. Y. Hwang, K. Baumgaertel, B. L. Roth, C. Kentros and M. Mayford (2012). "Generation of a synthetic memory trace." *Science* 335(6075): 1513-1516.

Gdalyahu, A., E. Tring, P. O. Polack, R. Gruver, P. Golshani, M. S. Fanselow, A. J. Silva and J. T. Trachtenberg (2012). "Associative fear learning enhances sparse network coding in primary sensory cortex." *Neuron* 75(1): 121-132.

Genzel, L. and E. M. Robertson (2015). "To Replay, Perchance to Consolidate." *PLoS Biol* 13(10): e1002285.

Girardeau, G., K. Benchenane, S. I. Wiener, G. Buzsaki and M. B. Zugaro (2009). "Selective suppression of hippocampal ripples impairs spatial memory." *Nat Neurosci* 12(10): 1222-1223.

Gore, F., E. C. Schwartz, B. C. Brangers, S. Aladi, J. M. Stujenske, E. Likhtik, M. J. Russo, J. A. Gordon, C. D. Salzman and R. Axel (2015). "Neural Representations of Unconditioned Stimuli in Basolateral Amygdala Mediate Innate and Learned Responses." *Cell* 162(1): 134-145.

Grewe, B. F., J. Grundemann, L. J. Kitch, J. A. Lecoq, J. G. Parker, J. D. Marshall, M. C. Larkin, P. E. Jercog, F. Grenier, J. Z. Li, A. Luthi and M. J. Schnitzer (2017). "Neural ensemble dynamics underlying a long-term associative memory." *Nature* **543**(7647): 670-675.

Guenther, C. J., K. Miyamichi, H. H. Yang, H. C. Heller and L. Luo (2013). "Permanent genetic access to transiently active neurons via TRAP: targeted recombination in active populations." *Neuron* 78(5): 773-784.

Guzowski, J. F. (2002). "Insights into immediate-early gene function in hippocampal memory consolidation using antisense oligonucleotide and fluorescent imaging approaches." *Hippocampus* 12(1): 86-104.

Guzowski, J. F. and J. L. McGaugh (1997). "Antisense oligodeoxynucleotide-mediated disruption of hippocampal cAMP response element binding protein levels impairs consolidation of memory for water maze training." *Proc Natl Acad Sci U S A* 94(6): 2693-2698.

Han, J. H., S. A. Kushner, A. P. Yiu, C. J. Cole, A. Matynia, R. A. Brown, R. L. Neve, J. F. Guzowski, A. J. Silva and S. A. Josselyn (2007). "Neuronal competition and selection during memory formation." *Science* 316(5823): 457-460.

Han, J. H., S. A. Kushner, A. P. Yiu, H. L. Hsiang, T. Buch, A. Waisman, B. Bontempi, R. L. Neve, P. W. Frankland and S. A. Josselyn (2009). "Selective erasure of a fear memory." *Science* 323(5920): 1492-1496.

Hawkins, R. D., T. W. Abrams, T. J. Carew and E. R. Kandel (1983). "A cellular mechanism of classical conditioning in *Aplysia*: activity-dependent amplification of presynaptic facilitation." *Science* 219(4583): 400-405.

Hayashi-Takagi, A., S. Yagishita, M. Nakamura, F. Shirai, Y. I. Wu, A. L. Loshbaugh, B. Kuhlman, K. M. Hahn and H. Kasai (2015). "Labelling and optical erasure of synaptic memory traces in the motor cortex." *Nature* 525(7569): 333-338.

He, J., K. Yamada and T. Nabeshima (2002). "A role of Fos expression in the CA3 region of the hippocampus in spatial memory formation in rats." *Neuropsychopharmacology* 26(2): 259-268.

Hebb, D. (1949). *The Organization of Behavior* (New York: Wiley & Sons).

Hoeffler, C. A., K. K. Cowansage, E. C. Arnold, J. L. Banko, N. J. Moerke, R. Rodriguez, E. K. Schmidt, E. Klosi, M. Chorev, R. E. Lloyd, P. Pierre, G. Wagner, J. E. LeDoux and E. Klann (2011). "Inhibition of the interactions between eukaryotic initiation factors 4E and 4G impairs long-term associative memory consolidation but not reconsolidation." *Proc Natl Acad Sci U S A* 108(8): 3383-3388.

Hofer, S. B., T. D. Mrsic-Flogel, T. Bonhoeffer and M. Hubener (2009). "Experience leaves a lasting structural trace in cortical circuits." *Nature* 457(7227): 313-317.

Holtmaat, A. and P. Caroni (2016). "Functional and structural underpinnings of neuronal assembly formation in learning." *Nat Neurosci* 19(12): 1553-1562.

Hu, H., J. Gan and P. Jonas (2014). "Interneurons. Fast-spiking, parvalbumin(+) GABAergic interneurons: from cellular design to microcircuit function." *Science* 345(6196): 1255-1263.

Igaz, L. M., M. R. Vianna, J. H. Medina and I. Izquierdo (2002). "Two time periods of hippocampal mRNA synthesis are required for memory consolidation of fear-motivated learning." *J Neurosci* 22(15): 6781-6789.

Isaacson, J. S. and M. Scanziani (2011). "How inhibition shapes cortical activity." *Neuron* 72(2): 231-243.

Johansen, J. P., J. W. Tarpley, J. E. LeDoux and H. T. Blair (2010). "Neural substrates for expectation-modulated fear learning in the amygdala and periaqueductal gray." *Nat Neurosci* 13(8): 979-986.

Joo, J. Y., K. Schaukowitz, L. Farbiak, G. Kilaru and T. K. Kim (2016). "Stimulus-specific combinatorial functionality of neuronal c-fos enhancers." *Nat Neurosci* 19(1): 75-83.

Kandel, E. R. (2001). "The molecular biology of memory storage: a dialogue between genes and synapses." *Science* 294(5544): 1030-1038.

Kandel, E. R. (2012). "The molecular biology of memory: cAMP, PKA, CRE, CREB-1, CREB-2, and CPEB." *Mol Brain* 5: 14.

Kandel, E. R., Y. Dudai and M. R. Mayford (2014). "The molecular and systems biology of memory." *Cell* 157(1): 163-186.

Kastellakis, G., D. J. Cai, S. C. Mednick, A. J. Silva and P. Poirazi (2015). "Synaptic clustering within dendrites: an emerging theory of memory formation." *Prog Neurobiol* **126**: 19-35.

Kastellakis, G., A. J. Silva and P. Poirazi (2016). "Linking Memories across Time via Neuronal and Dendritic Overlaps in Model Neurons with Active Dendrites." *Cell Rep* **17**(6): 1491-1504.

Katche, C., P. Bekinschtein, L. Slipczuk, A. Goldin, I. A. Izquierdo, M. Cammarota and J. H. Medina (2010). "Delayed wave of c-Fos expression in the dorsal hippocampus involved specifically in persistence of long-term memory storage." *Proc Natl Acad Sci U S A* 107(1): 349-354.

Katche, C., G. Dorman, C. Gonzalez, C. P. Kramar, L. Slipczuk, J. I. Rossato, M. Cammarota and J. H. Medina (2013). "On the role of retrosplenial cortex in long-lasting memory storage." *Hippocampus* 23(4): 295-302.

Katche, C. and J. H. Medina (2017). "Requirement of an Early Activation of BDNF/c-Fos Cascade in the Retrosplenial Cortex for the Persistence of a Long-Lasting Aversive Memory." *Cereb Cortex* 27(2): 1060-1067.

Kawashima, T., H. Okuno and H. Bito (2014). "A new era for functional labeling of neurons: activity-dependent promoters have come of age." *Front Neural Circuits* 8: 37.

Kelleher, R. J., 3rd, A. Govindarajan, H. Y. Jung, H. Kang and S. Tonegawa (2004). "Translational control by MAPK signaling in long-term synaptic plasticity and memory." *Cell* 116(3): 467-479.

Kepecs, A. and G. Fishell (2014). "Interneuron cell types are fit to function." *Nature* 505(7483): 318-326.

Kessels, H. W. and R. Malinow (2009). "Synaptic AMPA receptor plasticity and behavior." *Neuron* 61(3): 340-350.

Kida, S., S. A. Josselyn, S. Pena de Ortiz, J. H. Kogan, I. Chevere, S. Masushige and A. J. Silva (2002). "CREB required for the stability of new and reactivated fear memories." *Nat Neurosci* 5(4): 348-355.

Kim, J., J. T. Kwon, H. S. Kim, S. A. Josselyn and J. H. Han (2014). "Memory recall and modifications by activating neurons with elevated CREB." *Nat Neurosci* 17(1): 65-72.

Klausberger, T. and P. Somogyi (2008). "Neuronal diversity and temporal dynamics: the unity of hippocampal circuit operations." *Science* 321(5885): 53-57.

Kogan, J. H., P. W. Frankland, J. A. Blendy, J. Coblenz, Z. Marowitz, G. Schutz and A. J. Silva (1997). "Spaced training induces normal long-term memory in CREB mutant mice." *Curr Biol* 7(1): 1-11.

Kubik, S., T. Miyashita and J. F. Guzowski (2007). "Using immediate-early genes to map hippocampal subregional functions." *Learn Mem* 14(11): 758-770.

Lai, C. S., T. F. Franke and W. B. Gan (2012). "Opposite effects of fear conditioning and extinction on dendritic spine remodelling." *Nature* 483(7387): 87-91.

Lamprecht, R. and Y. Dudai (1996). "Transient expression of c-Fos in rat amygdala during training is required for encoding conditioned taste aversion memory." *Learn Mem* 3(1): 31-41.

Lamprecht, R., S. Hazvi and Y. Dudai (1997). "cAMP response element-binding protein in the amygdala is required for long- but not short-term conditioned taste aversion memory." *J Neurosci* 17(21): 8443-8450.

Lashley, K. (1950). In search of the engram. *Symp. Soc. Exp. Biol.* 4, 454–482.

Lee, D. (2015). "Global and local missions of cAMP signaling in neural plasticity, learning, and memory." *Front Pharmacol* 6: 161.

Letzkus, J. J., S. B. Wolff and A. Luthi (2015). "Disinhibition, a Circuit Mechanism for Associative Learning and Memory." *Neuron* 88(2): 264-276.

Liu, X., S. Ramirez, P. T. Pang, C. B. Puryear, A. Govindarajan, K. Deisseroth and S. Tonegawa (2012). "Optogenetic stimulation of a hippocampal engram activates fear memory recall." *Nature* 484(7394): 381-385.

Livingstone, M. S., P. P. Sziber and W. G. Quinn (1984). "Loss of calcium/calmodulin responsiveness in adenylate cyclase of rutabaga, a *Drosophila* learning mutant." *Cell* 37(1): 205-215.

Martin, K. C., D. Michael, J. C. Rose, M. Barad, A. Casadio, H. Zhu and E. R. Kandel (1997). "MAP kinase translocates into the nucleus of the presynaptic cell and is required for long-term facilitation in *Aplysia*." *Neuron* 18(6): 899-912.

McGaugh, J. L. (2000). "Memory--a century of consolidation." *Science* 287(5451): 248-251.

Morrison, D. J., A. J. Rashid, A. P. Yiu, C. Yan, P. W. Frankland and S. A. Josselyn (2016). "Parvalbumin interneurons constrain the size of the lateral amygdala engram." *Neurobiol Learn Mem* 135: 91-99.

Muller GE, Pilzecker A. 1900. Experimentelle Beiträge zur Lehre von Gedächtnis. Z. Psychol. 1:1–300

Nader, K., G. E. Schafe and J. E. LeDoux (2000). "The labile nature of consolidation theory." *Nat Rev Neurosci* 1(3): 216-219.

Nakayama, D., H. Iwata, C. Teshirogi, Y. Ikegaya, N. Matsuki and H. Nomura (2015). "Long-delayed expression of the immediate early gene *Arc/Arg3.1* refines neuronal circuits to perpetuate fear memory." *J Neurosci* 35(2): 819-830.

Ognjanovski, N., S. Schaeffer, J. Wu, S. Mofakham, D. Maruyama, M. Zochowski and S. J. Aton (2017). "Parvalbumin-expressing interneurons coordinate hippocampal network dynamics required for memory consolidation." *Nat Commun* 8: 15039.

Ohkawa, N., Y. Saitoh, A. Suzuki, S. Tsujimura, E. Murayama, S. Kosugi, H. Nishizono, M. Matsuo, Y. Takahashi, M. Nagase, Y. K. Sugimura, A. M. Watabe, F. Kato and K. Inokuchi (2015). "Artificial association of pre-stored information to generate a qualitatively new memory." *Cell Rep* 11(2): 261-269.

Packer, A. M., L. E. Russell, H. W. Dalglish and M. Hausser (2015). "Simultaneous all-optical manipulation and recording of neural circuit activity with cellular resolution in vivo." *Nat Methods* 12(2): 140-146.

Ramirez, S., X. Liu, P. A. Lin, J. Suh, M. Pignatelli, R. L. Redondo, T. J. Ryan and S. Tonegawa (2013). "Creating a false memory in the hippocampus." *Science* 341(6144): 387-391.

Rashid, A. J., C. Yan, V. Mercaldo, H. L. Hsiang, S. Park, C. J. Cole, A. De Cristofaro, J. Yu, C. Ramakrishnan, S. Y. Lee, K. Deisseroth, P. W. Frankland and S. A. Josselyn (2016). "Competition between engrams influences fear memory formation and recall." *Science* 353(6297): 383-387.

Reijmers, L. G., B. L. Perkins, N. Matsuo and M. Mayford (2007). "Localization of a stable neural correlate of associative memory." *Science* 317(5842): 1230-1233.

Repa, J. C., J. Muller, J. Apergis, T. M. Desrochers, Y. Zhou and J. E. LeDoux (2001). "Two different lateral amygdala cell populations contribute to the initiation and storage of memory." *Nat Neurosci* 4(7): 724-731.

Rogerson, T., D. J. Cai, A. Frank, Y. Sano, J. Shobe, M. F. Lopez-Aranda and A. J. Silva (2014). "Synaptic tagging during memory allocation." *Nat Rev Neurosci* 15(3): 157-169.

Rossato, J. I., L. R. Bevilaqua, I. Izquierdo, J. H. Medina and M. Cammarota (2009). "Dopamine controls persistence of long-term memory storage." *Science* 325(5943): 1017-1020.

Roux, L., B. Hu, R. Eichler, E. Stark and G. Buzsaki (2017). "Sharp wave ripples during learning stabilize the hippocampal spatial map." *Nat Neurosci* 20(6): 845-853.

Ruediger, S., D. Spirig, F. Donato and P. Caroni (2012). "Goal-oriented searching mediated by ventral hippocampus early in trial-and-error learning." *Nat Neurosci* 15(11): 1563-1571.

Ruediger, S., C. Vittori, E. Bednarek, C. Genoud, P. Strata, B. Sacchetti and P. Caroni (2011). "Learning-related feedforward inhibitory connectivity growth required for memory precision." *Nature* 473(7348): 514-518.

Rumpel, S., J. LeDoux, A. Zador and R. Malinow (2005). "Postsynaptic receptor trafficking underlying a form of associative learning." *Science* 308(5718): 83-88.

Ryan, T. J., D. S. Roy, M. Pignatelli, A. Arons and S. Tonegawa (2015). "Memory. Engram cells retain memory under retrograde amnesia." *Science* 348(6238): 1007-1013.

Sanders, J., K. Cowansage, K. Baumgartel and M. Mayford (2012). "Elimination of dendritic spines with long-term memory is specific to active circuits." *J Neurosci* 32(36): 12570-12578.

Sano, Y., J. L. Shobe, M. Zhou, S. Huang, T. Shuman, D. J. Cai, P. Golshani, M. Kamata and A. J. Silva (2014). "CREB regulates memory allocation in the insular cortex." *Curr Biol* 24(23): 2833-2837.

Schacter, D.L., Eich, J.E., and Tulving, E. (1978). Richard Semon's Theory of Memory. *J. Verbal Learn. Verbal Behav.* 17, 721–743.



Schacter, D.L. (1982). *Stranger behind the engram: theories of memory and the psychology of science* (L. Erlbaum Associates).

Schafe, G. E., K. Nader, H. T. Blair and J. E. LeDoux (2001). "Memory consolidation of Pavlovian fear conditioning: a cellular and molecular perspective." *Trends Neurosci* 24(9): 540-546.

Semon, R. (1904). *Die Mneme als erhaltendes Prinzip im Wechsel des organischen Geschehens* (Leipzig: Wilhelm Engelmann).

Semon, R. (1909). *Die mnemischen Empfindungen* (Leipzig: Wilhelm Engelmann).

Semon, R. (1921). *The Mneme* (G. Allen & Unwin Limited).

Semon, R. (1923). *Mnemic Philosophy* (Allen & Unwin).

Sheng, M., G. McFadden and M. E. Greenberg (1990). "Membrane depolarization and calcium induce c-fos transcription via phosphorylation of transcription factor CREB." *Neuron* 4(4): 571-582.

Sheng, M., M. A. Thompson and M. E. Greenberg (1991). "CREB: a Ca(2+)-regulated transcription factor phosphorylated by calmodulin-dependent kinases." *Science* 252(5011): 1427-1430.

Silva, A. J., J. H. Kogan, P. W. Frankland and S. Kida (1998). "CREB and memory." *Annu Rev Neurosci* 21: 127-148.

Stanciu, M., J. Radulovic and J. Spiess (2001). "Phosphorylated cAMP response element binding protein in the mouse brain after fear conditioning: relationship to Fos production." *Brain Res Mol Brain Res* 94(1-2): 15-24.

Stark, E., L. Roux, R. Eichler and G. Buzsaki (2015). "Local generation of multineuronal spike sequences in the hippocampal CA1 region." *Proc Natl Acad Sci U S A* 112(33): 10521-10526.

Stark, E., L. Roux, R. Eichler, Y. Senzai, S. Royer and G. Buzsaki (2014). "Pyramidal cell-interneuron interactions underlie hippocampal ripple oscillations." *Neuron* 83(2): 467-480.

Stefanelli, T., C. Bertollini, C. Luscher, D. Muller and P. Mendez (2016). "Hippocampal Somatostatin Interneurons Control the Size of Neuronal Memory Ensembles." *Neuron* **89**(5): 1074-1085.

Tanaka, K. Z., A. Pevzner, A. B. Hamidi, Y. Nakazawa, J. Graham and B. J. Wiltgen (2014). "Cortical representations are reinstated by the hippocampus during memory retrieval." *Neuron* **84**(2): 347-354.

Tao, X., S. Finkbeiner, D. B. Arnold, A. J. Shaywitz and M. E. Greenberg (1998). "Ca<sup>2+</sup> influx regulates BDNF transcription by a CREB family transcription factor-dependent mechanism." *Neuron* **20**(4): 709-726.

Taylor, K. K., K. Z. Tanaka, L. G. Reijmers and B. J. Wiltgen (2013). "Reactivation of neural ensembles during the retrieval of recent and remote memory." *Curr Biol* **23**(2): 99-106.

Tonegawa, S., X. Liu, S. Ramirez and R. Redondo (2015). "Memory Engram Cells Have Come of Age." *Neuron* **87**(5): 918-931.

Tonegawa, S., M. Pignatelli, D. S. Roy and T. J. Ryan (2015). "Memory engram storage and retrieval." *Curr Opin Neurobiol* **35**: 101-109.

Tricoire, L., K. A. Pelkey, B. E. Erkkila, B. W. Jeffries, X. Yuan and C. J. McBain (2011). "A blueprint for the spatiotemporal origins of mouse hippocampal interneuron diversity." *J Neurosci* **31**(30): 10948-10970.

Trifilieff, P., C. Herry, P. Vanhoutte, J. Caboche, A. Desmedt, G. Riedel, N. Mons and J. Micheau (2006). "Foreground contextual fear memory consolidation requires two independent phases of hippocampal ERK/CREB activation." *Learn Mem* **13**(3): 349-358.

Trouche, S., P. V. Perestenko, G. M. van de Ven, C. T. Bratley, C. G. McNamara, N. Campo-Urriza, S. L. Black, L. G. Reijmers and D. Dupret (2016). "Recoding a cocaine-place memory engram to a neutral engram in the hippocampus." *Nat Neurosci* **19**(4): 564-567.

Walters, E. T. and J. H. Byrne (1983). "Associative conditioning of single sensory neurons suggests a cellular mechanism for learning." *Science* **219**(4583): 405-408.

Wagner, M. J., T. H. Kim, J. Savall, M. J. Schnitzer and L. Luo (2017). "Cerebellar granule cells encode the expectation of reward." *Nature* **544**(7648): 96-100.

Wolff, S. B., J. Grundemann, P. Tovote, S. Krabbe, G. A. Jacobson, C. Müller, C. Herry, I. Ehrlich, R. W. Friedrich, J. J. Letzkus and A. Luthi (2014). "Amygdala interneuron subtypes control fear learning through disinhibition." *Nature* **509**(7501): 453-458.

Xia, Z. and D. R. Storm (2012). "Role of signal transduction crosstalk between adenylyl cyclase and MAP kinase in hippocampus-dependent memory." *Learn Mem* **19**(9): 369-374.

Xu, T., X. Yu, A. J. Perlik, W. F. Tobin, J. A. Zweig, K. Tennant, T. Jones and Y. Zuo (2009). "Rapid formation and selective stabilization of synapses for enduring motor memories." *Nature* **462**(7275): 915-919.

Yang, G., F. Pan and W. B. Gan (2009). "Stably maintained dendritic spines are associated with lifelong memories." *Nature* **462**(7275): 920-924.

Yassin, L., B. L. Benedetti, J. S. Jouhanneau, J. A. Wen, J. F. Poulet and A. L. Barth (2010). "An embedded subnetwork of highly active neurons in the neocortex." *Neuron* **68**(6): 1043-1050.

Yin, J. C., J. S. Wallach, M. Del Vecchio, E. L. Wilder, H. Zhou, W. G. Quinn and T. Tully (1994). "Induction of a dominant negative CREB transgene specifically blocks long-term memory in *Drosophila*." *Cell* **79**(1): 49-58.

Yiu, A. P., V. Mercaldo, C. Yan, B. Richards, A. J. Rashid, H. L. Hsiang, J. Pressey, V. Mahadevan, M. M. Tran, S. A. Kushner, M. A. Woodin, P. W. Frankland and S. A. Josselyn (2014). "Neurons are recruited to a memory trace based on relative neuronal excitability immediately before training." *Neuron* **83**(3): 722-735.

Zhou, Y., J. Won, M. G. Karlsson, M. Zhou, T. Rogerson, J. Balaji, R. Neve, P. Poirazi and A. J. Silva (2009). "CREB regulates excitability and the allocation of memory to subsets of neurons in the amygdala." *Nat Neurosci* **12**(11): 1438-1443.

# Acknowledgements

I could start by thanking Pico for giving me the opportunity to do my PhD thesis in his lab. But before that, I would like to thank him for making me want to do a PhD in the first place. After two masters in two continents, one day a talk in the Neurizons meeting at Goettingen made an impression that still persists. Pico, now it is the time to thank you for the passion you instilled that day. Every discussion and argument, every success and failure in these years has taught me far beyond neuroscience. Thank you for being the mentor with whom I could always share the fun of experiments, for believing in me and guiding me all the way.

I would like to thank my thesis committee members, Silvia and Botond for the discussions and resources, the support and guidance during and beyond the committee meetings. A lot of the ideas sparked at those meetings with your suggestions and made these years so much more fun.

I would like to thank Flavio. More than the experimental techniques, you showed me how to best organize my thoughts into experiments that helped me throughout the PhD. Thanks to Purni for being very good friend who helped me ease into the lab.

Melissa and Fernando, thank you, for sheltering me with your friendship. Your presence made this city a home and this lab a sanctuary. Fernando, I finally learnt to 'feel the staining', thank you for the discussions at 710. Melissa, you are the best friend I always had wished for but never believed I would have. You endure the worst in me and bring out the best. I love you for caring and scolding, for all the precious memories. Nothing in my work or talks or reports or thesis or life in Basel would have been the same without you being there to make them better.

A special thanks to Kerstin for being a great friend and supporting me all along. Thank you to Matteo, Maria Spolidoro, Giulia, Agne, Arghya, Maria Lahr, Olga, Sebastian, Komal, Lara and Lisa for discussing science and not-so-science, for cool ideas and even better coffee times.

I want to thank my father for showing me throughout my life what meant to be a scientist, my sister for being my 207<sup>th</sup> bone and loving me no matter what and my mother for everything I am. Ma, thank you, for so many reasons that I could write another thesis. But, in your heart, you know them already because you know me better than I know myself. Finally, my gratitude to the one who kept me together whenever I was afraid and lost, thank you for keeping your promises.

# Curriculum Vitae

## Personal Details-

Ananya Chowdhury

Current Address- Erlenstrasse 52

Basel 4058

Switzerland

Phone number- +41789327501

Email I.D- ananya.chowdhury@fmi.ch, ananyakgp@gmail.com

## Academic Record-

- PhD Program- International PhD Program, Friedrich Miescher Institute for Biomedical Research (FMI), Basel, Switzerland. 2012-2017.
- Masters' Program- International Max Planck Research School (IMPRS), Neuroscience Program, Goettingen, Germany. 2010-2012. Grade-A.
- Masters (MSc)- Jawaharlal Nehru University, New Delhi, India. 2008-2010. Grade- 8.7 out of 9 CGPA.
- Bachelors (BSc)- Banaras Hindu University, Uttar Pradesh, India. 2005-2008. Grade-78.7%.
- 12th Standard- Central Board (CBSE), Kharagpur, India. 2004. Grade-91.8%.
- 10th Standard- West Bengal Board, Kharagpur, India. 2002. Grade-90.12%.

## Research Experience-

- PhD Project at FMI- PhD studies under the supervision of Prof. Dr. Pico Caroni, Friedrich Miescher Institute for Biomedical Research (2012-2017). The topic of my research is 'Cellular and Network mechanisms for Learning and Memory Consolidation' and it is partially supported by NCCR grant.
- Master's Project at IMPRS- 6 months' project under Dr. Moritz Rossner, Max Planck Institute of Experimental Medicine, Goettingen in the topic titled 'Behavioral Analysis of TCF4 (novel schizophrenia risk factor) transgenic mouse under chronic social stress and Effect of loss of TCF4 in the morphology of cortical neurons.'

□ Lab rotations in IMPRS Program-

a) 2 months' lab rotation in the topic titled 'Characterization of synaptosomes using biochemical techniques and high resolution imaging' under the supervision of Dr. Silvio Rizzoli, European Neuroscience Institute (ENI), Goettingen, Germany.

b) 2 months' lab experience of using STED Microscopy in the hippocampal brain slices under Dr. Katrin Willig, in the department of Dr. Stefan Hell, Max Plank Institute of Biophysical Chemistry, Goettingen, Germany.

c) 2 months' lab rotation in the topic titled 'Effect of Social Chronic Stress and Enrichment of environment on the social and cognitive behaviour of the wild type mice' under the supervision of Dr. Moritz Rossner, Max Planck Institute of Experimental Medicine, Goettingen, Germany.

□ Master's Project at JNU, India- 1-year project under Dr. Sushil K Jha, School of Life Sciences, Jawaharlal Nehru University, New Delhi, India in the topic titled 'Role of sleep on reward-learning and memory consolidation'.

**Publications-**

1: Chowdhury A and Caroni P. Time Units for Learning Involving Maintenance of System-wide cFos Expressing Neuronal Assemblies. Under review, Nature Neuroscience, 2017.

2: Karunakaran S\*, Chowdhury A\*, Donato F, Quairiaux C, Michel CM, Caroni P. PV plasticity sustained through D1/5 dopamine signaling required for long-term memory consolidation. Nat Neurosci. 2016 Mar;19(3):454-64. doi: 10.1038/nn.4231. Epub 2016 Jan 25. PubMed PMID: 26807952. [\*: Equal Contribution]

3: Donato F\*, Chowdhury A\*, Lahr M, Caroni P. Early- and late-born parvalbumin basket cell subpopulations exhibiting distinct regulation and roles in learning. Neuron. 2015 Feb 18;85(4):770-86. doi: 10.1016/j.neuron.2015.01.011. PubMed PMID: 25695271. [\*: Equal Contribution]

4: Caroni P, Chowdhury A, Lahr M. Synapse rearrangements upon learning: from divergent-sparse connectivity to dedicated sub-circuits. Trends Neurosci. 2014 Oct;37(10):604-14. doi: 10.1016/j.tins.2014.08.011. Epub 2014 Sep 22. Review. PubMed PMID: 25257207.

5: Badowska DM, Brzózka MM, Chowdhury A, Malzahn D, Rossner MJ. Data calibration and reduction allows to visualize behavioural profiles of psychosocial influences in mice towards clinical domains. Eur Arch Psychiatry Clin Neurosci. 2015 Sep;265(6):483-96. doi: 10.1007/s00406-014-0532-6. Epub 2014 Sep 19. PubMed PMID: 25236183.

6: Chowdhury A\*, Chandra R\*, Jha SK. Total sleep deprivation impairs the encoding of trace-conditioned memory in the rat. Neurobiol Learn Mem. 2011 Mar;95(3):355-60. doi: 10.1016/j.nlm.2011.01.009. Epub 2011 Feb 2. PubMed PMID: 21295147. [\*: Equal Contribution]

### **Conferences Attended-**

- The Brain Conferences- "Learning, Memory and Synaptic Plasticity", 2017, Rungstedgaard, Copenhagen, Denmark. Presented poster.
- GRC (Gordon Research Conference)- "Optogenetic Approaches to Understanding Neural Circuits and Behaviour", 2016, Sunday River, Maine, USA. Presented poster.
- The NCCR-Synapsy Conference- "The Neurobiology of Mental Health", 2016, Geneva, Switzerland. Presented poster.
- The Ascona Meetings on Neuronal Circuits- "The Assembly and Function of Neuronal Circuits", 2015, Ascona, Switzerland. Presented a short talk titled-'Protracted offline reenactment of learning for information binding and long-term memory consolidation'.
- The Brain Conferences- "Bridging Neural Mechanisms and Cognition", 2015, Rungstedgaard, Copenhagen, Denmark. Presented a short talk titled- 'Parvalbumin Basket Cell Subpopulations Exhibiting Distinct Roles in Learning'.
- The Brain Conferences- "The Neurobiology of Synapses and their dysfunction", 2013, Stresa, Italy.
- FENS Forum Conference- 2012 (Barcelona, Spain), 2014 (Milan, Italy), 2016 (Copenhagen, Denmark)

### **Fundings Received-**

- Recipient of the 'Stipend of the Excellence Foundation for the Promotion of the Max Planck Society', 2010-2011.